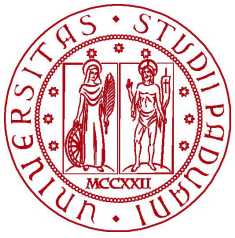

UNIVERSITÀ
DEGLI STUDI
DI PADOVA

Sede Amministrativa: Universitá degli Studi di Padova

Dipartimento di Ingegneria Idraulica, Marittima, Ambientale e Geotecnica

SCUOLA DI DOTTORATO DI RICERCA IN: Scienze dell'Ingegneria Civile e Ambientale

CICLO XXIV

# ASPECTS OF RIVERINE HYDRO-MORPHO-BIODYNAMICS AT WATERSHED SCALE

**Direttore della Scuola**: Ch.mo Prof. Stefano Lanzoni

**Supervisore**: Ch.mo Prof. Giampaolo Di Silvio

**Dottorando**: Michael Nones

*a Arianna*

# Aknowledgements

My thanks to the Professor Giampaolo Di Silvio, who is been able to stimulate my interest in research and provided me a lot of suggestions and incentive, and to the Professor Helmut Habersack for his precious suggestions during the revision of my thesis.

Many thanks to Paolo Ronco and Giacomo Fasolato, who gave me the numerical model which I used for doing my studies, and to Massimo Guerrero, who helped me in a new topic of my PhD work.

Thanks to Luca Guarino (AdB Adige) and the staff of Corila and Cnr-Ismar, who helped me to develop some researches.

Many thanks to the XXIV ciclo team, for the time spent together, and for the support given me.

Infine un ringraziamento ai miei genitori per tutto il sostegno datomi in questi anni.

# Contents

# List of Figures

# List of Tables

# Sommario

L'integrazione di varie discipline scientifiche sta diventando sempre piú importante nel definire in maniera compiuta l'evoluzione di un intero sistema fluviale, sia dal punto di vista spaziale che temporale.
Questo lavoro di tesi si prefigge lo scopo di analizzare l'evolversi di un fiume sottoposto ad interazioni idrologiche, morfologiche e biologiche.
Tale analisi viene fatta a scala di bacino, adottando un modello numerico 1-D integrato con un sottomodello quasi 2-D. Entrambi i modelli sono capaci di utilizzare ed integrare i dati reperibili lungo un corso d'acqua, che spesso risultano carenti sia qualitativamente che quantitativamente, soprattutto nel caso di grandi fiumi non strumentati, tipici dei paesi in via di sviluppo.
Tale approccio permette quindi di studiare l'evolversi di un complesso sistema fluviale a grande scala e a lungo termine, in quanto i tempi computazionali richiesti dal codice semplificato risultano piuttosto contenuti. I risultati ottenuti sono indicativi di una tendenza evolutiva del fiume a media risoluzione, che puó essere utile in differenti studi, anche come dato di input per successive modellizzazioni di maggior dettaglio.
Nel primo capitolo si evidenziano tutti i meccanismi di formazione e trasporto dei sedimenti, in modo tale da fornire una panoramica sui vari modelli che si possono adottare per descrivere l'evoluzione morfologica di un sistema fluviale. Oltre a tale descrizione, in questo capitolo vengono messe in evidenza anche le differenti conformazioni fluviali presenti in natura, suddivise sulla base della loro morfologia dominante.
La mancanza di dati specifici, sia dal punto di vista dell'idrologia che della morfologia e della biologia, comporta l'applicazione di un modello, sia pure non di dettaglio, capace di descrivere i principali processi dell'idrodinamica, della morfodinamica e della crescita della vegetazione riparia lungo il corso del fiume.
Questo modello, sostanzialmente 1-D, si basa sulle semplificazioni connesse all'imposizione del moto localmente uniforme. Al modello 1-D viene associato un sottomodello quasi 2-D, capace di fornire una descrizione sintetica della sezione trasversale del fiume. Tale sottomodello si rende necessario per l'analisi di grandi sistemi fluviali, dei quali spesso non si dispone di un rilievo batimetrico di dettaglio. Nel secondo

e nel terzo capitolo viene quindi fatta un'analisi di tali modelli, evidenziando i pregi ed i difetti delle varie semplificazioni effettuate.

Lo sviluppo della vegetazione riparia é fortemente influenzato dalle forzanti agenti su di essa, sia quelle idrologiche che quelle morfologiche. Allo stadio attuale, esistono solo alcuni studi sito-specifici o di carattere puramente qualitativo che analizzano compiutamente l'interazione tra le forzanti fluviali e la vegetazione riparia. In questa tesi si é quindi voluto provare a descrivere l'influenza dell'idrologia e della morfologia sullo sviluppo della vegetazione, semplificando il piú possibile i meccanismi coinvolti. Viene quindi proposta tale analisi, evidenziandone i limiti legati all'assenza di dati sperimentali tali da permettere una buona taratura del modello.

Nei successivi due capitoli vengono riportate due differenti applicazioni del modello completo: la prima al fiume Paraná e la seconda al fiume Zambezi.

L'applicazione al fiume Paraná viene fatta per mettere in evidenza la bontá del modello nel descrivere l'evoluzione fluviale, anche mediante un raffronto con un modello commerciale unidimensionale quale Hec-Ras. Tale applicazione é stata fatta anche per verificare l'impostazione generale e le formulazioni adottate nella descrizione della sezione sintetica e dell'interazione tra le forzanti fluviali e lo sviluppo della vegetazione riparia.

Lo studio del fiume Zambezi vuole invece verificare come l'alterazione delle portate a causa degli sbarramenti idroelettrici presenti lungo il corso d'acqua influenzi fortemente sia la morfologia che la biologia dell'ambiente fluviale, con effetti sia a medio che a lungo termine. Questa analisi é stata fatta con l'intento di analizzare le variazioni planimetriche e batimetriche susseguenti all'alterazione del regime idrologico naturale di un corso d'acqua causata dalla costruzione di sbarramenti idroelettrici.

Nell'ultimo capitolo vengono discussi i risultati generali ed introdotti i possibili sviluppi futuri, sottolineando come tutti i modelli semplificati analizzati in questo lavoro di tesi necessitino di ulteriori verifiche e validazioni, anche attraverso l'analisi di ulteriori dati sperimentali.

# Abstract

The integration of various scientific disciplines is becoming more and more important to define the complete evolution of an entire river system, both in time and in space.
The aim of this thesis is to analyze the evolution of a river subjected to hydrological, morphological and biological interactions. This analysis is done at watershed scale, by using a numerical 1-D model plus a quasi 2-D sub-model. These models are able to integrate the available data, often scarce both qualitatively and quantitatively, especially in large unsurveyed rivers, typical of less developed countries.
The models analysis allows to study the evolution of a river system at large space-scale and long-time scale, because the computational effort required by simplified models are quite low. The results of these models are indicative of a trend of the evolution of the river, in space and time, which can be useful in different studies, for example as input for other detailed models.
In the first Chapter we analyze the principal mechanisms of formation and transport of sediments, making an overview of the various models that can be adopted to describe the morphological evolution of a river system. In addition to this description, in this chapter we study the different conformations of riverbeds, classified on the basis of their geometry and morphology.
The lack of detailed data, from the point of view both of geometry and biology, implies the application of a non-detailed model, able to describe the hydrodynamic, morphodynamic and biological main processes of the river along its course. This model, essentially 1-D, is based on simplifications related to the hypothesis of the Local Uniform Flow. The 1-D model is associated to a quasi 2-D sub-model, able to provide a synthetic description of the river cross-section. This sub-model is useful for the analysis of large river systems, for which often we do not have bathymetric surveys. In the second Chapter and in the third Chapter is made a detailed analysis of these models, highlighting the advantages and disadvantages of the various simplifications.
The growth of the riparian vegetation is strongly influenced by the forcing terms present in a river, related to hydrology and morphology. In Literature there are only a few site-specific studies or purely qualitative

analysis, which study the interaction between the forcing terms and the riparian vegetation. The aim of this thesis is trying to model the influence of hydrology and morphology on the growth of the riparian vegetation, by a simplification of all the possible mechanisms involved. In this Chapter we have reported a detailed analysis of our studies, highlighting the limitations related to the lack of experimental data needed for a good calibration of our quasi 2-D sub-model.

In the next two Chapters two different applications of the complete model are given: the first one about the Paraná River, and the second one about the Zambezi River.

The application to the Paraná River has been made to highlight the goodness of the model for describing the evolution of the river, even compared to a commercial 1-D model as the Hec-Ras code. That application was also made to verify the general approach and the formulation used in the description of the synthetic river cross-section and the interaction between the river forcing terms and the growth of the riparian vegetation.

The study of the Zambezi River is useful to see how the alteration of flow due to hydropower dams along the river strongly influences both morphology and biology of the river, with medium and long term effects. This analysis evaluates the planimetric and bathymetric changes subsequent to an alteration of the natural flow regime of a river due to the construction of hydroelectric reservoirs.

In the last Chapter we have discussed the general results and the future developments, underlining, however, that the simplified models used in this work require further verifications, also against the analysis of more experimental data.

# Chapter 1

# Erosion and Sedimentation

## 1.1 Introduction

Sediment research has been marked by an intensive progress in the last decades, as the problem of the sediment management is becoming very important in several regions of the world. This problem concerns different aspects of human life, for example the hydropower production (e.g. in the Lower Zambezi River) or the fluvial navigation (e.g. along the Paraná River).

The theme of erosion and sedimentation must be seen as key factor in many different socio-economical environments, but assumes special importance in the contest of Less Developed Countries (Africa or South America), since there are various problems linked to erosion, transport and sedimentation. For example, surface erosion and trasportation of fine sediments create big problems in many areas along the Middle and the Lower Paraná River in Argentina, and these problems increase year by year also due to the climatic variations: sediment deposition alters the river patterns and reduces the fluvial navigation, necessary for the development of the region, and surface erosion reduces cropland areas (Nones et al., 2011c).

The soil erosion has a direct relationship with the reservoir sedimentation: this theme is particularly interesting in regions where water supply of agriculture and people depends on surface water stired in reservoirs, created by the construction of dams, and sediment management is necessary to preserve the reservoir storage capacity (Bruk, 2003), as the Lower Zambezi region. Since the most favorable sites for the construction of dams have already been utilized, sediment management has the purpose to extend as much as possible the useful life of existing or new storage reservoirs (Ronco, 2008).

In this Chapter we analyze the principal forms of sediment formation and transport, and make a short summary about the morphological models and their principal simplifications. Furthermore, we analyze the

common shapes of riverbeds, related to the channel geometry and the annual hydrology of a river network.

## 1.2 Principal forms of sediment motion

Erosion of the watershed slopes and the dynamics of the sediments involve a variety of different processes, which may be analyzed and classified under different point of view. Under the action of direct water (rainfall, overland flow, channeled flow, etc.) or indirect water (infiltration, freezing, melting of the snow, etc.) the sediments are removed from the surface of the watershed and conveyed downstream to the river and to the sea.

Depending on the prevalent extension of the process, we can distinguish different basic forms of sediment movement: mass or volume (principally developed at 3-D spatial scale), surface (mainly developed at 2-D scale) and linear (chiefly developed at 1-D scale).

The mass movement corresponds to landslides, occasionally produced in the steepest slopes of the watershed; the surface erosion can take place in undulated, scarcily vegetated surface; the linear transport occurs in the stream network. Obviously, there are numerous intermediate forms, as, for example, rills erosion (surface/linear movements), gullies erosion (mass/surface/linear movements) or debris flows (mass/linear movements) (Di Silvio, 2004).

If the rainfall is extremely scarce (e.g. in desert or in arid zones), wind is the most effective cause of the surface erosion.

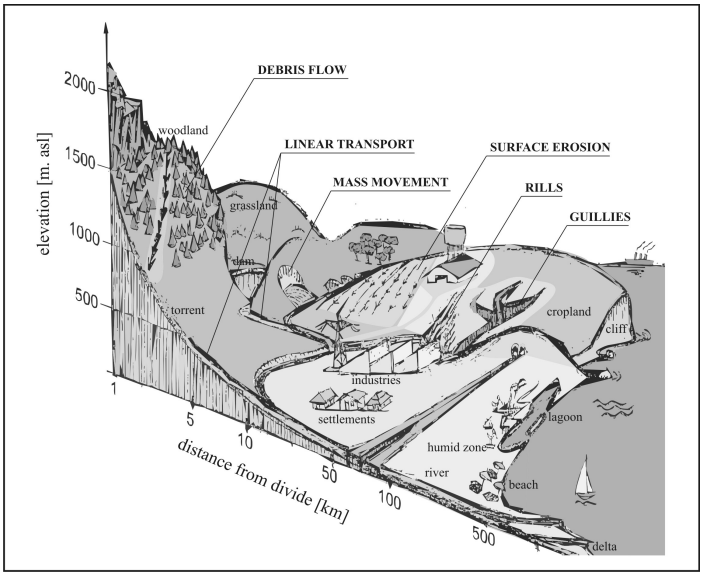


**Figure 1.1:** Basic forms of sediment motion in a watershed in temperate zones (adapted from Di Silvio, 2006).

In the next figure we have reported a simple diagram of the principal zones of distinct sediment behaviour in a river catchment. Headwater areas are predominantly erosional. Mid-reaches are principally transfer zones and erosion and deposition are quite balanced. The lowest sections of rivers, near the sea, are mainly depositional (Naiman et al., 2005).

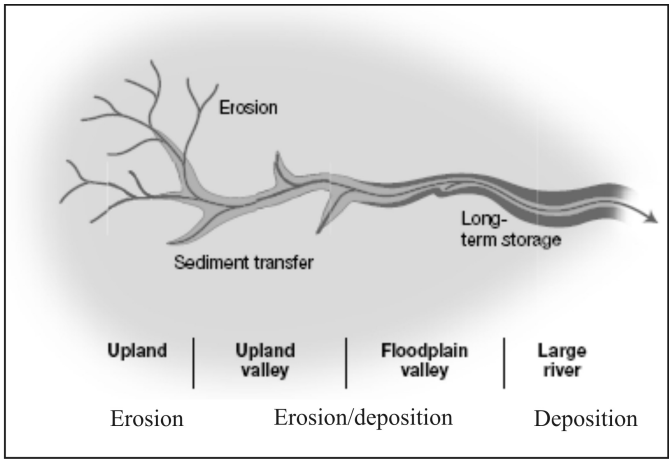


**Figure 1.2:** Principal zones of sediment behaviour in a watershed; adapted from Church, 2002.

### 1.2.1 Volume erosion

Mass movement corresponds to the detachment of sediments as a bulk from their original position (namely landslides), when the active forces (gravity) become higher than the passive forces (friction and cohesion). This kind of movement is an important source of material for many rivers and, in some cases, the most important one (e.g. in alpine climate or in humid tropical forests).

Mud flows and debris flows are some intermediate forms of sediment motion between mass movements and linear transport, which require a relatively small minimum steepness to be started. While their motion depends on particle and fluid dynamics (typical of linear transport), their triggering is controlled by static forces, depending on friction, cohesion, slope and saturation of the permeable material (typical of mass movements).

Various models have attempted to simulate the interactions of more different contributions which can activate these erosion processes (Montgomery et al., 1994; Baum et al., 2002).

### 1.2.2 Surface erosion

Surface erosion, developing mainly over two dimensions, represents the most important source of sediments where vegetation does not provide a sufficient cover of the bare soil from the rainfall (or wind) impact.

This means that the surface erosion is particularly important in cropland areas, especially where the type of soil is more vulnerable, while measures against erosion and correct cultivation practices are not good applied.

Erosion and sediment transport models can be subdivided into three main categories (Merritt et al., 2003), depending on the physical processes simulated, the model algorithms describing these processes and the data dependence of the model:

- empirical or statistical models;
- physical based models;
- conceptual models.

The distinctions between these models is not so clear and therefore can be somewhat subjective. They are likely to contain a mix of modules from each of these categories.

The most important Institution in the study of the soil erosion was the U.S. Department of Agriculture, which has proposed the U.S.L.E. (Universal Soil Loss Equation) model (Wischmeier et al., 1978). The structure of this formula (eq. 1.1) tries to take into account all factors: kinetic energy impact of rainfall combined with the intensity of rainfall, proportional to overland flow discharge (erosivity factor $R$); resistance of the soil, quantified by means of descriptive tables (erodibility factor $K$); slope length, also proportional to overland flow discharge (length factor $L$); slope steepness, related to overland flow velocity (steepness factor $S$); protection by vegetation depending on plants, crop and vegetative phase (cover factor $C$); management practices (practice factor $P$).

$$A = R \cdot K \cdot L \cdot S \cdot C \cdot P \tag{1.1}$$

In this formula the term $A$ indicates the area subjected to soil erosion.

The U.S.L.E. formula provides the values of sediment production at the “plot-or field scale” for a given period of time. For obtaining the corresponding data at watershed scale, it is necessary to apply a routing process, which transforms the local sediment production into the integral sediment yield. The U.S.L.E. model (or some of its variations, reported in Williams, 1975 and Renard et al., 1997), is generally the simplest and most widely applied of the empirical models, especially for large basins.

Instead of the U.S.L.E. model, it is possible to use another empirical method, known as the E.P.M. (Erosion Potential Method), reported in various studies (Gavrilovic, 1988; Gavrilovic et al., 2004; Stefanovic et al, 2003; Stefanovic et al, 2004). This method is particularly useful for describing the potential erosion along torrents or mountain rivers.

In contrast with the empirical models (as the U.S.L.E. models or the E.P.M. model), in the last years they have been developed the so-called "physically based" models, which are constituted by some theoretical differential equations, expressing the mass balance of water and sediments, and by algebraic equations, describing each of the physical processes involved (Laflen et al., 1991; Rulli et al., 2007; Basile et al., 2010).

The physical processes involved in water flow and sediment dynamics are more complicated on the watershed slopes than in rivers, and so it is much more difficult to simulate them realistically. For this reason, empirical models, controlled by few coefficients (scarcely recognizable from the physical point of view, but quite consistent and confirmed by a great number of experiments) can give much better results that physically based models, controlled by a large number of coefficients (generally unknown and based on hardly plausible physical and geometrical schematizations).

Conceptual models are usually based on the representation of a catchment as a series or by a combination of hydraulic storage like reservoirs, channels, etc. (Tyagi et al., 2008). These models tend to include a general description of the catchment processes, without including the specific details of the interactions, which require detailed catchment informations. Parameters values for conceptual models have been obtained through calibration against measured data, and so these models tend to suffer from problems associated with the identifiability of these parameters.

### 1.2.3 Linear transport

Linear transport taking place along only one direction (longitudinal) and the motion of sediments is produced by persistent and channelized water flow. This process is mainly responsible for the river evolution (aggradation/degradation processes) in the hydrographic network.

Linear transport assumes various modes (bedload, suspended load and some intermediate forms), but attempts have been made towards a conceptual unification of these forms of transport, through the concept of the "adaptation length" (Ronco, 2008). The adaptation length represents the distance required by clear water entering a uniform flow stream flowing over a river bottom with uniform grain size composition to reach the uniform sediment transport conditions. This quantity is related to the particle grain size and to the characteristic of the water flow. The adaptation length can be evaluated by different approaches (Galappatti, 1983; Armanini et al., 1988; Bolla Pittaluga et al., 2003; Pryce et al., 2003) and its effects should be taken into account in sediment transport computation.

In real rivers, bed material appears to be coarser than the transported material, and a complete model must consider the transport of each grain size classes. When trating different grain size classes, we must make attention to the interference of particles of different diameter (namely the "Hiding-Exposure" effect)

(Egiazaroff, 1965; Parker et al., 1982; Wu et al., 2000).

If we analyze the evolution of a river system over a long period of time, it is possible to note that the transported material (e.g. the material intercepted by a reservoir) appears to be definitely finer than the average composition of the river bottom.

## 1.3 Morphological models

Morphological processes may be seen as the product of repeated succession of different phases of sediment motion: erosion, transport and deposition. In some cases, one of these phases is dominant.

If we analyze the entire morphological processes, it is important to keep in mind the time-and space-scale under consideration. The time-scale of each system may be associated to the corresponding space-scale via a typical process velocity (Ronco, 2008).

A large number of morphological models have been developed at different time and space scales and with various degrees of detail and approximation and are available in Literature (Merritt et al., 2003).

In this section we make a short analysis about the available linear transport models, based on the scale of these models.

### 1.3.1 Small scale models

Detailed small-scale models have been developed principally for research purpose.

Many of these models have the aim to reproduce the movement of individual particles under the action of other particles and water flow and are usually based on a lagrangian approach. They should be able to reproduce the detailed behaviour of small scale systems (Strom et al., 2004; Strom et al., 2007) and may be useful to explain the hydraulic resistance mechanisms, to show the validity and the limitations of some transport formula, to investigate the dynamics of the movable bottom of rivers and to describe the motion of hyper-concentrated liquid-solid mixtures.

### 1.3.2 Intermediate scale models

These models are used mainly for practical applications.

They are typically extended to the size of a river reach and applied for relatively short time duration (only few years). All the sub-systems processes are incorporated via simple predictors, usually algebraic equations developed under some equilibrium hypothesis.

Intermediate scale models are obtained by averaging the Reynolds equations (obtained by averaging

the Navier-Stokes equations over turbulences) over appropriate space dimensions. These models can be applied to relatively large portions of the hydrographic network.

The most common commercial models are 1-D, averaged over the river cross-sections. These models can simulate the variations of the bottom profile (in terms of erosion and deposition) along the river (Cui et al., 1996; Cao et al., 2002; Papanicolau et al., 2004; Wu et al., 2004; Cui et al., 2005; Curran et al., 2005; Wright et al., 2005).

Rather common, however, are becoming 2-D models (namely averaged over the river depth) (Ye et al., 1997; Stockstill et al., 1997; Nicholas et al., 1998; Jia et al., 1999; Defina, 2000; Kassem et al., 2002; Defina, 2003; Cea et al., 2007; Abad et al., 2007; Lago et al., 2010). These models can simulate the process at river width-scale (migrating and stationary bars, braiding and bifurcations, sediment exchange with floodplains, etc.). Bank collapse and reconstruction can be incorporated in a 2-D model, which therefore will be able to reproduce meander formation and propagation.

The reproduction of the meanders behaviour requires 3-D models (Jia et al., 1996; Ouillon et al., 1997; Wu et al., 2000; Wilson et al., 2003; Olsen, 2003; Jia et al., 2005; Nagata et al., 2005; Zedler et al., 2006), but their local effects can be approximately accounted for by 2-D models. Reproduction of density currents, often important in certain reservoirs, also requires 3-D models (Kassem et al., 2003). Also the reproduction of the plume of a river requires a 3-D description of its behaviour (Cugier et al., 2002).

Intermediate scale models are extremely sensitive to the boundary conditions, which can be prescribed at the upstream and the downstream ends of the river reach under investigation. Correct boundary conditions for morphological models should be given in terms of sediment input of each grain size fraction and in terms of water depth or bottom elevation (Sieben, 1997). Note that boundary conditions depend, in principle, on what is going on upstream and downstream the reach under consideration. For short-term simulations, sediment input upstream can be evaluated by some hypothesis based on local quasi-equilibrium conditions (Section 2.2.1); the same can be made for water level or bottom elevation downstream. For long-term simulations, however, the behaviour of the entire river system should be explicitly accounted for.

### 1.3.3 Large scale models

Although 1-D models have been sometimes applied to relatively large natural watersheds for specific flood events, not so many examples are available in Literature of morphodynamic modelling at very long (historical or even geological) time-scale, except in few very schematized situations (e.g. simple geometry, constant water flow, uniform grain size composition), as reported in Coulthard et al., 2007 and De Rosa, 2008.

The effects of geometrical, hydrological and sedimentological non-uniformities along the main channel

have not been investigated for long-term, large-scale simulations of natural rivers and relevant watersheds. In fact, averaging non-uniformities in non-linear equations produces various residual terms, which should be properly assessed and eventually modelled only with appropriate sub-models.
It may be interesting exploring the possibilities offered by various long-term morphological models, where the average is performed only over the time. In practice, these large-scale models filter the morphological fluctuations due to short-term components and compute only the long-term evolution of the rivers.
Long-term models have been especially developed for studying the evolution of estuaries (de Vriend et al., 1993; de Vriend, 1996; Dal Monte et al., 2004) or lagoons (Di Silvio et al., 2010b); but these models can, in principle, be applied also to natural river systems.

## 1.4 Morphology of natural rivers

Is possible to analyze the morphology of a natural river is described by the plan and the dimensions of its transversal cross-sections (Leopold et al., 1957; Rosgen, 1994; Garde, 2006).
Variability in the sediment delivery ratio, hydraulic discharge and channel slope give rise to different spatial and temporal variations in channel morphology and river patterns (Montgomery et al., 1998).
Generally, the water tends to arrange itself according to the path which allows the lower loss of energy through friction. This loss of energy occurs along the contact surface between the fluid and the bottom of the river, and so we can observe that the river tends to minimize its wetted perimeter.
The rivers that carry large amounts of coarse material need large channels and current with high velocity to maximize their sediment transport, and so they tend to develop broad and shallow channels; while the rivers which carry finer sediments need lower energy and so develop deep and narrow channels.
The shape of a river channel is a function of two different tendencies: the minimization of the loss of energy by friction and the maximization of the transport capacity of their sediments. The shape, the dimensions and the plan of the riverbed will vary in response to the changes of the water discharge and/or the sediment transport. These adjustements will fluctuate around an equilibrium configuration of the river (Fasolato et al., 2011).
The dominant discharge represents the key feature of a riverbed, because it is considered as the formative discharge of the river patterns. In Literature, it can be considered, as dominant discharge, the bankfull discharge (Parker et al., 2007; Wilkerson et al., 2010).
In our study, instead of the bankfull discharge, we use the equivalent discharge (Ronco et al., 2006) as dominant discharge. The concept and the conputation of the equivalent discharge is analized in detail in the Appendix B.1.

### 1.4.1 Shape of the riverbeds

Most natural rivers have mobile bed, and so their shape varies in response to the variation of the forcing terms (river discharge, geological configuration, geometry, etc.) and the sediments, which form the riverbed and the floodplains. These sediments are subjected to different forms of erosion, transport and deposition (Section 1.2).

The fixed-bed rivers are typical of mountains areas and are enclosed by rocky banks; their transport capacity is more than the presence of the sediments, and so, along these rivers, the deposition is quite negligible.

The mobile-bed rivers are classified on the basis of the following characteristics (Leopold et al., 1957):

- sinuosity of the main channel (ratio between the length of the river and the length of the alluvional valley);
- presence of one single channel or various multiple channels;
- prevailing sediment transport system;
  a) bed load, typical in the braided rivers;
  b) mixed load, typical in the meandering rivers;
  c) suspended load, typical in the anastomosing rivers.

Some descriptions and analysis about the evolution of the river patterns are reported in Literature (Rosgen, 1994; Howard, 1996; Dade et al., 1998; Twidale, 2004; Naiman et al., 2005).

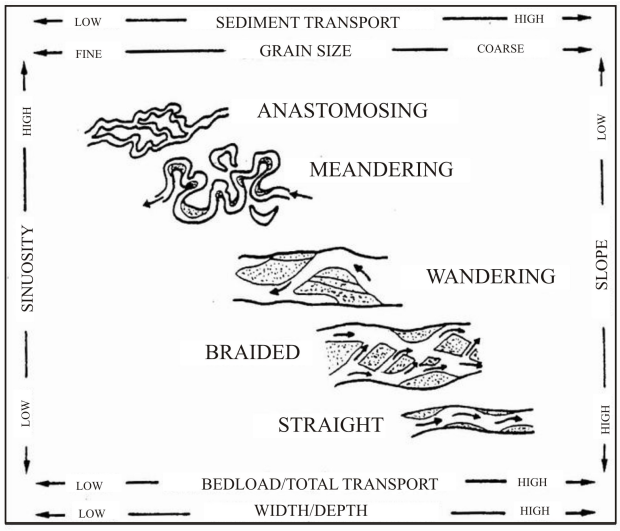


**Figure 1.3:** Classification of the principal shapes of riverbeds.

| riverbed | sediment transport | grain size composition | sinuosity | slope | bedload/ total transport | width/ depth |
|---|---|---|---|---|---|---|
| Anastomosing | ⇓⇓ | ⇓⇓ | ⇑⇑ | ⇓⇓ | ⇓⇓ | ⇓⇓ |
| Meandering | ⇓ | ⇓ | ⇑ | ⇓ | ⇓ | ⇓ |
| Wandering | ⇔ | ⇔ | ⇔ | ⇔ | ⇔ | ⇔ |
| Braided | ⇑ | ⇑ | ⇓ | ⇑ | ⇑ | ⇑ |
| Straight | ⇑⇑ | ⇑⇑ | ⇓⇓ | ⇑⇑ | ⇑⇑ | ⇑⇑ |

**Table 1.1:** Characteristics of the principal shapes of riverbeds.

### 1.4.2 Anastomosing rivers

Anastomosing rivers are composed by two or more stable channels, which have a sinuos path and, in general, we can treat them as meandering channels interconnected. The stability of the channels are favored by the presence of riparian vegetation along the banks.
This morphological configuration, quite rare in nature, seems to be characterized by situations of lower variability of river discharge, lower suspended load and almost total absence of bedload transport (Makaske, 2001).

### 1.4.3 Meandering rivers

The meandering rivers are frequent in the lower floodplains and in coastal zones (e.g. the Lower Zambezi River or the Lower Paraná River). This configuration presents a single river channel deeper than a braided channel and composed by fine sediments (Leopold et al., 1964). The water covers the lower part of the channel during the entire hydrological year. The meandering channel migrate between natural levees within a zone wide 15-20 times the channel. The evolution of the meander occurs trought the erosion of the concave bank and the deposition on the convex bank (Langbein, 1966).
Some case studies and modelling about the formation and the behaviour of a meandering river is reported in Literature (Bradley et al., 1984; Olsen, 2003; Lanzoni et al., 2006; Luchi et al., 2010).

### 1.4.4 Wandering river

The wandering rivers are an intermediate configuration between braided and meandering rivers. These water courses are composed of alternate bars and a single active channel; sometimes they can be present secondary channels, but they become active only with high flow.
The wandering rivers become straight rivers when floods occur and the water covers all the bars.

### 1.4.5 Braided rivers

The braided rivers are present in very different environments and are characterized by floodplains principally composed by gravel, often very large and with relatively high bottom slopes (e.g. the upper reach of the Middle Paraná River).
Their formation is function of high-energy conditions with steep slopes of the riverbed, high and variable discharge, great availability of sediment, high transport capacity of bedload material and non-cohesive banks. The cross-sections are very wide and shallow (the width to depth ratio is generally greater than 40). This allows the activation of secondary water circulations that can promote the formation of various bars along the channel. The formation of a bar begins with the lateral erosion of the banks, that causes an excessive river width, due to the decrease of the local transport capacity of the current, and a small accumulation of sediment into the riverbed. The presence of the bars diverges the main flow, causing further lateral erosion of the banks and thus emphasizing the development of other bars and the enlargement of the main channel. The braided rivers are characterized by great and frequent movement of the bars and the active channels.
In natural rivers we can observe two basic types of bars and their intermediate forms:

- bars subjected to erosion and/or accretion, without vegetation and composed by coarse and non-cohesive material;

- bars that are reached only by extreme events, topographically higher and covered by vegetation, composed by fine and cohesive material, which stabilize the deposits.

Analysis of the behaviour of braided rivers are reported in various studies (Mosley, 1982; Griffiths, 1989; Bristow et al., 1993; Xu, 1996; Gran et al., 2001).

### 1.4.6 Straight rivers

This is a quite rare morphological configuration, because, also if the main channel has a straight path, the current flows into a winding bed, in conjuction with the presence of alternating riffles and pools (Huang et al., 2010).
In nature, the straight reaches are generally less than ten times the total width of the main channel. Channels can be assumed to be essentially straight if the sinuosity (the ratio of centerline arc length to downvalley length) is less than 1.2 (Chitale, 1970).

### 1.4.7 Anabraching rivers

Anabranching rivers consist of multiple channels separated by vegetated semi-permanent alluvial islands excised from exisiting floodplain or formed by within-channel or deltaic accretion. These rivers occupy a wide range of environments from low to high energy, however, their existence has never been adequately explained. They occur concurrently with other types of channel patterns.

Anabranching rivers represent a relatively uncommon, but widespread and distinctive, group that, because of particular sediments, energy-gradient and other hydraulic conditions, operate most effectively as a system of multiple channels separated by vegetated floodplain islands (Nanson et al., 1996).

# Chapter 2

# 1-D Hydro-Morphodynamic Model

## 2.1 Introduction

Morphological processes in river systems (erosion and deposition, variation of bottom profile, evolution of grain size composition) can be described by various 1-D differential equations: for modelling the liquid phase we use the De St. Venant equations and for describing the solid phase we adopt the Exner equation and the Hirano equation.

Even if 1-D models are relatively simple, they present various problems when applied, in their complete form, to long-term simulations at watershed scale. Apart from the complexity of their complete non-linear equations, an other problem is related to the scarcity of extended and accurate informations of the entire river (namely various bathymetric surveys along the water course).

In order to integrate the scarce available topographic data with some supplementary informations, a particular form of 1-D model has been developed, based on the hypothesis that any reasonably portion of rivers can be considered in quasi-equilibrium conditions (Ronco, 2008).

The hypothesis of quasi-equilibrium conditions represents a basis for a theoretical analysis of various problems related to the optimal use of 1-D models, which use a smoothing procedure to averaging the irregularities of the water course, with an acceptable loss of accurancy and resolution. Appropriate averaging operations permits us to increase the size of computational steps both in space and in time, with an important reduction of the numerical effort. On the other hand, space averaging over a sufficiently long river reach permit us to use an approximate 1-D model, which reduces the computational effort and makes possible its application for long-time simulations at watershed scale (Fasolato et al., 2011), as the case of the Zambezi River or the Paraná River.

The effects of averaging operations on spatial irregularities have been investigated, in terms of resolution and accurancy, for 2-D models of floodplains (Gee et al., 1990; Bates et al., 1992; Bates et al., 1995; Hardy et al., 1999) and for physically-based models of watershed slopes (Beven, 1989), but no general criterion has been provided for selecting the most appropriate computational grid size.
In this Chapter we report the general criterion of the "morphological box", necessary to recognize the minimum computational steps, which should be used if the approximate model (quasi-uniform flow) is applied instead the regular 1-D model (quasi-steady flow), as proposed by Ronco, 2008.

## 2.2 Mathematical structure of the 1-D model

The complete 1-D hydro-morphodynamic model is consituted by a system of differential equations, which expresses:

- the continuity equation of the water flow (eq. 2.1);
- the energy balance along the stream (eq. 2.2);
- the overall sediment balance between the stream and the bottom, expressed by the Exner equation (eq. 2.4);
- the sediment balance of each granulometric class present in the mixing layer of the bottom, computed by the Hirano equation (Hirano, 1971) (eq. 2.5).

$$\frac{\partial Q}{\partial x} + \frac{\partial A}{\partial t} = 0 \tag{2.1}$$

$$\frac{\partial}{\partial x}\left(H + Z + \alpha_c \cdot \frac{Q^2}{2g \cdot A^2}\right) = -\frac{\beta_c}{g} \cdot \frac{\partial U}{\partial t} - j \tag{2.2}$$

$$U = \frac{Q}{A} \tag{2.3}$$

where $Q$ is the river discharge, $A$ represents the wetted area of the cross-section, $x$ is the distance along the river, $t$ indicates the time step, $H$ is the water depth, $Z$ is the bottom elevation of the river respect to

a datum, $U$ represents the velocity of the current (eq. 2.3), $g$ is the acceleration due to the gravity and $j$ indicates the energy slope.
The coefficients $\alpha_c$ and $\beta_c$, accounting for the energy and momentum distribution on the cross-section (Coriolis forces), are assumed here both equal to one.

$$\sum_{i=1}^{N} \frac{\partial P_i}{\partial x} = -B \cdot \frac{\partial Z}{\partial t} \tag{2.4}$$

where $P_i$ is the solid discharge of the $i$-th class of sediment ($i$=1, 2, ..., N) and $B$ is the width of the active channel.

$$\delta \cdot B \cdot \frac{\partial \beta_i}{\partial t} = -\frac{\partial P_i}{\partial x} \cdot \beta_i^* \cdot \frac{\partial Z}{\partial t} \tag{2.5}$$

where $\delta$ is the thickness of the active layer, $\beta_i$ is the percentage of the $i$-th grain size class $d_i$ present in the active layer and $\beta_i^*$ is the percentage below the active layer, assuming different values during the erosion or deposition phase.
The following expressions describe:

- the hydraulic resistance of the water flow, expressed by the Chézy equation (eq. 2.6);
- the sediment transport of each grain size class, under the hypothesis of immediate adaptation of the solid transport to the local condition, expressed by an equation of the Engelund-Hansen type (Engelund et al., 1967) (eq. 2.7);
- the Hiding-Exposure effect for each grain size class $d_i$, which reduces the larger mobility of smaller particle and vice versa, expressed by the Egiazaroff equation (Egiazaroff, 1965) (eq. 2.8).

$$Q = U \cdot B \cdot H = \chi \cdot H^{3/2} \cdot B \cdot \sqrt{j} \tag{2.6}$$

where $\chi$ indicates the resistance coefficient of the river.

$$P_i = \alpha' \cdot \beta_i \cdot \xi_i \cdot \frac{Q^m \cdot j^n}{B^p \cdot d_i^q} \tag{2.7}$$

$$\xi_i = \left[ \frac{d_i}{\sum_{i=1}^{N} \beta_i \cdot d_i} \right]^s \tag{2.8}$$

where the coefficient $\alpha'$ is proportional to the ratio between the sediment transport and the flow discharge along the river and the exponents $m$, $n$, $p$, $q$, $s$ depend on the category of river under consideration, and are computed from some experimental analysis (Di Silvio, 2006).

### 2.2.1 Simplifications of the water flow equations

The continuity equation (eq. 2.1) and the energy equation (eq. 2.2) may be subjected to a series of simplifications, if the flood hydrograph is relatively flat compared with the energy slope $j$, as the case of most large rivers.
This condition corresponds to assuming the expression:

$$\frac{\partial Q}{\partial x} = \frac{2}{3} \cdot \frac{1}{U} \cdot \frac{\partial Q}{\partial t} \tag{2.9}$$

instead of the eq. (2.1), by assuming the kinematic wave hypothesis, and to dropping the time-depending term in eq. (2.2), under the hypothesis of quasi-steady water flow.

$$\frac{\partial}{\partial x} \left( H + Z + \alpha_c \cdot \frac{Q^2}{2g \cdot A^2} \right) = -j \tag{2.10}$$

A stronger simplification consists in the assumption of the instantaneous propagation of the liquid phase, expressed by the following equation, instead of the eq. (2.9).

$$\frac{\partial Q}{\partial x} = 0 \tag{2.11}$$

Another simplification consists in assuming the equivalence between the bottom slope and the energy line slope, under the hypothesis of quasi-uniform water flow, instead of the eq. (2.10).

$$\frac{\partial Z}{\partial x} = -j \tag{2.12}$$

The eq. (2.11) is acceptable if the distance between two main tributaries of the river is relatively short compared to the length of the principal wave of a typical flood event (Fasolato, 2008).
The eq. (2.12) is valid for a relatively long flood hydrograph provided that the river channel is prismatic

and the bottom slope is uniform. If the river channel geometry is irregular, the local energy line slope and the local bottom slope are not the same, but we can analyze the river averaging over appropriate length (namely the concept of the morphological box).

A theoretical analysis of the hypothesis of Local Uniform Flow is reported in Literature (Fasolato et al., 2011).

### 2.2.2 The equivalent uniform river reach

For analyzing the morphodynamic evolution of a river reach at watershed scale is useful to introduce the concept of the equivalent uniform river reach.

A short portion of a river between the confluence of two main tributaries conveys a water discharge $Q$. If this portion is much shorter than the flood wave length, we may assume than the discharge $Q$ is constant along the river reach (eq. 2.11). For a given cross-section of the river we may define the water elevation $Y(x,t)$, with respect to a datum, the corresponding active river width $B(x,t)$, the cross-section bottom elevation $Z(X,t)$ and the water depth $H(x,t)$.

We can assume that the water flow is the annualy equivalent discharge $Q_{eq}$ (Ronco et al., 2009), which conveys the annualy averaged solid discharge $\overline{P_s}$. For this particular discharge we define the equivalent uniform river reach, as the rectangular channel characterized by the averaged values along the reach of the active river width $\overline{B}$, the water depth $\overline{H}$, the bottom composition $\overline{\beta_i}$ and the bottom slope $\overline{i_b}$ equal to the energy line slope $\overline{j}$.

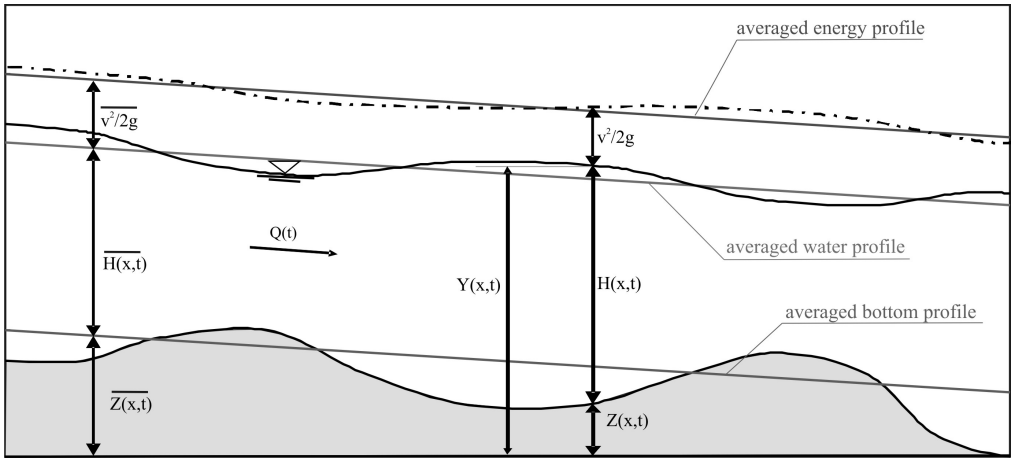


**Figure 2.1:** Scheme of the Local Uniform Flow simplifications.

The above quantities are mutually related by the empirical expressions of water flow (eq. 2.6) and

sediment transport (eq. 2.7) as a function of the energy slope.

$$\overline{Q} = \overline{U} \cdot \overline{B} \cdot \overline{H} = \chi \cdot \overline{H}^{3/2} \cdot \overline{B} \cdot \sqrt{\overline{j}} \tag{2.13}$$

$$\overline{P_s} = \sum_{i=1}^{N} \overline{P_i} = \alpha^{'} \cdot \beta_i \cdot \xi_i \cdot \frac{\overline{Q}^m \cdot \overline{j}^n}{\overline{B}^p \cdot d_i^q} \tag{2.14}$$

### 2.2.3 Equivalent discharge

The notion of the equivalent river discharge is related to the hypothesis of Local Uniform Flow, by the parallelism between the averaged bottom slope $\overline{i_b}$ and the averaged energy line slope $\overline{j}$ (eq. 2.12).
This discharge, indeed, is defined as the constant water flow which conveys the solid discharge $\overline{P_s}$, corresponding to the annual sediment yield of the river reach.
The mathematical formulation of the equivalent discharge is reported in the Appendix B.1.

# Chapter 3

# Synthetic representation of river cross-sections

## 3.1 Introduction

During the past centuries the dynamics of many fluvial systems have been affected by human impact. Several studies (Marchetti, 2002; Surian et al., 2003; Naiman et al., 2005; Kramer et al., 2008) have analyzed the morphological response of rivers to anthropogenic disturbances (water utilization, gravel mining, construction of dams, etc.), showing that important variations take generally place not only along the water course (such as changes of bottom profile and grain size composition), but also across the river section (such as cross-sections width and density of the riparian vegetation).

Important studies are related to the effects of human alteration on river systems: they concern the analysis of the impact in terms of hydrology (Magilligan et al., 2005), morphology (Simon, 1989; Hupp et al., 1991; Church, 1995; Kondolf, 1997; Brandt, 2000; Davies et al., 2000; Surian et al., 2003; Zhou et al., 2004; Petts et al., 2005; Zaghloul, 2006; Wang et al., 2007) or ecology (Baxter, 1977; Bonetto et al., 1989; Gordon et al., 2006; Tealdi et al., 2011). These works are mostly related to a small detailed scale, although we are often interested in the evolution of the entire river basin over a long period of time.

River modelling should take into account the interactions between three principal factors: hydrodynamics, morphodynamics and biodynamics (growth and reduction of the riparian vegetation), which, in principle, have 3-D (Wilson et al., 2005; Li et al., 2009) or, at least, 2-D features (Rosatti et al., 2008).

Different studies show that the riparian vegetation is greatly influenced by the fluvial hydrological regime, through the control exerted by the river on water table depth, flooding and hyporheic fluxes (Micheli et

al., 2002a; Mitsch et al., 2007). The spatial patterns of riparian vegetation are an indication of this strong influence: sparse vegetation is principally associated with high river discharge variability, while uniform vegetation is mainly typical of more regulated river (Camporeale et al., 2006). Where present, vegetation modifies or contributes to determine width, height and stability of the river surface. The elevation of the considered surfaces above the channel bottom, the corresponding stream velocity and turbulence during floods and the sediment sizes forming these surfaces, appear to influence (and be influenced by) riparian vegetation growth (Osterkamp et al., 1984).

Various studies (Osterkamp et al., 1984; Hupp et al., 1985) determine the relationship between riparian vegetation patterns and fluvial landforms, while other studies (Mahoney et al., 1998) identify the geomorphological features of locations in which seedlings are most likely to germinate and survive. The riparian species are sorted along the river in relation to the gradient of the water table and the flow discharge (Bendix et al., 2000).

Some field works (Friedman et al., 1999; Johnson, 2000; Auble et al., 1994; Lite et al., 2005) have shown that the river discharge and the depth of the water table are the fundamental mechanisms for controlling the growth of the riparian vegetation. Flood events cause the inundation of a plot, during which a vegetated site is submerged by the stream. Riparian vegetation may benefit from floods, which supply moisture, seeds and nutrients (Naiman et al., 1997; Tewari et al., 2003), but floods are often related to negative impacts on vegetation, due to physical damage (Yanosky, 1982), uprooting and sediment removal (Osterkamp et al., 1987), anoxia (Kozlowski, 1984; Naumburg et al., 2005) and burial (Hupp, 1988; Friedman et al., 1999), as well as vegetation loss due to bank retreat.

The random time variability of the river hydrology plays a crucial role in the evolution of the riparian vegetation (Tockner et al., 2000; Stromberg, 2001; Steiger et al., 2005). By the same token, also the random spatial variability of the river morphology acts in the same direction.

Some conceptual qualitative models (McKenney et al., 1995; Richter et al., 2000; Gurnell et al., 2001) and regression analysis between the growth of the vegetation and the river discharge (Stromberg et al., 1991) or the duration of the inundation (Franz et al., 1977; Auble et al., 1994) account for probabilistic aspects of hydrological variability, but these models do not address riparian vegetation dynamics using an approach that is both probabilistic and processes based. On the other hand, the lack of analytical approaches limits the study of the riparian vegetation to numerical simulations (Pearlstine et al., 1985; Brookes et al, 2000; Lytle et al., 2004).

Recent studies have the aim to simulate the stochastic dynamics of the riparian vegetation by using simplified approaches related to the hydrological constraints typical of a river system (Camporeale et al., 2006; Muneepeerakul et al., 2007; Camporeale et al., 2010; Tealdi et al., 2011).

In many cases, river evolution needs to be investigated in space and time, respectively at watershed scale and over long-time simulations. For this purpose, in the present study we have transferred some of the cited concepts into a numerically fast 1-D hydro-morphodynamic model to describe water and sediment movement along the river (Di Silvio et al., 1989). This model, based on the LUF (Local Uniform Flow) hypothesis, has been throughly discussed and validated in Fasolato et al., 2011, as reported in the Chapter 2. Moreover, the 2-D aspects of hydrological, morphological and vegetational processes are taken into account by a cross-section sub-model of the river profile and its vegetation cover. The entire model, however, is basically 1-D, being the evolution of the river cross-section solely controlled by the longitudinal variations of some variables. A first version of the model (Di Silvio et al., 2010a) has been substantially improved here, especially in the part regarding the computation of the vegetated cross-section, the description of the active river width and the analysis of the growth of the riparian vegetation.

It is important to note that the basic 1-D model runs at multiannual time-scale ($\tau$) and simulates the long-term evolution at historical or geological scale. The quasi 2-D sub-model describes the hydrological and vegetational changes at sub-annual (seasonal) time scale ($t/\tau$), but the transversal morphological evolution is also represented at the multi-annual time-scale ($\tau$) like the longitudinal morphological evolution.

The next image (Figure 3.1) summarizes the interactions between the main forcing factors incorporated in the quasi 2-D model (left side) and in the 1-D model (right side). As we will see more in detail in the following, the flow-duration curve (hydrology) influences both the shape of the river cross-section (morphology) and the carrying capacity of the vegetation (biology); on the other hand, the carrying capacity and the cross-section profile control together the presence of grass, shrubs and trees (riparian vegetation). As riparian vegetation represents an obstacle that determines the active river width, its density clearly reflects on the river water flow (hydraulics); but, on the same time, it is also affected by the flow characteristics, e.g. by its velocity (capacity of extirpation). The interactions between hydraulics and longitudinal morphology are accounted for by the model at multi-annual scale (1-D morphodynamics); this last model also controls the general configuration of the cross-section profile (quasi 2-D morphology) through an overall morphological parameter (e.g. the one proposed by Leopold et al., 1957).

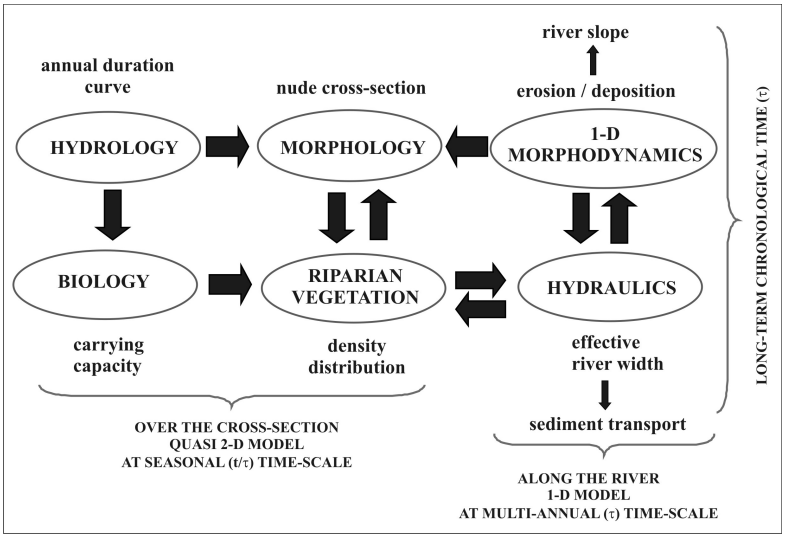


**Figure 3.1:** Principal interactions present in a river system at different time-scale

## 3.2 Hydrological forcing: flow-duration curve

From the previous Figure 3.1 one notes that hydrology is the only totally external driving force, namely not influenced by the other ones.

Hydrology may be represented by the three-parameters flow duration curve:

$$Q(t/\tau) = [Q_{max}(\tau) - Q_{min}(\tau)] \cdot e^{-\gamma(\tau)\cdot\frac{t}{\tau}} + Q_{min}(\tau) \tag{3.1}$$

with the variability coefficient $\gamma(\tau)$ expressed by:

$$\gamma(\tau) = \frac{Q_{max}(\tau) - Q_{min}(\tau)}{Q_{mean}(\tau) - Q_{min}(\tau)} \tag{3.2}$$

where $Q_{max}(\tau)$ is the maximun annual flow, $Q_{min}(\tau)$ represents the minimum annual flow and $Q_{mean}(\tau)$ indicates the mean annual discharge. These three quantities generally oscillate from year to year ($\tau$), and may also be subject to both anthropic and natural long-term modifications.

## 3.3 Morphological forcing: nude cross-section profile

Let us recall that the application of the pure 1-D model under LUF hypothesis (Nones et al., 2009; Ronco et al., 2010) only requires to know the active river width (namely the width free from vegetation conveying

the transported sediments), used to compute the annual sediment discharge with the selected transport formula. This width was assumed to be constant at the long-term time-scale $\tau$ as well as the seasonal time-scale $t/\tau$, and was somehow assessed as on average of the satellite images.

With our approach, the water width is not considered constant anymore, but depending on the water flow duration curve $Q(t/\tau)$. In surveyed rivers the active width is defined to be the one corresponding to the equivalent discharge $Q_{eq}(\tau)$ (Ronco et al., 2009), computed by a 1-D water flow model assuming a completely nude cross-section (bare soil) with a correspondingly low hydraulic resistance. In absence of vegetation (as it would be in laboratory conditions), the active width coincides with the total one, while the shape of the cross-section is exclusively controlled by the morphodynamic processes. We shall then assume that the active width depends on some flow-related quantities, for example the river discharge $Q(t/\tau)$ (eq. 3.1). Note that the active width $B[Q(t/\tau)]$ computed from the surveyed nude cros-section would be much wider if one applies a more realistic resistance coefficient which would account for the vegetation (very likely present in the real cross-sections).

In any case, we will assume that, as suggested by various Authors (Bhowmik et al., 1979; Yalin, 1992; Singh, 2003; Parker et al., 2007; Vianello et al., 2007; Valiani et al., 2009; Wilkerson et al., 2010), the active river width of any cross-section may be expressed as:

$$B(t/\tau) = \alpha \cdot Q(t/\tau)^{\beta} \tag{3.3}$$

In any surveyed nude cross-section the coefficient $\alpha$ and the exponent $\beta$ can be directly computed by fitting the topographic measured data with the corresponding river discharges. With this purpose, a great number of surveyed highland, lowland and piedmont rivers (mostly from territories with moderately humid temperate climate, namely Italian rivers) have been subject to a 1-D steady-flow computations by the numerical code Hec-Ras 4.1 (US Army Corps of Engineers, 2010), under the hypothesis of no vegetation (as in laboratory conditions) and with a resistance coefficient $\chi$=50 $m^{1/2}/s$, according to the Chézy formulation.

In the case of unsurveyed rivers, it is possible, in principle, to determine the river width from satellite images, as they are usually available at different dates and hours for different flow conditions of the river. Therefore the total width $B_{tot}[Q(t/\tau)]$ is known for different discharges, as for the case of surveyed rivers. The important difference, however, is that in a topographic survey the total width $B_{tot}(t/\tau)$ coincides with the nude cross-section (no vegetation), while in satellite images $B_{tot}(t/\tau)$ includes both the active width $B(t/\tau)$ and the vegetated width $B_{sv}(t/\tau)$ (eq. 3.4), because we can not directly distinguish the submerged vegetation from the water surface. For determining the vegetated width (eq. 3.4) we developed an iterative

method (Appendix C.7), based on the concept of the vegetational carrying capacity, described in the following sections.

$$B_{sv}(t/\tau) = B_{tot}(t/\tau) - B(t/\tau) \tag{3.4}$$

## 3.4 Biological forcing: riparian vegetation

For simulating the dynamics of the riparian vegetation, it is necessary to quantify its interactions with the most important constraints imposed by the river (hydrology and morphology) (Francis et al., 2005). These interactions will be described by introducing the concept of the "carrying capacity" of the vegetation (Murray, 2002; Molles, 2008; Yukalov et al., 2009). A general definition of the carrying capacity at the ecosystem level could be "the level to which a process or variable may be changed within a particular ecosystem, without driving the structure and function of the ecosystem over certain acceptable limits" (Duarte et al., 2003). In particular, the carrying capacity of a biological population in a given environment is the population size that the environment can sustain indefinitely, given the food, habitat, water and other necessities available in the environment. In population biology, the carrying capacity is defined as the maximal load of the environment (Hui, 2006), which is different from the concept of population equilibrium, as reported in Gabriel et al., 2005. In other words, the carrying capacity of an environment is its maximum persistently supportable load (Carton, 1986).

In the present contest, the aggregate carrying capacity $K(t/\tau)$ is an intrinsic feature of the riparian area, depending on the constraints locally acting, defined as the "actual" percentage of vegetation cover with respect to the vegetation cover in "optimal" conditions (here assumed as 100%, i.e. total cover, corresponding to no constraints). We define the vegetation cover as the overall riparian population (grass, shrubs and trees) prevailing in the specific morpho-climatic conditions, with no distinction of species and age classes. Constraints consist in all the typical disturbances present in the riparian area.

Each disturbance $i$ ($i$=1,2,...,$n$) affects the single carrying capacity $K_i(t/\tau)$ depending on the water flow and, therefore, on the corresponding submergence time (or flow duration) $(t/\tau)$. For this reason the aggregate carrying capacity $K(t/\tau)$ is defined as the productory of the $n$ carrying capacities corresponding to the contribution of each single time-depending disturbance $i$, such as flood, drown, drought, lateral erosion, flow velocity, ice, salinity, etc.

$$K(t/\tau) = \prod_{i=1}^{n} K_i(t/\tau) \tag{3.5}$$

For defining the effects of the river constraints on the riparian vegetation, it is more convenient to define the single damage $\Delta_i(t/\tau)$ as the complement to one of the corresponding single carrying capacity $K_i(t/\tau)$.

$$\Delta_i(t/\tau) = 1 - K_i(t/\tau) \tag{3.6}$$

In this way it is possible to express each component of the carrying capacity via the corresponding value of the single damage and the aggregate carrying capacity as:

$$K(t/\tau) = \prod_{i=1}^{n} K_i(t/\tau) = \prod_{i=1}^{n} [1 - \Delta_i(t/\tau)] \tag{3.7}$$

Not so many quantitative informations are available in Literature for expressing the aggregate carrying capacity $K(t/\tau)$, or the aggregate damage $\Delta(t/\tau)$, of the riparian areas as defined above (Karrenberg et al., 2002).

In this work we evaluate the aggregate carrying capacity (eq. 3.5) as the combined action of the four chief damages, related to hydrology and morphology, invariably acting in a certain cross-section of the river: anoxia, wilting, extirpation and erosion of the lateral banks.

Each damage $\Delta_i(t/\tau)$ is assumed to be related to specific hydrological and morphological quantities.

- $\Delta_A$ (Anoxia), linearly depending on the submergence time;
- $\Delta_W$ (Wilting), linearly depending on the vertical distance of the free surface from the water table;
- $\Delta_E$ (Extirpation), linearly depending on the unit power of the current;
- $\Delta_B$ (Bank erosion), linearly depending on the river propensity to braiding, expressed by the width to depth ratio.

### 3.4.1 Damage by Anoxia

For a simpler evaluation the exponential duration curve of the water flow (eq. 3.1) has been transformed in an equivalent power curve:

$$Q(t/\tau) = \left[\left(1 - \frac{t}{\tau}\right) \cdot (Q_{max}(\tau)^q - Q_{min}(\tau)^q) + Q_{min}(\tau)^q\right]^{\frac{1}{q}} \tag{3.8}$$

where the submergence time $t/\tau$ is expressed as:

$$\frac{t}{\tau} = 1 - \frac{Q(t/\tau)^q - Q_{min}(\tau)^q}{Q_{max}(\tau)^q - Q_{min}(\tau)^q} \tag{3.9}$$

and the exponent $q$, related to the median discharge $Q_{50}(\tau)$, is computed by the equation:

$$q(\tau) = \frac{1.38}{\gamma(\tau)} = 1.38 \cdot \left[ \frac{Q_{mean}(\tau) - Q_{min}(\tau)}{Q_{max}(\tau) - Q_{min}(\tau)} \right] \tag{3.10}$$

where $\gamma$ (eq. 3.2) represents the coefficient of hydrological variability of the river.
By assuming a linear relationship between damage and submergence time (eq. 3.9), the single damage due to anoxia is:

$$\Delta_A(t/\tau) = \delta_A \cdot \left[ 1 - \frac{Q(t/\tau)^q - Q_{min}(\tau)^q}{Q_{max}(\tau)^q - Q_{min}(\tau)^q} \right] \tag{3.11}$$

The single carrying capacity due to anoxia is computed with the expression:

$$K_A(t/\tau) = 1 - \Delta_A(t/\tau) \tag{3.12}$$

When the river discharge is maximum, with time $t/\tau$=0, the damage due to the anoxia is negligible, and the carrying capacity $K_{A,0}$ is equal to one. On the contary, for the minimum discharge, with time $t/\tau$=1, the total damage $\Delta_{A,1}$ attains a maximum, put equal to the marginal damage $\delta_A$, very likely typical of the prevailing vegetational population.

### 3.4.2 Damage by Wilting

The damage $\Delta_W(t/\tau)$ due to the wilting has been assumed here proportional to the distance $H_w(t/\tau)$ of the free surface from the water table (eq. 3.14).
In this model we assume that the water table has the same elevation of the minimum water level in the river.
By assuming the Chézy formula for the active cross-section, the water depth $H[Q(t/\tau)]$ is given by the expression:

$$H(t/\tau) = \left[ \frac{Q(t/\tau)^{1-\beta}}{\alpha \cdot \chi \cdot \sqrt{j}} \right]^{2/3} \tag{3.13}$$

where $\chi$ is the Chézy coefficient and $j$ is the slope of the energy line.
Eq. (3.13) provides the distance (eq. 3.14) and the damage associated to wilting (eq. 3.15).

$$H_W(t/\tau) = H[Q(t/\tau)] - H[Q_{min}(\tau)] \tag{3.14}$$

$$\Delta_W(t/\tau) = \delta_W \cdot \frac{Q(t/\tau)^{\frac{2}{3}(1-\beta)} - Q_{min}(\tau)^{\frac{2}{3}(1-\beta)}}{Q_{max}(\tau)^{\frac{2}{3}(1-\beta)} - Q_{min}(\tau)^{\frac{2}{3}(1-\beta)}} \tag{3.15}$$

$$K_W(t/\tau) = 1 - \Delta_W(t/\tau) \tag{3.16}$$

When the submergence time $t/\tau$ is equal to one ($Q(t/\tau) = Q_{min}(\tau)$), there is no wilting and the carrying capacity $K_{W,1}$ is maximum; while, for the maximum discharge ($t/\tau$=0), the single damage $\Delta_{W,0}$ reaches its maximum, put here equal to the marginal damage $\delta_W$.

### 3.4.3 Damage by Extirpation

The damage $\Delta_E(t/\tau)$ related to the extirpation (uprooting) is assumed here to be proportional to the unit power of the current, namely to $U(t/\tau)^3$.
The velocity of the current $U(t/\tau)$ is expressed by using the Chézy formula:

$$U(t/\tau) = \frac{Q(t/\tau)^{\frac{1-\beta}{3}} \cdot \chi^{2/3} \cdot j^{1/3}}{\alpha^{1/3}} \tag{3.17}$$

The single damage due to extirpation results to be:

$$\Delta_E(t/\tau) = \delta_E \cdot \frac{Q(t/\tau)^{(1-\beta)} - Q_{min}(\tau)^{(1-\beta)}}{Q_{max}(\tau)^{(1-\beta)} - Q_{min}(\tau)^{(1-\beta)}} \tag{3.18}$$

and the corresponding carrying capacity is:

$$K_E(t/\tau) = 1 - \Delta_E(t/\tau) \tag{3.19}$$

When the submergence time is equal to one (minimum discharge), there is no extirpation and the carrying capacity $K_{E,1}$ is maximum, while, for the maximum discharge, the damage $\Delta_{E,0}$ due to extirpation has its maximum, equal to the marginal damage $\delta_E$.

### 3.4.4 Damage by Bank erosion

The last contribution by hydro-morphology to the carrying capacity is related to the lateral bank erosion due to river straying.

The relevant damage $\Delta_B(t/\tau)$ is proportional to the ratio between the active width $B(t/\tau)$ and the hydraulic depth $H(t/\tau)$. In fact, various studies show an important role of this ratio in the two-dimensional bottom stability of rivers and may therefore be assuemd as an indicator of their propensity to braiding. A detailed computation of this ratio is reported in the Appendix C.5.

$$\Delta_B(t/\tau) = \delta_B \cdot \left[\frac{Q(t/\tau)}{Q_{min}(\tau)}\right]^{\frac{5\beta-2}{3}} \tag{3.20}$$

$$K_B(t/\tau) = 1 - \Delta_B(t/\tau) \tag{3.21}$$

When the submergence time $t/\tau$=1 and the river discharge is minimum, the damage $\Delta_{B,1}$ due to the bank erosion is equal to the marginal damage $\delta_B$, while, when the discharge increases, it depends both on the hydrology via the ratio $Q(t/\tau)/Q_{min}(\tau)$ and the morphology, expressed by the exponent $\beta$.

### 3.4.5 Computation of the marginal damages

There is not direct informations available about the single values of the marginal damages, very likely site-specific and depending on both the local morpho-climatic conditions and the corresponding prevailing population. Some informations, however, is available about the maximum aggregate damage, which can be tolerated by the riparian population, in the course of the year, under the combined action of the forcing terms as anoxia, wilting, extirpation and bank erosion.
The maximum aggregate damage (corresponding to the minimum aggregate carrying capacity) reasonably occurs with the extremal hydrological conditions ($t/\tau$=1 and $t/\tau$=0) and can therefore be assimilated to the maximum annual mortality rate, estimated by some Authors equal to 90% (Karrenberg et al., 2002). We may put therefore:

$$\begin{aligned} K_1 &= 1 - \Delta_{i,1}(\tfrac{t}{\tau} = 1) = 1 - \textstyle\prod_{i=1}^{n}(1 - \delta_{i,1}) \cong 0.10 \\ K_0 &= 1 - \Delta_{i,0}(\tfrac{t}{\tau} = 0) = 1 - \textstyle\prod_{i=1}^{n}(1 - \delta_{i,0}) \cong 0.10 \end{aligned} \tag{3.22}$$

It is possible to rewrite the previous equation with the value of each single marginal damage, for each extremal hydrological condition.

$$\begin{aligned} K_1 &= (1 - \delta_A) \cdot (1 - \delta_B) = 0.10 \\ K_0 &= (1 - \delta_W) \cdot (1 - \delta_E) \cdot \left(1 - \delta_B \cdot \left[\tfrac{Q_{max}(\tau)}{Q_{min}(\tau)}\right]^{\frac{5\beta-2}{3}}\right) = 0.10 \end{aligned} \tag{3.23}$$

For computing the values of the marginal damages we can analyze two different configurations:

- no high flow velocity into the river;
- no important variations of the river discharge.

If we assume there is no high flow velocity into the river we can neglect the damage due to extirpation $\Delta_E(t/\tau)$ and bank erosion $\Delta_B(t/\tau)$.
Under these assumptions, the previous eq. (3.23) becomes:

$$\begin{aligned} K_1 &= (1-\delta_A) = 0.10 \\ K_0 &= (1-\delta_W) = 0.10 \end{aligned} \tag{3.24}$$

and so the resulting value of the marginal damages $\delta_A$ and $\delta_W$ are equal to 0.90.
Under the hypothesis of no important variations of the river discharge during the year, we can assume that the damage due to anoxia and to wilting is negligible, and the eq. (3.23) becomes:

$$\begin{aligned} K_1 &= (1-\delta_B) = 0.10 \\ K_0 &= (1-\delta_E)\cdot\left(1-\delta_B\cdot\left[\frac{Q_{max}(\tau)}{Q_{min}(\tau)}\right]^{\frac{5\beta-2}{3}}\right) = 0.10 \end{aligned} \tag{3.25}$$

In this case it is possible to compute the values of the other two marginal damages $\delta_E$ and $\delta_B$: also they are equal to 0.90.
In the following table we have summarize the resulting values of the marginal damages:

| Type of damage | Marginal damage |
|---|---|
| Anoxia | $\delta_A$=0.90 |
| Wilting | $\delta_W$=0.90 |
| Extirpation | $\delta_E$=0.90 |
| Bank erosion | $\delta_B$=0.90 |

**Table 3.1:** Marginal damages for the carrying capacity.

## 3.5 Determination of the active river width

The aggregate carrying capacity $K(t/\tau)$ is the product of the four components $K_i(t/\tau)$ (eq. 3.5) and depends on both the hydrology and the morphology of the river. If we suppose to know the values of the marginal damages related to anoxia $\delta_A$, wilting $\delta_W$, extirpation $\delta_E$ and bank erosion $\delta_B$, as well as the hydrology of the river in terms of maximum and minimum discharge and variability coefficient (respectively $Q_{max}(\tau)$,

$Q_{min}(\tau)$ and $\gamma(\tau)$), we can write the function $K_i(t/\tau)$ (eqs. 3.11, 3.15, 3.18 and 3.20) for any value of the shape factor $\beta$.

As already said in Section 3.3, the exponent $\beta$ of the active river cross-section (eq. 3.3) is not directly known, but it can be found from the definition of the carrying capacity $K(t/\tau)$ as density of the vegetal population in equilibrium, namely:

$$K(t/\tau) = \frac{dB_{sv}(t/\tau)}{dB_{tot}(t/\tau)} \tag{3.26}$$

By considering the relation between the active river width and the water flow (eq. 3.3) and the equation for expressing the submerged river width (eq. 3.4), one finds:

$$K(t/\tau) = 1 - \frac{dB(t/\tau)/d(t/\tau)}{dB_{tot}(t/\tau)/d(t/\tau)} = 1 - \frac{\alpha \cdot \beta \cdot Q(t/\tau)^{\beta-1} \cdot dQ(t/\tau)/d(t/\tau)}{dB_{tot}(t/\tau)/d(t/\tau)} \tag{3.27}$$

The previous equation can be solved by a trial-and-error method, whenever the values of the marginal damages $\delta_A$, $\delta_W$, $\delta_E$ and $\delta_B$ are known or assumed under the hypothesis reported in the Section 3.4.

## 3.6 Long-term evolution of the riparian vegetation

If long-term hydrological conditions are stationary (e.g. if $Q_{eq}(\tau)$ does not vary with $\tau$ from one period to another one), the density of vegetation $P(t/\tau, \tau)$ coincides with the total carrying capacity $K(t/\tau)$; otherwise $P(t/\tau, \tau)$ will vary with $\tau$ and follow $K(t/\tau)$, according to an adaptation process expressed by a logistic curve.

$$\frac{dP(t/\tau, \tau)}{d\tau} = r \cdot P(t/\tau, \tau) \cdot \left[1 - \frac{P(t/\tau, \tau)}{K(t/\tau)}\right] \tag{3.28}$$

where $r$ is the net vegetation growth rate, which is assumed constant in time.

It is to be noted that, in most practical case, the equivalent discharge $Q_{eq}(\tau)$ (eq. B.11) can be considered stationary and equal to, say, its decadic average. However, to explain correctly the pluri-annual cycles of vegetation, eq. (3.28) should be applied.

In equation (3.28), the early, unimpeded net growth rate is modelled by the first term $+r \cdot P(t/\tau, \tau)$. The value of the net growth rate $r$ represents the proportional increase of the population $P(t/\tau, \tau)$ in one unit of time. Later, as the population grows, the second term, which multiplied out is $-r \cdot \left[P^2(t/\tau, \tau)/K(t/\tau)\right]$, becomes larger than the first one as some members of the population $P(t/\tau, \tau)$ interfere with each other by competing for some critical resource, such as food or living space. This antagonistic effect is called

"bottleneck effect", and is modelled by the value of the parameter $K(t/\tau)$. The competition diminishes the combined growth rate, until the value of $P(t/\tau,\tau)$ ceases to grow (maturity of the population).

There are two different steady states or equilibrium states for eq. (3.28), namely $P(t/\tau,\tau)$=0 and $P(t/\tau,\tau)$=$K(t/\tau)$, that is when $dP(t/\tau,\tau)/d\tau$=0. $P(t/\tau,\tau)$=0 is unstable since linearization about it (that is, $P(t/\tau,\tau)^2$ is neglected compared with $P(t/\tau,\tau)$) gives $dP(t/\tau,\tau)/d\tau \approx r \cdot P(t/\tau,\tau)$, and so $P(t/\tau,\tau)$ grows exponentially from any small initial value. The other equilibrium $P(t/\tau,\tau) = K(t/\tau)$ is stable: linearization about it (that is, $(P(t/\tau,\tau) - K(t/\tau))^2$) is neglected compared with $|P(t/\tau,\tau) - K(t/\tau)|$) gives $d(P(t/\tau,\tau) - K(t/\tau))/d\tau \approx r \cdot (P(t/\tau,\tau) - K(t/\tau))$ and so $P(t/\tau,\tau) \to K(t/\tau)$ as $t \to \infty$.

The carrying capacity $K(t/\tau)$ represents the size of the stable steady state population, while $r$ is a measure of the rate at which it is reached; that is, it is a measure of the biological dynamics: we could incorporate it in the time by a transformation from $t$ to $rt$. Thus $1/r$ is a representative time-scale of the response of the model to any change in the population (Murray, 2002).

The ratio $P(t/\tau,\tau)/K(t/\tau)$ is been called "environmental resistance" to population growth. As the size of population, $P(t/\tau,\tau)$, gets closer and closer to carrying capacity $K(t/\tau)$, environmental factors increasingly impede further population growth (Molles, 2008).

# Chapter 4

# Morphological evolution of the Paraná River

## 4.1 Introduction

The aim of the present study is the analysis of the morphodynamic evolution of the Middle and Lower Paraná River occurred during the XX century, in the light of interdecadal climate variability (Maciel et al., 2010) and morphological constrains. These results will be hopefully extended to predict future morphological trends, e.g. due to climatic change.
In this Chapter, after a brief description of the study site, which includes the Paraná River from Corrientes to Villa Constitución (a 865 km long reach), two 1-D numerical models are compared with regards to hydraulic and morphodynamic changes occured along the river:

- Hec-Ras 4.0 by U.S. Army (U.S. Army Corps of Engineers, 2008), widely accepted within the river engineers community, that simulates river hydro-morphodynamics for relative short periods (i.e. from 10 to 100 years), provided that topographic detailed survey of river cross-sections, not always available, especially in case of large rivers, is implemented to represent the watercourse;

- the hydro-morphodynamics model (LUFM), which assumes the validity of the Local Uniform Flow (LUF) hypothesis (Chapter 2) and describes the river evolution at very long time-scale (i.e. from 100 to 1000 years), using a synthetic description of river cross-sections derived from various satellite data (Chapter 3).

The purpose of this study is the analysis of the capacity of the long-term model with the widely used Hec-Ras model and its calibration against a comprehensive data set of one of the largest world rivers, including a topographic survey of 76 cross-sections, level-time series measured at 17 stations along the river, hydrological and sedimentological data taken from Literature (Amsler et al., 2005; Castro et al., 2007) and field data collected along the river reach between San Martin and Rosario during a campaign carried out in 2009 (Guerrero et al., 2011).

We analyze the aggradation-degradation tendencies and the transversal evolution of the river as resulted by Hec-Ras and by LUFM for the XX century, also at the light of various historical maps.

## 4.2 Site of study: the Middle and the Lower Paraná River

The Paraná River is the main tributary of the Plata Basin, which has a total area of about $3.2 \cdot 10^6$ km$^2$. The Plata River is the Ocean inlet of the city of Buenos Aires (Argentina), mainly characterized by fresh waters due to the elevated discharges coming from the Paraná and the Uruguay rivers.

The following figure (Figure 4.1) shows the location of the Paraná River and the studied river reach from Corrientes to Villa Constitución. The Paraná River flows from north to south through Brazil and Argentina for around 5000 km; the area covered by its watershed is about $2.5 \cdot 10^6$ km$^2$; its mean annual discharge is around 12000-15000 m$^3$/s and the total sediment transport is around 130-135$\cdot 10^6$ t/y (Amsler et al., 2005). The river represents one of the most important navigation ways in South America, with a transported cargo around 100 million of tons.

With regards to sediment yield and runoff, the sub-basin contributions are clearly distinct within the Paraguay-Paraná system. The 80% of the runoff comes from the Brazilian Paraná watershed, i.e. the Upper Paraná River; vice versa the 80% of sediments is supplied by the Bermejo River, a western tributary of the Paraguay River (Figure 4.8).

Downstream of the city of Corrientes (Argentina), where is located the Paraguay-Paraná junction, there are no more significant contributions to the river water discharge. For this reason we apply the two models by using only the hydrological data measured at the gauging station of Corrientes.

In any case, the Middle and the Lower Paraná, two reaches of the entire Paraná River with a total length of around 900 km from Corrientes to the Delta, play a key role in the sediment transport processes and related morphodynamics. In fact, clay and silt materials (80% of solid discharge) coming from the Bermejo sub-basin and are transported as wash load and feed, during the flood periods, the Paraná Delta and wetlands, up to 30 km wide plains; while the remaining 20%, i.e. 20-25$\cdot 10^6$ t/y of river bed fine sand is transported as bedload and suspended load and accomplishes to modify the channel morphology (i.e. bed

slope, channel sinuosity and bifurcations).

Previous studies on the morphodinamic evolution of the Paraná River showed different behaviors for the Middle and the Lower Paraná during the last century, although the same yearly averaged streamflow and sediment transport were observed. In particular, the channel sinuosity and the planimetric divagation, inferred from some historical maps, at the Lower Paraná appeared not to be straightforward correlated to the hydrological variability during the XX century, while a more important correlation was observed for the Middle Paraná (Amsler et al., 2005; Castro et al., 2007).

According to past studies (Garcia et al., 1998; Garcia et al., 2002), streamflows and precipitations have the same tendency variations during the last century: in particular, a dry period, lasted nearly 30 years, was observed in the basin in the midst of the century.

Notwithstanding the river basin hydrology and land use changed at the beginning of the 1970s, consistently increasing the annual streamflow regime, historical maps of the 30 km long reach between San Martin and Rosario bear out a continuously and progressive oversimplification of river planimetric morphology (Figure 4.4), toward a lower width to depth ratio. The Lower Paraná River reach did not recover the extremely braided morphology characterizing the beginning of the XX century with a similar hydrology; on the contrary, the midst century morphodynamics is exacerbated. On the other hand, the Middle Paraná recovered the braided morphology of the beginning of the century.

In the present work, the distances of the navigation route from Buenos Aires are used to name the river cross-sections.

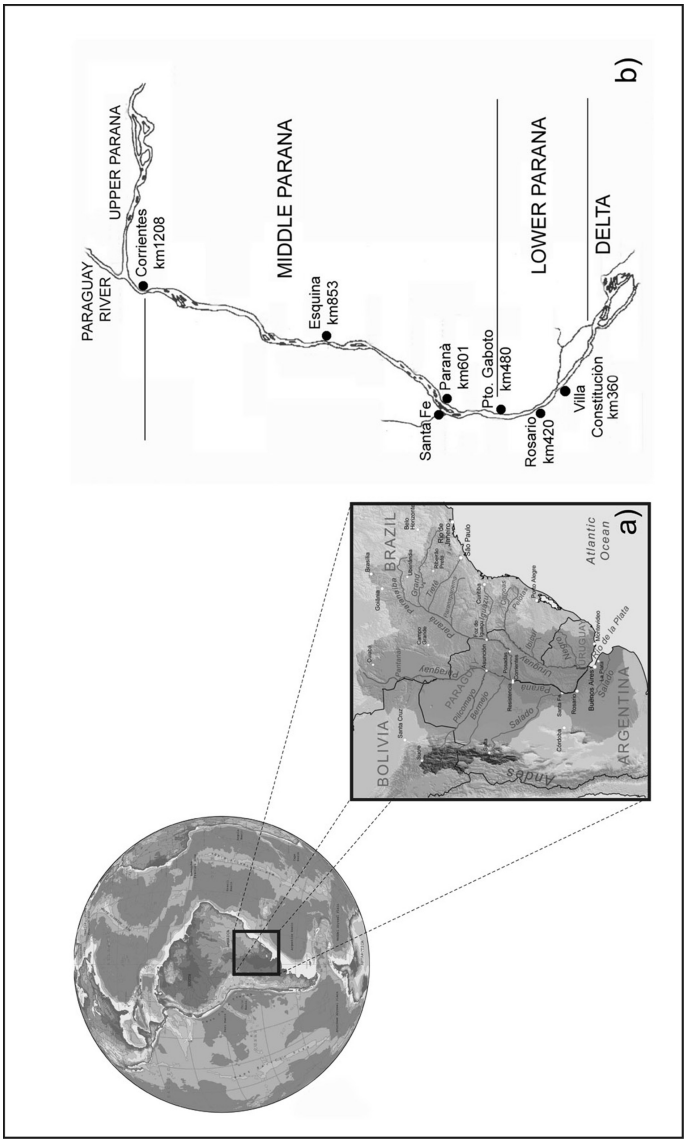


**Figure 4.1:** The Paraná River basin.

## 4.3 Available data

### 4.3.1 Hydrology

Different Authors (Garcia et al., 1996; Garcia et al., 1998; Camilloni et al., 2002; Garcia et al., 2002; Orfeo et al., 2002; Maheu et al., 2003; Amsler et al., 2005; Minetti et al., 2010) notice a great variability of the hydrology along the Paraná River during the XX century.

In the next figure (Figure 4.2) we have reported the monthly river discharge measured at the gauging station of Corrientes, situated at the beginning of the Middle Paraná River (Fig. 4.1). Downstream this station there are not significant contributions from tributaries or other alterations of the river discharge (i.e. reservoirs, agricultural samples, etc.). For these reasons we consider only the monthly discharge measured at the station of Corrientes for our simulations (Section 4.4).

We can observe a humid period between the 1910 and 1930, then a reduction of the river discharge during the dry period 1930-1970 and then an other very humid period from 1970 till now.

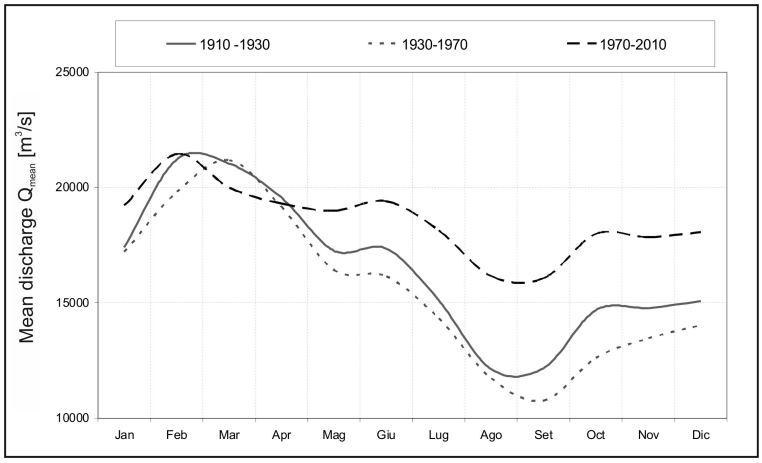


**Figure 4.2:** Variation of the river discharge during the XX century.

### 4.3.2 Geometry

As the case of other large rivers, as the Lower Zambezi River (Chapter 5), we take the geometry of the river from various satellite images. We analyze the Landsat 7 images of the river of the period 1999-2007 taken from the USGS database (USGS, 2011).

For each morphological box we measure the total river width $B_{tot}(t/\tau)$ directly from the satellite images, with a spatial resolution of 8 km (namely about 10 section for each morphological box). For computing the mean river width of the morphological box we make an average of these data over the entire length of the morphological box (80 km). We repeat these operations for each discharge that we analyze (namely for each day of acquisition of the images). In this way we obtain an annual duration curve of the total river width for each morphological box.

As example, in the next figure (Figure 4.3) we have reported two images: one related to the upper part of the river reach, just downstream Corrientes, and another one related to the lower part of the Paraná River, near Villa Consitución. We can notice the braided path of the river downstream the city of Corrientes and a

more straight path in the lower part of the river, upstream the Delta. In these cases the river discharge is quite the same, closer to the median discharge ($Q_{50}(\tau)$ ≈15000 $m^3/s$).

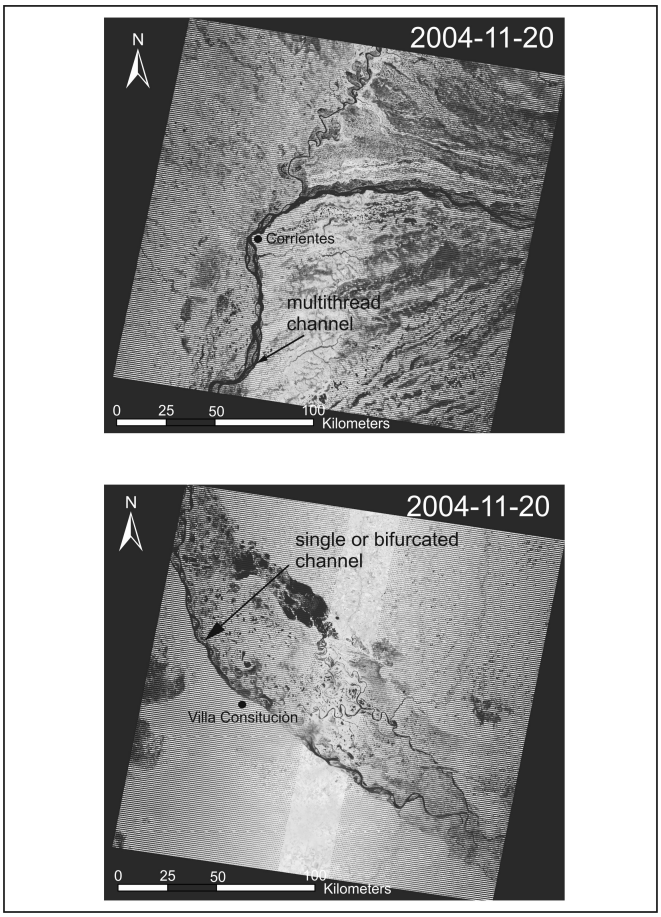


**Figure 4.3:** Satellite images of the reach downstream Corrientes (M.B. 1) ad upstream Villa Constitución (M.B 10).

In the next figure we have reported the morphological changes occurred at the Lower Paraná reach around Rosario and San Martin cities taken from various historical maps supplied by the Instituto Nacional del Agua (*INA*). In bold line we have indicated the later date. The reported navigation distances of inner ports start from the ocean inlet of the Plata River (Castro et al., 2007).

Analyzing these maps, we can observe a continuously and progressive oversimplification of the planimetric morphology of the channel, and the tendency of the Paraná River to becoming more straight from an initial braided configuration. The ratio between the river width and the water depth is decreasing, and the channel is deepening (Claris, 2011).

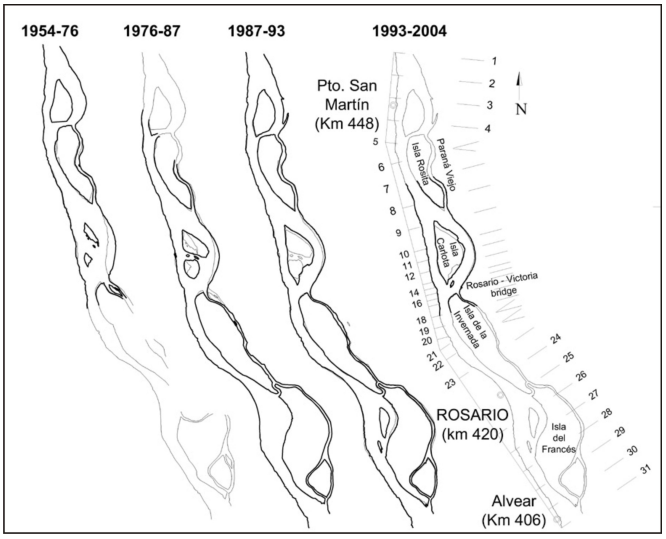


**Figure 4.4:** Morphological changes at Lower Paraná reach around Rosario and San Martin cities (courtesy of Instituto Nacional del Agua).

The bottom slope used in the application of the two models is provided by a bathimetric survey made by the *INA* during the 1970s.

For the application of the simplifications assumed by the LUFM model, the slope of this river reach is averaged over each morphological box, as we can see in the Figure 4.5. The simplifications valid for the LUFM model (Chapter 2 and Chapter 3) permits us to apply this model also to unsurveyed rivers, where is possible to take the bottom slope (or the free surface slope) from a DTM, as reported in the Chapter 5. In this case we adopt the averaged slope derived from the bathymetric survey.

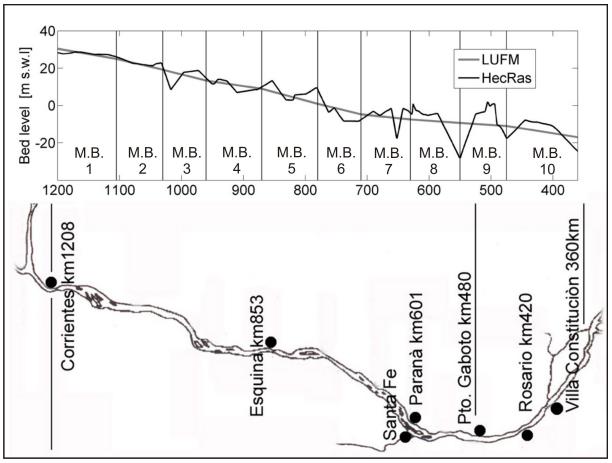


**Figure 4.5:** Initial longitudinal profile for the morphodynamics simulations. Comparison between the values used for the Hec-Ras model and the LUFM model.

### 4.3.3 Grain size composition

The grain size composition of the river is taken from Amsler et al., 2005. The geochemical characteristics of the suspended sediment load is also reported in Depetris et al., 2003.

In the next graph we report the measurements of the mean grain size composition of the river bottom at five gauging stations along the Middle and the Lower Paraná River. The label of the data indicates the distance from the mouth (namely the navigation way). We note that the grain size composition are quite constant along the river, with a median diameter $d_{50}$ of about 0.25 mm.

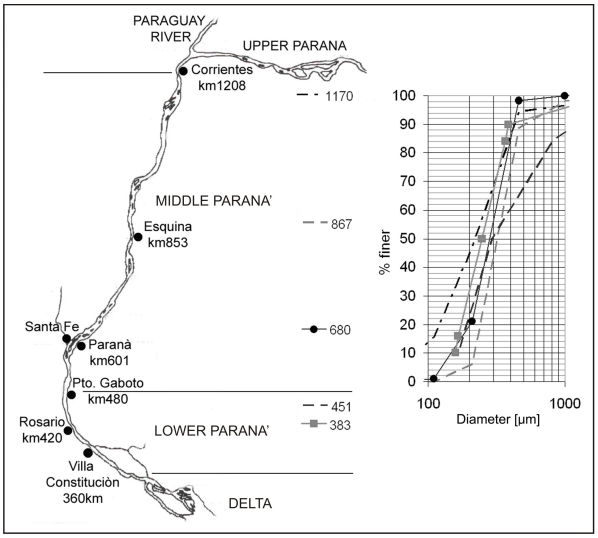


**Figure 4.6:** Sampling points of the granulometric data along the Middle and Lower Paraná River.

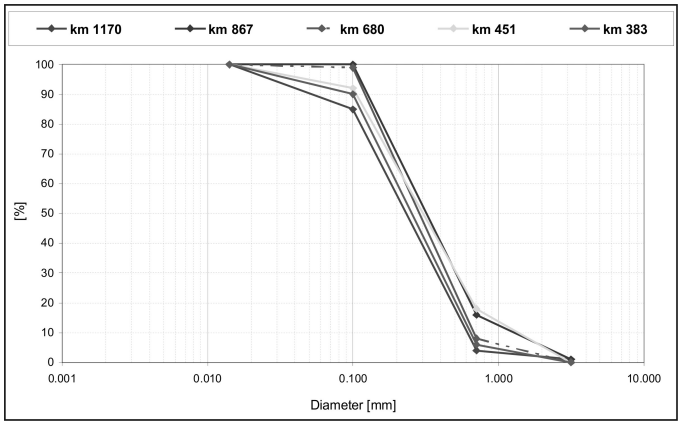


**Figure 4.7:** Computed grain size composition of the sediments in the Middle and Lower Paraná River.

### 4.3.4 Sediment transport

The data about the sediment transport related to the Bermejo River have been measured at the gauging station of Corrientes in the period 1993-2007 (Amsler et al., 2009). Unfortunately, these data, necessary for the calibration of the sediment transport formula (eq. 2.14), are taken only occasionally. For the calibration of the sediment transport formula applied in the LUFM model we have used the data coming from Claris, 2011.

Another analysis of the suspendend sediment along the Middle Paraná River is reported in some other studies (Drago et al., 1988; Alarcón et al., 2003).

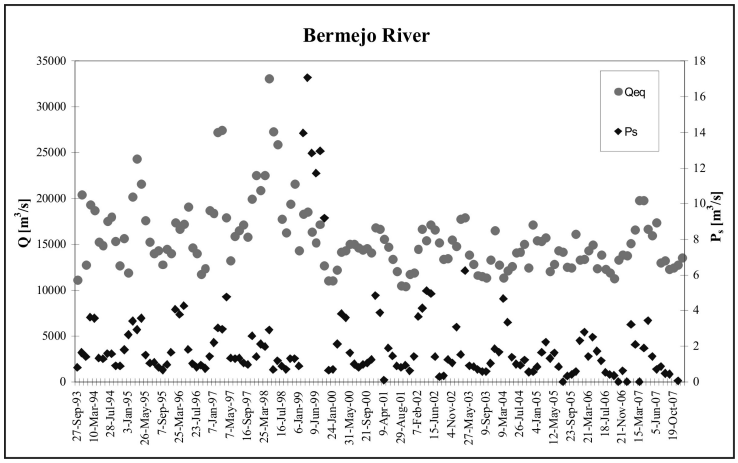


**Figure 4.8:** Sediment transport of the Bermejo River during the period 1993-2007.

### 4.3.5 Riparian vegetation

In Literature there are few data about the vegetation pattern along the Middle and Lower Paraná River. The only available works are referred to the evolution of the vegetation in some islands in the delta of the river (Malvárez, 1999; Kandus et al., 2004; Kalesnik et al., 2008; Kalesnik et al., 2011), but downstream the river reach which we are studing. In this zone the studies suggest that any given site factors, such as hydrologic regime, topographic position and sediment composition, strongly influences both the vegetational zonation and the succession process. Thus, vegetation replacement pathways differ depending on the particular conditions of the site (Kandus et al., 2004).

## 4.4 Comparison between two 1-D models

We will analyze the future evolution of the Paraná river from Corrientes to Villa Costitución (865 km) and so we must calibrate the long-term hydro-morphodynamic model described in the previous Chapters (Chapter 2 and Chapter 3).
We compare two 1-D numerical models:

- the Hec-Ras 4.0 by US Army, which is widely accepted within the river engineers community. This code simulates river hydro-morphodynamics along stream flow mean direction for relative short periods (i.e. 10 to 100 years), but it needs a topographic detailed survey of river cross-sections which is not always available, especially for large rivers;

- our hydro-morphological model, which assumes the validity of the Local Uniform Flow hypothesis (Fasolato et al., 2011) and describes the evolution of the river at very long time scale (i.e. 100 to 1000 years) (Chapter 2), using a synthetic description of the river cross-sections width and their biological behaviour (Chapter 3).

The comparison aims to validate the long term model against the widely tested US army model on a comprehensive data set of one of the largest world river, including topographic cross-sections made by the *INA*, hydrological and sedimentological data taken from Literature (Amsler et al., 2005; Castro et al., 2007) and field data coming from the San Martin-Rosario campaign (Guerrero et al., 2011).

### 4.4.1 The Hec-Ras 4.0 model

The Hec-Ras 4.0 code is a free numerical model, widely used to compute water surface profile and energy line slopes for river dynamics analysis in one dimension. It contains four different components: steady state and unsteady flow computation modules, sediment transport modelling in quasi-unsteady flow state and water quality analysis.
The hydraulics is solved by the continuity equation and the energy equation (De St. Venant eqs.), while the morphodynamic module couples the sediment continuity equation (Exner eq.) to different sediment transport formula.

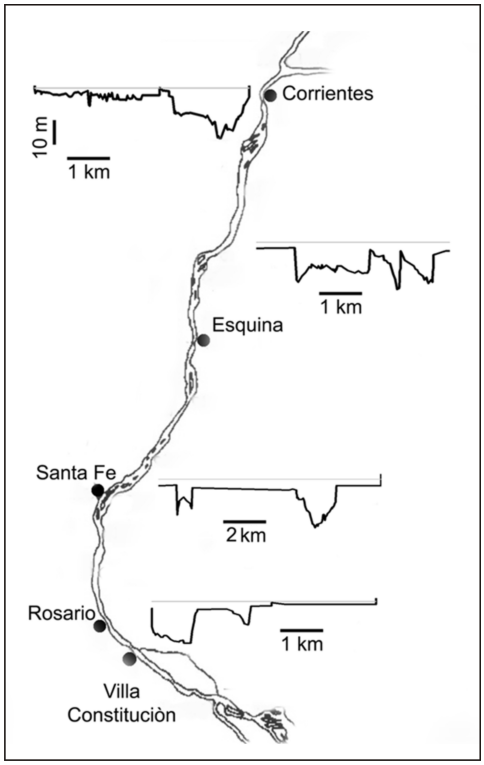


**Figure 4.9:** The modelled reach of the Paraná River and four cross-sections (Corrientes, Esquina, Santa Fe and Rosario), as represented by the Hec-Ras model.

In this application, the river hydrodynamics is calibrated in terms of floodplains width (around 10 km) and bed roughness, equal to 0.025 s/m$^{1/3}$ as order of magnitude, by using measurements of water elevations and free-surface slopes, which are available for the period 1994-1999 at 17 cross-sections.
The 1-D morphodynamics validation is carried out in terms of bed sediment transport rate and effective discharges from Literature (Amsler et al., 2005; Amsler et al., 2007; Castro et al., 2007).
The topographic survey of 76 cross-sections, performed by the *INA* during the 1970s, is used to discretize the river channel in the numerical model, while known time series of level at Villa Constitución (downstream) and at Asunción (upstream, Paraguay) and the rating curve at Ituzaingó (upstream, Upper Paraná) are imposed as boundary conditions.
The water elevations, measured at 17 water stage stations along the river, are used to calibrate and validate the numerical model.
The calibration of the Hec-Ras code achieves a very good agreement between simulated and observed water levels with few small deviations during flood periods, when floodplain enlargements, at some areas, drive two dimensional hydrodynamics, which is not directly simulated by a 1-D model (Figure 4.12).

The morphodynamics module validation at Corrientes (1200 km)-Villa Constitución (350 km) reach follows the carried out hydraulics calibration. The upstream and downstream conditions are respectively the recorded discharge at Corrientes (a monthly time series) and the discharge-water stage relation at Villa Constitución by Evarsa S.A., based on 15 years long period of data:

$$\begin{aligned} Q &= 0.44 \cdot (h + 12.036)^{3.82} && \text{for} \quad h \leq 6m \\ Q &= 567.22 \cdot h^2 + 344.86 \cdot z + 5393.5 && \text{for} \quad h \geq 6m \end{aligned} \tag{4.1}$$

where $h$ is the water stage record.

Furthermore, the equilibrium load is imposed at Corrientes.

The humid period (1970-2000) is simulated in order to validate the total transport formula, by the Engelund-Hansen equation (Engelund et al., 1967), against the Literature data of sediment transport $P_s$ and related effective discharge $Q_{eff}$ (Amsler et al., 2007). The effective discharge $Q_{eff}$ is the flow which cumulates most of the channel bed sediments (Biedenharn et al., 2000), i.e., the product of the interval frequencies and the solid discharges occurring in the interval as assessed for the corresponding hydrological conditions. The sediment transport formula is applied in the model by fixing the grain size distributions as inferred from bed samples at various cross-sections along the studied river reach (Section 4.3.3).

The wash load (clay and silt) coming from the Bermejo River sub-basin is not simulated since it is widely accepted that it does not significantly affect river channel morphodynamics, but the delta consolidation and floodplains accretion.

The results of some river reaches are reported in the following tables in more details, focusing on Middle and Lower part of the river: Villa Urquiza-Paraná city (10 km long) and Diamante-San Martín (85 km long) reaches results are averaged for the Middle Paraná; San Martín-Rosario (30 km long) reach represents the averaged results for the Lower Paraná. The comparison between results from the simulation and various Literature data (Castro et al., 2007) is given in terms of effective discharge (Table 4.1) and in terms of sediment discharge (Table 4.2), for both the Middle and the Lower Paraná.

| $\mathbf{Q}_{eff}$ [m$^3$/s] | | | | |
|---|---|---|---|---|
| | *Middle Paraná* | | *Lower Paraná* | |
| | Computed | Literature | Computed | Literature |
| 1970-1979 | 15000 | 15100 | 16700 | 17500 |
| 1980-1989 | 17000 | 16500 | 20500 | 20500 |
| 1990-2001 | 16800 | 16300 | 20200 | 20400 |

**Table 4.1:** Effective discharge $Q_{eff}$ during the period 1970-2000: comparison between computed and data taken in Literature (Castro et al., 2007).

| $\mathbf{P}_s$ [$10^6$ t/y] | | | | |
|---|---|---|---|---|
| | *Middle Paraná* | | *Lower Paraná* | |
| | Computed | Literature | Computed | Literature |
| 1970-1979 | 23 | 22 | 49 | 41 |
| 1980-1989 | 32 | 28 | 75 | 85 |
| 1990-2001 | 28 | 23 | 58 | 63 |

**Table 4.2:** Sand discharge $P_s$ during the period 1970-2000: comparison between computed and data taken from Literature (Castro et al., 2007).

The Hec-Ras model is also applied to assess the effective discharge for the XX century dry period (1950-1970) revealing important differences in contrast to the humid period.

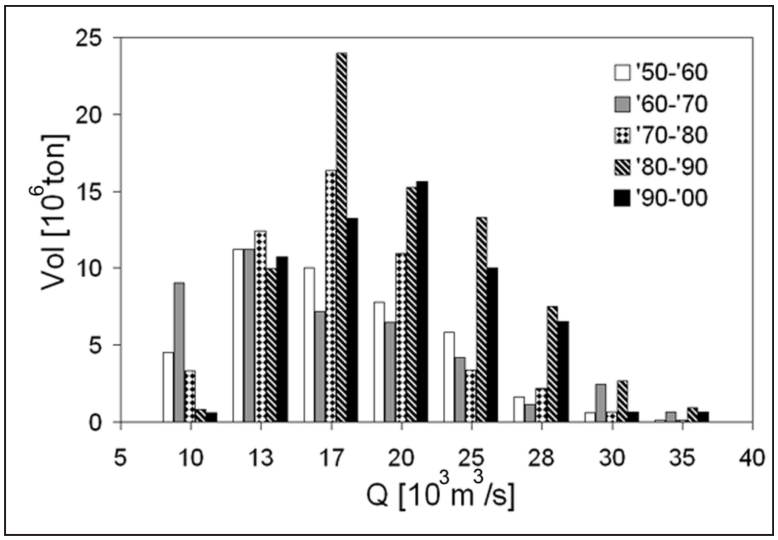


**Figure 4.10:** Period 1950-2000: effective discharge $Q_{eff}$ for the Diamante-Rosario reach.

Finally, the morphodynamic simulation of the XX century provides the occurred variations of the bottom profile (aggradation-degradation process) along the longitudinal axis of river channel from Corrientes to Villa Constitución, which is compared with Local Uniform Flow Morphodynamic model results.
In the following figure we have reported the trend of the top river width computed by the Hec-Ras model. We can observe that the bankfull discharge is around 17000 $m^3/s$; in fact, it is possibile to observe that, over this threshold, the top river widths change their trend in various morphological boxes.

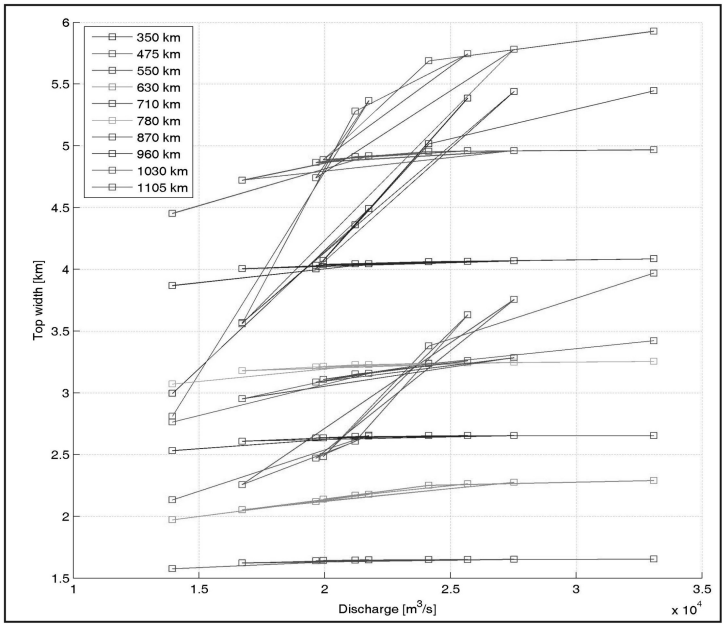


**Figure 4.11:** Top width of the Paraná River simulated by the Hec-Ras model.

### 4.4.2 The Local Uniform Flow Morphodynamic model

The proposed Local Uniform Flow Morphodynamic (LUFM) model (Di Silvio et al., 1989) couples the 1-D equations describing the water flow (i.e. modified De St. Venant Equations) and the equations describing the solid phase (i.e. Exner and Hirano Equations). This model is described in detail in the Chapter 2 and in the Chapter 3.

Conventional numerical models, even if only 1-D, are extremely time-consuming and require extensive and detailed topographic description, especially in case of long-term simulations of large river morphodynamics at watershed scale, as this case. As described in the previous chapter, acceptable simplifications are therefore introduced in the hydraulic equations, such as the kinematic propagation of the water flow and the Local Uniform Flow (LUF) hypothesis, under which the uniform flow is assumed to be fulfilled on average at the appropriate length and duration scales, i.e. the morphological box and evolution window respectively (Chapter 2). A theoretical criterion based on the analytical solution of the morphodynamic equations indicates that the size of these intervals mainly depends on the Froude number and on the perturbation period of the typical flood event (Fasolato et al., 2011). Another detailed description of this hydro-morphodynamic model is reported in Ronco et al., 2010.

For the Paraná River representation (from Corrientes to Villa Constitución) the resulting 10 morphological

boxes (i.e. bounded sub-reaches in Figure 4.5) have a length of about 80 km, while the evolution window is around 15 years.

The next equation (eq. 4.2) (analogous to the Engelund-Hansen formula) is applied to compute the sediment transport $P_s(\tau)$, which is based on the energy slope $j(\tau)$, the river active width $B(\tau)$, the sediment equivalent diameter $d_{eq}(\tau)$, and the equivalent discharge $Q_{eq}(\tau)$, at each morphological box:

$$P_s(\tau) = \alpha^{'} \cdot \frac{Q_{eq}(\tau)^m \cdot j(\tau)^n}{B(\tau)^p \cdot d_{eq}(\tau)^q} \tag{4.2}$$

Since the LUFM model is developed for long-term analysis, the mentioned river features are averaged over long periods $\tau$. For this study, the computed results are representative of the entire studied period 1910-2010.

The exponent $m$ is calibrated by assuming the equilibrium between the long-term means of the equivalent discharge $Q_{eq}(\tau)$ and the sediment transport $P_s(\tau)$ as resulted by averaging the measured time series of river discharge and sediment transport rate (Amsler et al., 2007). The other calibration exponents $n$, $p$, $q$ are function of $m$ and of other river features (Di Silvio et al., 1996b; Ronco et al., 2009). During the simulation, the calibration parameters are maintained as constant, allowing to assess the sediment transport $P_s(\tau)$.

In the present study, the LUFM model is coupled to a quasi 2-D representation of the river cross-section evolution. This sub-model computes the active cross-section width as a function of the discharge and is be applied in the simulation instead of assuming a fixed width (Chapter 3).

Satellite images indicate the multi-thread channel morphology characterizing the Paraná River. As an example, Figure 4.3 reports two analyzed images, one for the Middle Paraná River (downstream Corrientes) and the other one for the Lower Paraná River (upstream Villa Constitución). Multi- or single/bifurcated-thread morphology is observed at upstream part of the river or at the Lower Paraná respectively.

With the aim to compare LUFM and Hec-Ras models, the recent morphological evolution for the entire XX century has been simulated with the same hydrological conditions. While the Hec-Ras model has been applied to the 1970's bathymetric survey assuming the calibrated bed roughness around 0.015-0.035 $s/m^{1/3}$ (Claris, 2011), constant in time, but variable along the river; the LUFM model does not require any calibration, if satellite images corresponding to a given discharge are available.

For the years preceding the 2000 (when only few satellite images are available), the active and the vegetated cross-section have been reconstructed by assuming the same constant value of the coefficient $a$ estimated in the recent time (eq. D.2). An analysis of this parameter is reported in the Appendix D.

## 4.5 Discussion of the results

An important difference between the two models used in this application regards the resistance coefficient, in fact the LUFM model requires a different calibration respect to the Hec-Ras code. Indeed, while in the Hec-Ras model the value of the Manning coefficient obtained by the calibration includes also the effects of the growth of the submerged vegetation with the surveyed (nude) cross-section, these effects are explicitly accounted for by the LUFM code, via the description of the submerged vegetated width in the synthetic cross-section sub-model (eq. 3.4).

The presence of vegetation reflects itself (directly) on the active river width and (indirectly) on the water level. The values of the resistance coefficient of Manning deduced by calibrating the Hec-Ras model against measured water levels are much larger than the values deduced by considering nude the surveyed cross-section.

A comparison between the results of the two models, on the other hand, is complicated by the fact than the necessary quantities for their implementation, calibration and verification have been measured in some different periods of time.

In the case of the Paraná River, for example, we have three different dataset:

- bathymetric survey carried on during the years 1970;
- water level records available for the years 1990;
- numerous satellite images available only after the 2000.

Reasonable hypothesis of "invariance" of the relevant quantities have been made for the two models. For example, for the Hec-Ras model it was assumed that the calibrated Manning coefficients (obtained by comparing the water level measured during the years 1990 to the water level computed with the 1970s bathymetric survey, as reported in Section 4.4.1), would change by section to section along the river, but remain invariant in time. By contrast, in the LUFM model we assume that the morphological coefficient $a$ (eq. D.2) would be invariant in time, although (slightly) variable in space.

In this respect, the comparison between the water levels computed by the two calibrated models and measured in four representative cross-sections (corresponding to the downstream end of the relevant morphological boxes) is reported in Figure 4.12. In this figure the grey line indicates the measured data averaged at monthly scale, the black line represents the monthly water level computed with the Hec-Ras model, while the squares indicate the data modelling by the LUFM code.

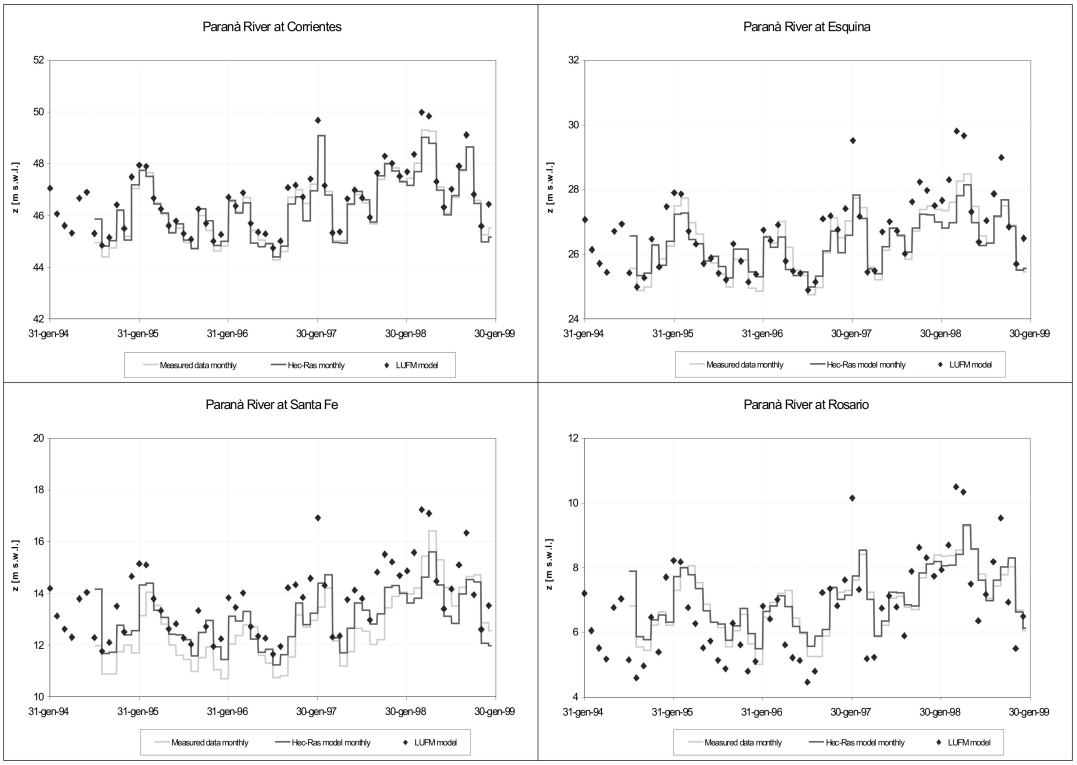


**Figure 4.12:** Comparison between Hec-Ras results and measured data in terms of water elevation at four cross-sections: Corrientes, Esquina, Santa Fe and Rosario.

The following figures report the significant results in terms of hydraulics (Figure 4.13), sediment transport (Figure 4.14), as 100-year averaged quantities, and final morphology (Figure 4.15) of the two models. The LUFM results are consistently comparable to the Hec-Ras box averaged results.

The simulated aggradation-degradation processes along the river appear quite similar for the two model results (Figure 4.15), notwithstanding the Hec-Ras model represents in detail the river cross-sections, with a longitudinal resolution around 10 km, while the LUFM model simplifies the geometry by applying a synthetic cross-section and reproducing the entire simulated reach with only 10 sub-reaches (morphological boxes), around 80 km of length for each one.

Actually, as expected, the simulated contribute to sediment transport by floodplains results negligible in comparison to the active channel contribute, notwithstanding the effect on the hydraulics. In particular, referring to the effective discharges (i.e. in the range 17000-20000 $m^3/s$) and to the active channel, the widths used both in Hec-Ras and LUFM models are similar from Villa Constitución (km 360) to the km 700 station (100 km upstream of Santa Fe), with only an exception in the last morphological box at the Lower Paraná. The upstream part of the river, from the km 700 station up to Corrientes, presents

significantly larger widths for the Hec-Ras model: LUFM model assessments remain lower than the widths computed by the Hec-Ras code. This result reflects the observed multithread morphology at the upstream morphological boxes. The larger width used in the Hec-Ras model also corresponds to a lower hydraulic radius of the active channel, with small deviation in the sub-reaches with similar widths.

The difference between the active widths exhibited by the two models (tendentially larger in Hec-Ras than in LUFM, even below the floodplain elevation), may be explained by the presence of vegetation obstructing part of the entire cross-section indicated by the bathymetric survey or by the satellite images. While the LUFM model explicitly predicts these obstructing portions, the Hec-Ras model compensates the excessive width by a corresponding increase of the resistance coefficient, which implies a respective decrease of hydraulic radius and energy slope.

It cannot be excluded, however, that the Hec-Ras backwater profile (Figure 4.14), has a lesser slope than the uniform flow profile of LUFM, forced to the bed profile. The local difference between energy slope and bottom slope. However, could be somehow accounted for in terms of longitudinal gradient of width, even if has not been made here.

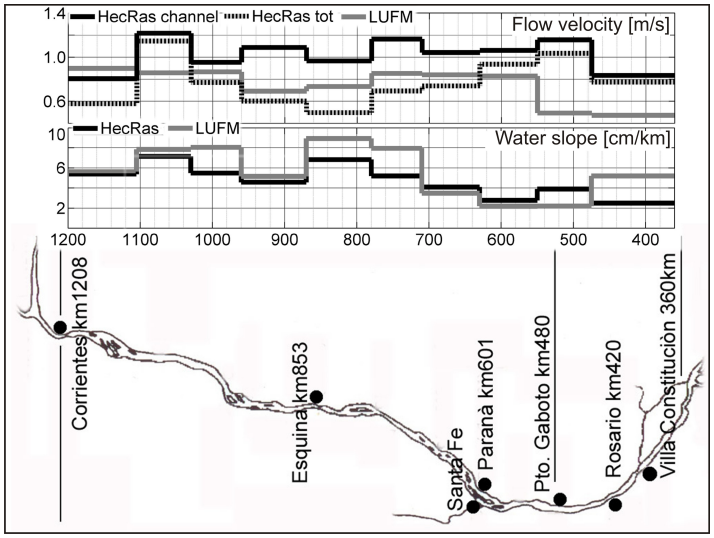


**Figure 4.13:** Comparison of the two models in terms of flow velocity and water slope.

Less obvious is the effect of a larger width (due to neglecting vegetation), assumed by the Hec-Ras model, on the flow velocity (Figure 4.13), the shear stress and the sediment transport (Figure 4.14). Therefore, the difference between the two models appears, in this case, mainly due to the scarce geometrical resolution of the LUFM model.

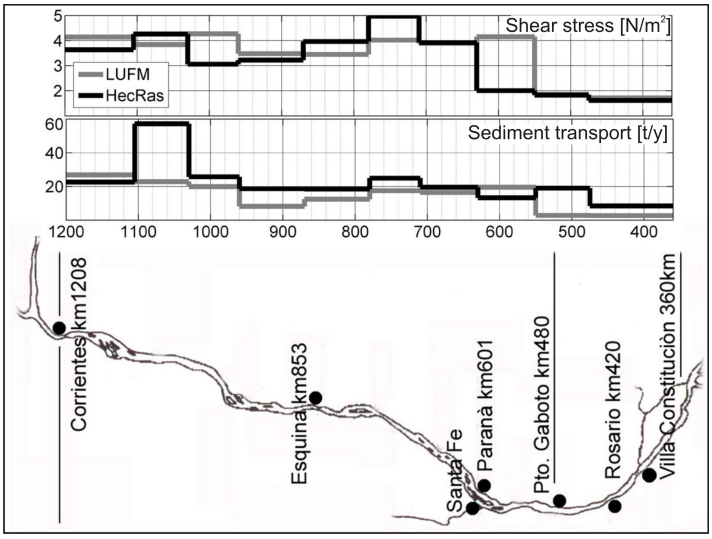


**Figure 4.14:** Comparison of the two models in terms of shear stress and sediment transport.

As shown in the next graph (Figure 4.15), the cumulated bed changes (deposition and erosion) show a good agreement between the two models. The river channel profile is quite stable, but presents different sub-reaches in terms of aggradation or degradation tendency. In particular, both models bear out that the Lower Paraná is characterized by an aggradation-deposition tendency within the XX century, while the Middle Paraná, in the reach between Pto. Gaboto (km 480) and Esquina (km 853), appears quite stable or slightly eroded.

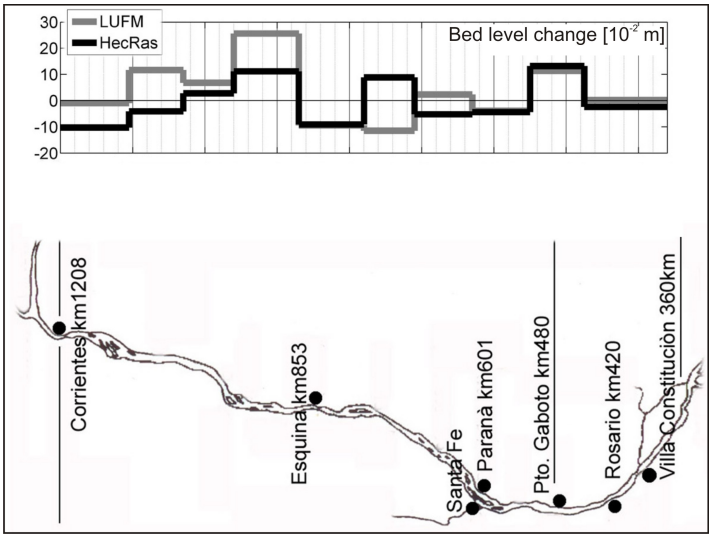


**Figure 4.15:** Comparison of the two models in terms of variation of bed elevation and correlation between river discharge and energy line slope.

The variability of the bed level along the river contributes to explain the different morphodynamics processes as observed by Castro et al., 2007 for the two areas in the XX century: the Lower Paraná tended to be a depositional area with a single thread morphology (Figure 4.3), while the downstream part of the Middle Paraná presented a not so clear trend to deposition or erosion, but was characterized by a braiding process in correspondence to humid sub-periods. The latter occurrence can be related to resulting negative correlation between discharge and water slope: the discharge increase would activate additional channels, inducing a mean velocity reduction in the total cross-sections and may extend the streamflow paths, eventually reducing the water slope.

Notwithstanding the lack of geometrical resolution, inherent to the LUF hypothesis, the synthetic description of the transversal cross-section presents some advantages with respect to an occasional (albeit very detailed) survey. Contrary to the fixed nude profile represented by the bathymetric survey, the synthetic cross-section is capable to account for the presence of riparian vegetation and to adapt itself to the long-term hydrological changes. The variation of the active river width, in fact, do not depend exclusively on the fixed cross-section profile (seasonal changes), but also on the evolution of the profile itself (long-term changes).

The LUFM model is able to simulate the long-term variations as indicates in Figure 4.16. The graph provides the values of the active width (corresponding to the equivalent discharge $Q_{eq}(\tau)$) for three typical hydrological periods (1970, 1990, 2010) in different locations. It is interesting to notice that the active river width $B$ tends to follow the long-term variations of the equivalent discharge, while the variations of the total width $B_{tot}$ (including vegetation and usually reported on the maps) are much less evident (Table 4.3). A more precise reproduction of the long-term changes of the river widths (both active and vegetated) may be obtained by relaxing the hypothesis of instantaneous adaption of width and vegetation to the annual hydrological cycle (Section 3.6).

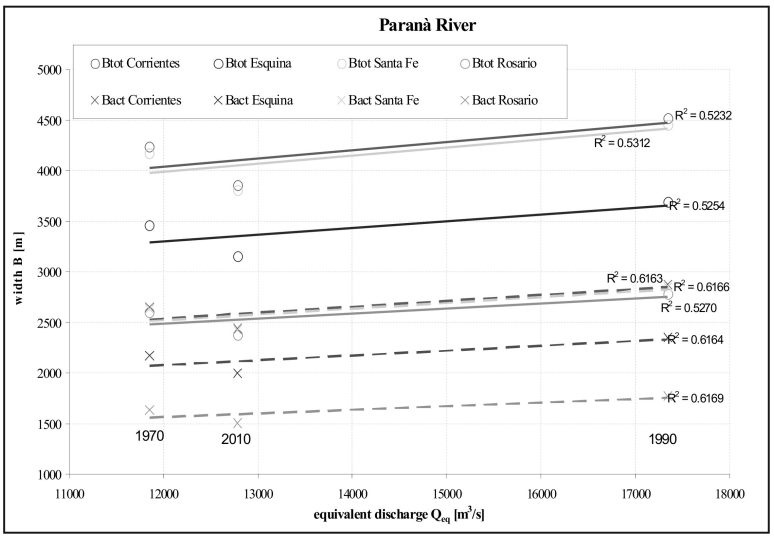


**Figure 4.16:** Evolution of the total (solid line) and active (dash line) river width, for the equivalent discharge, at four cross-sections: Corrientes, Esquina, Santa Fe and Rosario.

| $R^2$ | | | | |
|---|---|---|---|---|
| *station* | Corrientes | Esquina | Santa Fe | Rosario |
| *morphological box* | 1 | 5 | 8 | 10 |
| total river width $B_{tot}$ | 0.5232 | 0.5254 | 0.5312 | 0.5270 |
| active river width $B$ | 0.6163 | 0.6164 | 0.6166 | 0.6169 |

**Table 4.3:** Variation of the total and the active width during the last 30 years: coefficient of correlation between discharge and river width.

## 4.6 Conclusions

The LUFM model introduces some simplifications in the mathematical description of the river hydraulics and in the representation of the river morphology, whit the purpose to simulate long-term morphodynamics for large rivers with acceptable computational time and few topographic inputs.

The performed comparison between the LUFM model and the Hec-Ras model confirms the reliability of the LUFM morphodynamics simulations: the introduced schematization intend to reduce computational time and to avoid detailed topographic survey of cross-sections, needed for the Hec-Ras simulations. On the other hand, the synthetic cross-section sub-model presents some advantages with respect to an occasional bathymetric survey due to its capacity of adaptation to long-term hydrological changes. Some deviations between the two models in the hydraulics results arise, in fact, from the different representation of the river cross-section. In some degree, these deviations are dampened in the sediment transport results

and consequent morphology of the Paraná River, showing the LUFM effectiveness in modelling the 1-D morphodynamics of river active channel. The morphological results highlight as during the XX century the Lower Paraná River was a depositional area, while the Middle Paraná River between Pto. Gaboto and Esquina appears quite stable or slightly eroded, and characterized by a negative discharge-water slope correlation, which may justify the observed braiding tendency in this reach during humid periods.
As far as the reproductions of planimetric changes are concerned, an application of the non-equilibrium sub-model of the cross-section will be considered, introducing a progressive adaptation process.

# Chapter 5

# Morphological impact of dams on the Zambezi River

## 5.1 Introduction

The analysis of the effects of the construction of hydropower reservoirs on river system has been developed only in recent time. These studies concern the analysis of the impact of dams in terms of alteration of the river hydrology (Magilligan et al., 2005; Graf, 2006; Singer, 2007), morphology (Kondolf, 1997; Brandt, 2000; Surian et al., 2003; Zhou et al., 2004; Fasolato et al., 2006; Zaghloul, 2006; Wang et al., 2007; Ronco et al., 2009; Ronco et al., 2010), ecology (Baxter, 1977; Toner et al., 1997; Shafroth et al., 2002; Stanley et al., 2003; Hartmann, 2004; Gordon et al., 2006; Poff et al., 2007; Bombino et al., 2008; Hu et al., 2008; Camporeale et al., 2010; Tealdi et al., 2011) and biology (FAO, 2001). Some detailed reviews of these geomorphological works are reported in Petts et al., 2005 and McCartney, 2009.

The studies are chiefly related to a detailed scale of a single case-study, but we are interested to analyze the evolution of the entire river watershed at long-time scale. For this aim, we use a simplified 1-D model, which requires few input data and represents the most appropriate tool to investigate the effects of anthropic actions for large watersheds and for very long period of time (Ronco et al., 2009). This model, just descripted in Chapter 2, is particularly convenient for optimizing the sparse and scarce available information, typical of the analysis performed in undeveloped or developing countries. Various studies was performed on the Lower Zambezi River by applying this pure 1-D model (Ronco, 2008; Ronco et al., 2010).

The only geometric data required by the model are obtained analyzing a DEM taken from the EROS

database (Eros, 2000) and satellite images taken from the USGS database (USGS, 2011). One of the strong points of the model is the theoretical consequence of the Local Uniform Flow hypothesis (Fasolato et al., 2011) (namely that no detailed bathymetric surveys of the river cross-section are required, as reported in the Chapter 2).

The hydrological data consists in the flow-duration curve measured at the gauging station of Cahora Bassa before and after the construction of the Kariba and Cahora Bassa dams.

The sedimentological data coming from a campaign which has been made in some sections from Cahora Bassa to the Indian Ocean, while contemporary measurements of water flow and concentration have been carried on in a single cross-section, and permitting the calibration of the transport formula.

The model reproduces the evolution along the river in terms of bottom profile and grain size composition at the resolution scale of the morphological box (Ronco et al., 2010), as we can see in the previous Chapter 4. As, very often, there are most available bathymetric surveys, we have developed a quasi 2-D model, which describes the evolution of the transversal section of the river reach, also for accounting the growth of the riparian vegetation. In this chapter we make a comparison between the results of the pure hydro-morphodynamic 1-D model with the results of the coupled model (Chapter 3). As far as the morphological evolution of river profile and bottom composition are concerned, the main difference between the two models resides in the active river width, respectively fixed in the first model and time-variable in the second one.

## 5.2 Site of study: the Lower Zambezi River

### 5.2.1 An overview of the Zambezi River

The Zambezi River is the fourth-longest river in Africa and the largest flowing into the Indian Ocean from Africa (Davies et al., 2000). The total area of its basin is $1.39 \cdot 10^6$ km$^2$. This river has its source in Zambia and flows through Angola, along the borders of Namibia, Botswana, Zambia and Zimbabwe, to Mozambique, where it empties into the Indian Ocean (Figure 5.1). The entire river is long about 2500 km. The Zambezi system can be divided up into three separate sections, each differing in its landscape characteristics, geological template and biodiversity: the Upper Zambezi, the Middle Zambezi and the Lower Zambezi (Hughes et al., 1992; Main, 1992; Timberlake, 1998).

The Upper Zambezi flows into Angola for 240 km, then is joined by various tributaries, such as the Luena River and the Chifumage River. The Victoria Falls are considered the boundary between the Upper and the Middle Zambezi. About 240 km below Victoria Falls the river enters in the Lake Kariba, created in

1959 by the construction of the Kariba Dam. The Luangwa River and the Kafue River are the two largest left-hand tributaries of the Zambezi. At the confluence of the Luangwa River it enters Mozambique. The Middle Zambezi River ends where the river enters the lake of Cahora Bassa. Formerly the site of rapids known as Kebrabassa, the lake was created in 1974 by the construction of the Cahora Bassa Dam. The Lower Zambezi River is long about 650 km, from Cahora Bassa Dam to the Indian Ocean it is navigable, although the river is shallow in many places during the dry season. This shallowness arises as the river enters a broad valley and spreads out over a large area. Only at one point, the Lupata Gorge (320 km from its mouth), the river is confined between high hills: here it is scarcely 200 m wide; elsewhere it is from five to eight km wide. The river bed is sandy and the banks are low and reed-fringed. The delta may be considered to start at Mopeia, 150 km from the Indian Ocean, and the tidal influence is evident over the last 80 km (SCC, 2001). The Lower Zambezi watershed is typified by a broad floodplain, often with many parallel channels and shifting sandbanks, while the coastal portion includes extensive grasslands and freshwater swamps, dunes and mangroves. Although its geological history is not clear, this part of the basin has biological similarities to the Pungwe/Buzi system, and it is linked during floods to the Gorongosa area and Urema Trough (Timberlake, 2000).

Various studies have been published concerning the geological template of the Zambezi watershed (Orpen et al., 1989; Nugent, 1990; Thomas et al., 1992; Dollar, 1998; Salman et al., 1995, Shoko, 1999; Catuneanu et al., 2005), mainly dedicated to the comprehension of the regional tectonic evolution and implication on the middle and lower part of the basin. Focusing our attention on the lower part of the watercourse, the architecture of the section of the Lower Zambezi between Cahora Bassa Dam and Tambara is controlled by the west-east trending upper Zambezi graben and the middle Zambezi graben, which causes the river to flow in a NW-SE direction. Between Tambara and the Delta, the Zambezi River flows predominantly on Quaternary alluvium; this stretch of the river traverses the north-south trending East African Rift valley near Caia (Basson, 2004). Nothing is known about the lithology of the Zambezi basin beyond that published on the Mozambique geological map (Orpen et al., 1989). This permits, with some approximations, to locate the extent of the Cahora Bassa gorge from 35 km upstream the dam site, down to the confluence with Rio Mavuzi, 30 km upstream of the capital city of Tete; the total extent of the gorge is approximately 140 km long. Downstream of the gorge, the geological map only suggests a firm deposit of sediment down to the city of Tete, but without providing more information on the thickness of this layer (ING, 1987).

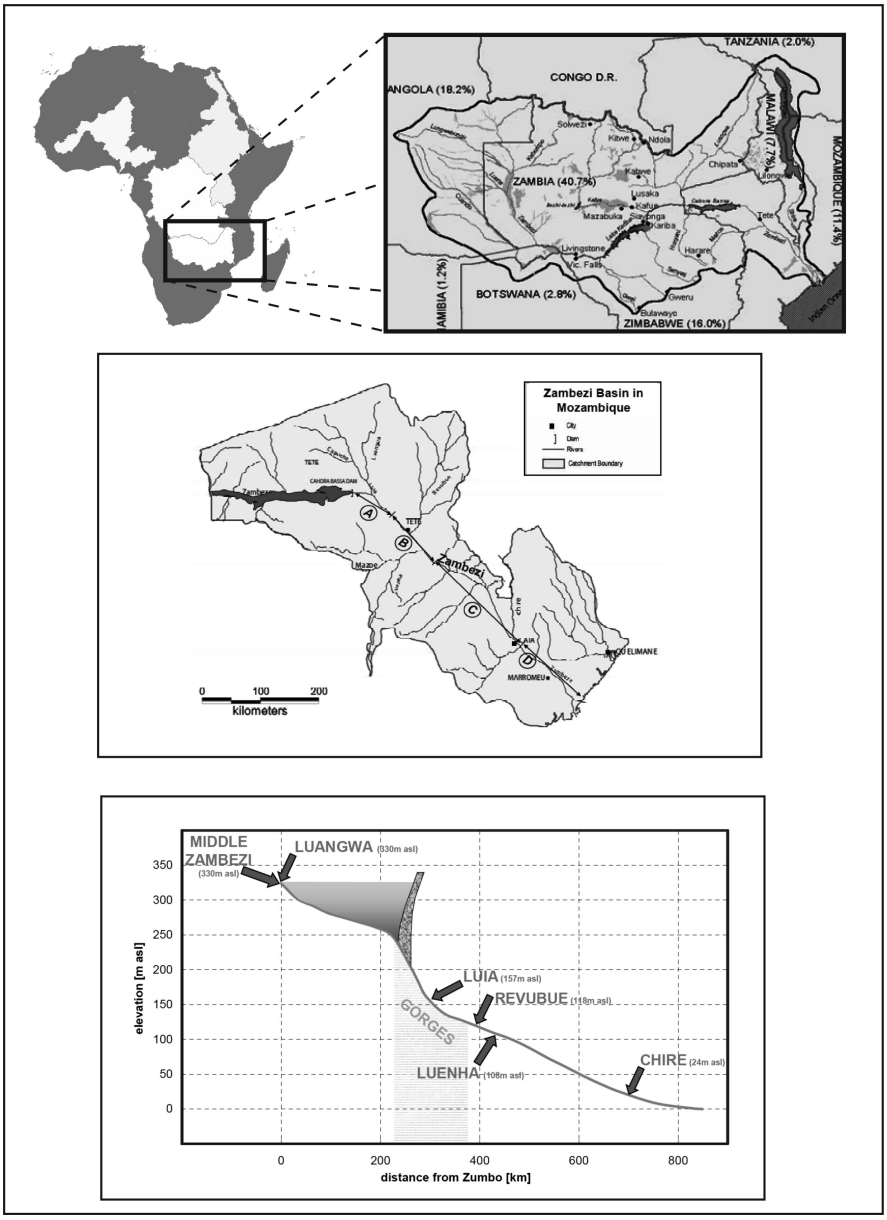


**Figure 5.1:** The Zambezi River basin and the longitudinal profile of the Lower Zambezi River.

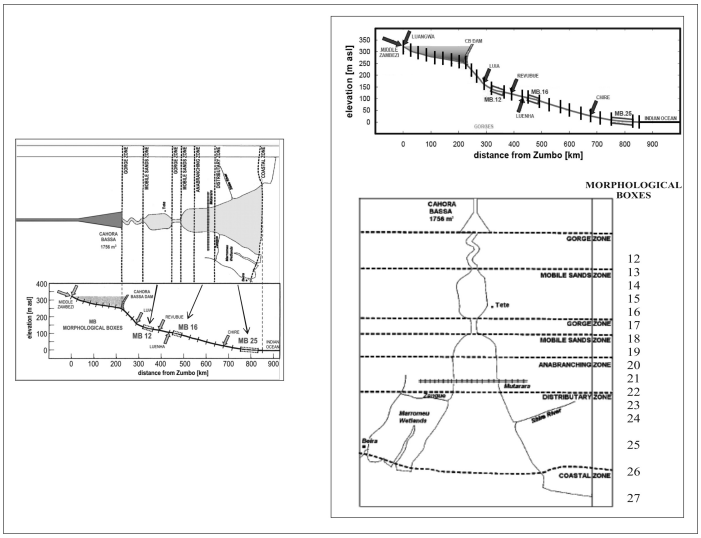


**Figure 5.2:** Morhological boxes along the Lower Zambezi River; adapted from Davies et al., 2000.

### 5.2.2 Major impoundments

Completed in 1959 at the Kariba gorge between Zambia and Zimbabwe, the Kariba Dam has a storage capacity of about $180.6 \cdot 10^9$ m$^3$ and creates a huge reservoir, with a surface area of 5577 km$^2$ at full supply level (Reeve, 1960; Davies et al., 2000). The lake created by this dam is one of the largest man-made lakes in the world, and the hydroelectric power-generating facilities at the dam provide electricity to Zambia and Zimbabwe.

Situated about 300 km downstream, the Cahora Bassa Dam (completed in 1975) has a storage capacity of $72.5 \cdot 10^9$ m$^3$ and creates a lake with a surface area of about 2660 km$^2$ (HCB, 2004).

In the future, the Cahora Bassa district will improve its energy production capacity and additional new impoundments are planned, namely Bakota Gorge, Devil's Gorge and Mupata Gorge (Matos et al., 2010), as reported in Figure 5.3.

With the construction of a great number of dams in its basin, when entering the territory of Mozambique the Zambezi River can be considered as a regulated river, which lost its natural pattern of flow variations in time and in quantity (Suschka et al., 1986), as we can see in Figure 5.4.

A lot of reports and papers were published concerning the impact of Kariba and Cahora Bassa reservoirs on the Zambezi River system. Many of them are focused on the ecological effects (biodiversity, fisheries, wetlands, etc.) of these impoundments (Bowmaker, 1960; Attwell, 1970; Hall et al., 1977; Du Toit, 1984; Dunham, 1989; Beilfuss et al., 1999), while very few addressed the problem of the morphological changes correlated to sediment and water fluxes altered by the presence of these large reservoirs (Guy, 1980;

Suschka et al., 1986; Beilfuss et al., 1999; Davies et al., 2000). No quantitative estimate of the rate of sediment accumulation has been found in the numerous reports that formed the basis for the design of the Cahora Bassa Dam scheme (Bolton, 1983). Even during the operational period, no monitoring of sediment accumulation has been carried on. A certain indication from the project design is the relatively small "dead capacity" chosen for the Cahora Bassa reservoir (Davies et al., 1975; HCB, 2004). Making some assumptions on the sediment production of the basin and the trapping capacity of the upstream Kariba reservoir and considering the sediment concentration occasionally measured on some tributaries, a previous study estimated the total rate of sediment input to Lake Cahora Bassa with a great uncertainty (Bolton, 1983). The damming of the Kariba and Cahora Bassa gorges has considerably changed the hydrological cycle of the Lower Zambezi. Data collected at the gauging station of Tete, in Mozambique (located 135 km downstream of the Cahora Bassa Dam, as reported in Figure 5.2) from 1951 until 2003, indicate that the presence of the impoundments regulates the pattern of the seasonal runoff, increasing its minimum value and decreasing its maximum value. The monthly runoff variation has much lower amplitude and the discharges are more uniformly distributed during the year: this situation changing the normal seasonal flow pattern. As far as the effects on river morphology are concerned, different Authors tried to evaluate the changes of the Lower Zambezi River after the completion of the Kariba Dam and Cahora Bassa Dam, but without getting at the same outcome (Suschka et al., 1986; Beilfuss et al., 1999; Davies et al., 2000). An Author attributes the removal of the sediment stored in the gorges zone, the incision of main flow channel with the stabilization of braid and bars in the transitional zone, the dominance of a single main channel that incises and conveys the majority of the flow in the braided zone, the reduction of the Zambezi Delta wetland mangrove swamp area and the increase of salt-water intrusion to these impoundments (Chenje, 2000). Following the construction of a dam, the reduction of the sediment load and the high flow tends to produce opposite effects, which propagate along the river. Unfortunately, at the moment, no systematic surveys of the morphological changes from the impact of the Kariba and Cahora Bassa dams are reported in Literature.

A numerical approach to these problems seems the only possible way of analysis. As already mentioned in the introduction, this analysis can be made only by a combination of a pure 1-D hydro-morphodynamic model (Chapter 2) providing the evolution of bottom elevation and grain size composition, although at non-detailed spatial and temporal scale (Ronco et al., 2010), with a quasi 2-D cross-section sub-model, (Chapter 3), able to reproduce the evolution of the river widths during the hydrological year.

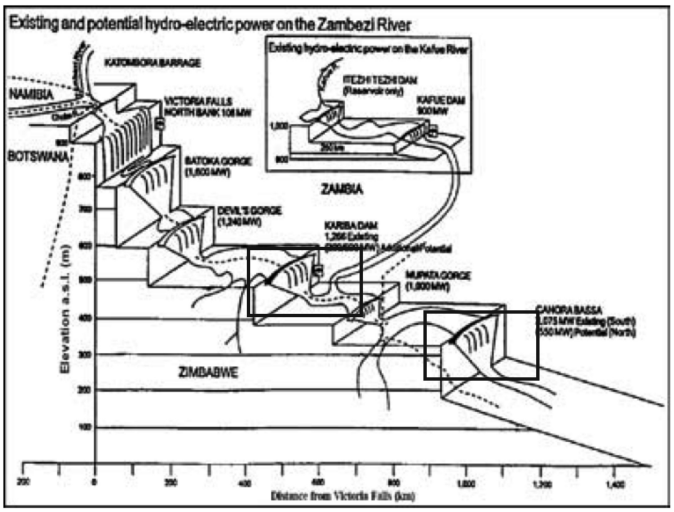


**Figure 5.3:** Schematic diagram of reservoirs and potential hydropower production of the Zambezi River basin; adapted from Ronco, 2008.

### 5.2.3 Hydrology

Some studies about the hydrology of the Lower Zambezi River have been carried out in the last years. One of them, in particular referred to the evolution of the delta environment, is reported in various papers (Beilfuss et al., 2001a; Beilfuss et al., 2001b), as a part of a detailed program for the integrated development and restoration of the Lower Zambezi valley.

The construction of the dams has considerably changed the hydrological cycle of high and low flows, as we can see in the next figure (Figure 5.4). This figure reports the discharge of the Lower Zambezi at the gauging station E320, located downstream the two dams, near the junction between the Zambezi River and the Revubue River. Data collected at this station until 2003 indicate that the presence of the two impoundments regulates the pattern of the monthly runoff, strongly increasing its minimum value (in August-November) and decreasing its maximum value (in February-April). As consequence, the monthly runoff variation has a much lower amplitude and the discharges are more distributed along the year, changing the normal seasonal flow pattern of the river (Table 5.1) (Ronco, 2008).

| | **1951-1958** | **1959-1974** | **1975-2003** |
|---|---|---|---|
| maximum monthly average runoff $Q_{max}$ [$10^6$ m$^3$] | 23360 | 13310 | 7789 |
| mean monthly average runoff $Q_{meam}$ [$10^6$ m$^3$] | 8161 | 6025 | 5748 |
| minimum monthly average runoff $Q_{min}$ [$10^6$ m$^3$] | 1021 | 2261 | 4195 |

**Table 5.1:** Variation of the monthly average runoff along the Lower Zambezi River.

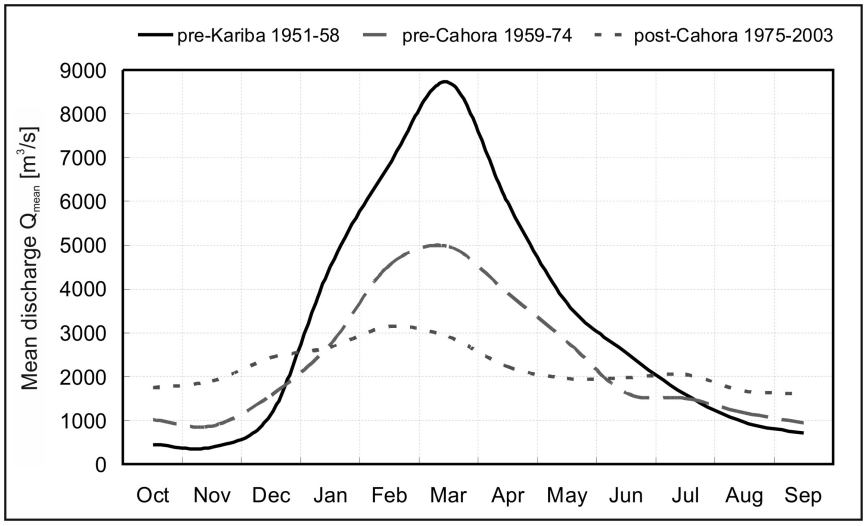


**Figure 5.4:** Variation of the discharge of the Lower Zambezi River measured at the gauging station E320.

### 5.2.4 Riparian vegetation

As reported in Literature, the typical riverine species of the Zambezi River are Mopane, Acaia-Combretum and Mangrove (Timberlake, 2000).

To simulate the vegetation dynamics of these species, it is necessary to quantify their interaction with the river constraints (Francis et al., 2005) by introducing the concept of the carrying capacity (Taylor et al., 1990; Murray, 2002; Duarte et al., 2003; Hui, 2006; Molles, 2008), as reported in a previous part of this thesis (Section 3.4). The carrying capacity $K(t/\tau)$ is an intrinsic features of the system, defined as the productory of all the contributions of each single time-depending disturbance, such as flood, drown, drought, lateral erosion, flow velocity, etc.

Not much quantitative informations are available for expressing the carrying capacity $K(t/\tau)$ of the Lower Zambezi River. However, as disturbances related to excess of water usually provide a decreasing with the submergence time, while disturbances related to deficit of water usually provide an increasing, one may infer that a reasonable productory will give a function with a maximum value $K_0(x)$ around $(t/\tau)$=0.50 (must frequent conditions), when the median discharge occurs. The real configuration of $K(t/\tau, x)$ will depend on the particular species along the Zambezi River. For this application, however, we assume a sort of "universal" carrying capacity variable along the river, provided in each cross-section by a relationship between hydrology and morphology of the active river cross-section (Chapter 3).

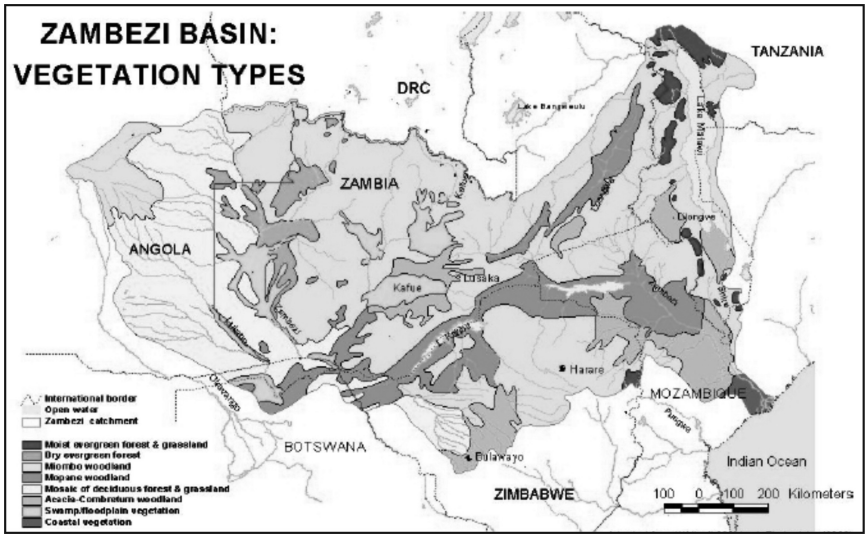


**Figure 5.5:** Vegetation of the Zambezi River Basin, adapted from Timberlake, 2000.

## 5.3 Analysis of the remote sensing images

### 5.3.1 Methods

The analysis was conducted along the Lower Zambezi River accounting for the various tributaries as external sources of water and sediments. The river was divided into a lot of morphological boxes with different length, related to the geometry of the river and to the velocity of the current (Ronco, 2008).
For every morphological box we identified the water (or bottom) slope by using the DEM of the Zambezi from the database HYDRO1K, related to the year 2000 (Eros, 2000).
The analized Landsat 7 images are taken from the USGS database (USGS, 2011) and are related to the period 1991-2003. The relationship between river width and river discharge (eq. 3.3) permits us to reconstruct the annual duration curve of each morphological box, as explained in the Chapter 3.
These satellite images, in principle, included both the nude portion of the river cross-section and the part covered by the riparian vegetation. The procedure for separating the two parts, by evaluating the vegetation density during the hydrological year, is reported in a previous part of this thesis (Section 3.5).
In the next figure (Figure 5.6) we have reported an analysis of some images taken at different time along the Lower Zambezi: the first two images represent the normal flow discharge of the river, while the second two represent the flood occured during the spring of 2001. We can observe a larger wet portion of the available river width when the flood occurs.

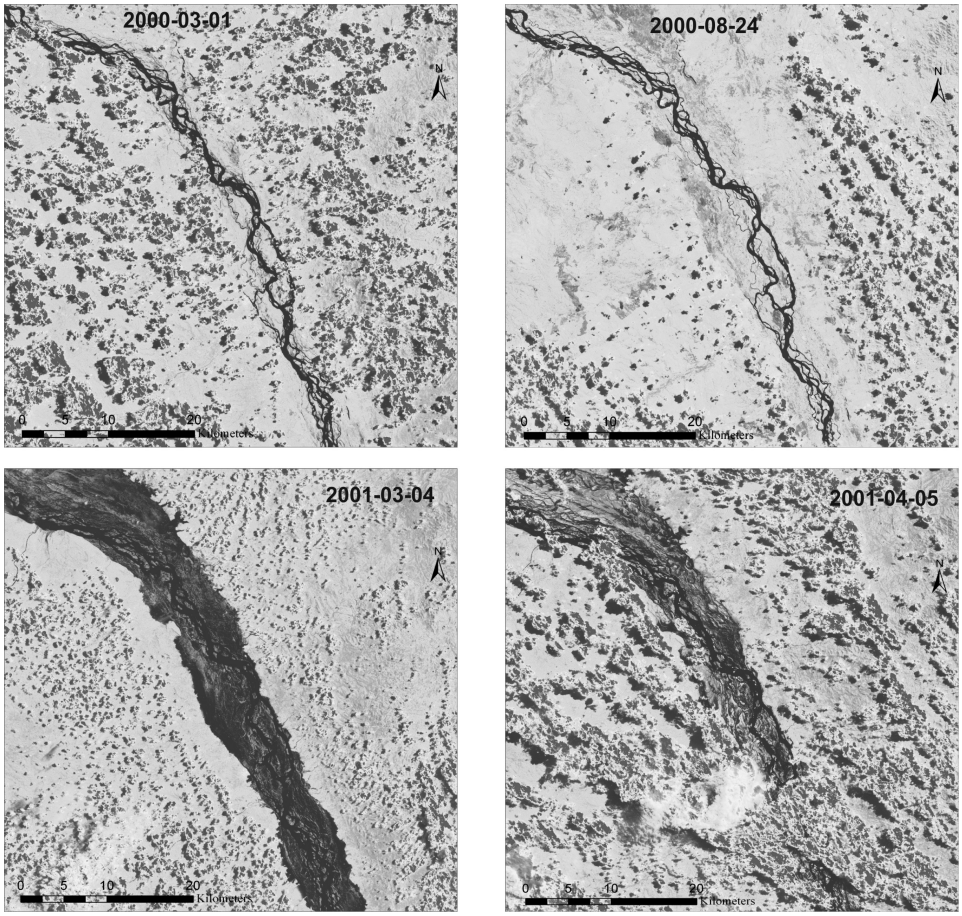


**Figure 5.6:** Variation of the discharge along the Lower Zambezi River upstream Caia, in Mozambique.

## 5.4 Results

Some simulations performed on the Lower Zambezi have shown that this part of the river seems to be subjected to a long-lasting process of general progressive deposition, which is apparently far from the equilibrium and it is slowly propagating in the downstream direction toward the Indian Ocean (Ronco et al., 2010). It should be noted that a long-term simulation should correctly be made by including all the sources of sediments, farther upstream from the present boundary conditions of the model.

In this study the attention has been concentrated to relatively shorter simulations in order to evaluate the relative medium term morphological and biological effects of the construction of the Kariba Dam and the Cahora Bassa Dam on the river bottom profile and on the variation of the cross-section profile due to the growth of the riparian vegetation.

### 5.4.1 Longitudinal evolution of the river

The model has been applied for simulating the morphological behaviour of the Lower Zambezi River since the year 1907, namely the period following the beginning of systematic hydrological measurements at the gauging station of Zumbo.

This has permitted an evaluation of the historical equivalent discharge entering the model, from the Zambezi River and from its main tributaries, together with the corresponding annual sediment transport up to 2003. Simulations have been carried out for another century after present, by assuming a synthetic hydrology with constant discharge, depending on the configuration considered.

These computations indicate that the course of the Lower Zambezi presents a general tendency to a progressive and constant deposition rate, especially concentrated in the flat reach downstream the Cahora Bassa gorges. The most striking result of the model is the fact that this undisturbed trend is only lightly affected by the presence of the two dams. This is probably due to the fact that the direct sediment input from the Middle Zambezi in the Cahora Bassa reservoirs is controlled by the elevation of the gorges and relatively low compared to the input from the tributaries downstream.

The study has been made downstream Cahora Bassa, following the year 1958 (just before the construction of the Kariba Dam), 1974 (just before the construction of the Cahora Bassa Dam), 2003 (the last year with measured hydrological data), and 2100. The analysis indicates different responses of the bottom, both in terms of change in elevation and mean grain size variation, under two different water flow configurations, which correspond to two hydrological configurations: no dams (real configuration until 1958, hypothetical natural configuration in the following period) and Kariba and Cahora Bassa dams, with both dams constructed (actual configuration since 1975). The results are summarized in the next figures (Figure 5.7 and Figure 5.8), where we have reported the comparison between the evolution of the river under the hypothesis of fixed or variable river width. The fixed river width are used in the model proposed by Ronco et al., 2010, while the variable river width is used in the model developed in this thesis.

As far as the bottom elevation is concerned, in absence of dams (natural conditions) apparently aggradation of the upper part of the river is progressive downstream of the gorges, where some tributaries flows into the Zambezi River. Along the intermediate reach the aggradation rate is almost nil, while a perceptible aggradation rate is again exhibited in the delta zone. The presence of the two dams creates an effect of sediment interception, which is rapidly felt. By contrast, after the construction the instantaneous opposite effect of water flow reduction from Cahora Bassa Dam has already been adsorbed.

It is possible to analyze the contemporary evolution of grain size composition corresponding to the bottom change discussed above. In absence of dams we notice the natural long-term progressive fining

of the bottom composition, which generally accompanies deposition. The opposite effects of water flow and sediment input reduction produced by the subsequent construction of two dams cannot be easily distinguished.

The time history of the bottom elevation and bottom grain size confirms our observations: the initial prevailing effects of water flow reduction, rapidly propagating downstream, are soon compensated by the opposite effect of sediment trapping (Ronco et al., 2010).

In the first figure (Figure 5.7), regarding the evolution of the river in natural conditions, it is possible to observe that the variation of the river width is not important in terms of variation of the bottom profile, in fact the bottom variation related to the fixed river width remains higher than the bottom variation related to variable river width during the entire simulation. The variation of the river width is more important in terms of grain size composition, in fact the mean diameter related to variable river width varies more quickly than the mean diameter related to fixed bottom.

The second figure (Figure 5.8) reports the evolution of the river due to the presence of the two dams (actual configuration). We can observe the importance of a variable river width when we study the evolution of a river related to a time-variable hydrography: when the discharge decreases (e.g. after the construction of the dams), the active river width also decreases, the bottom profile is more flat and the mean diameter decreases.

Under these consideration, we can notice that the hypothesis of fixed river width is valid only in rivers affected by an important anthropic presence, as the case of the Zambezi River.

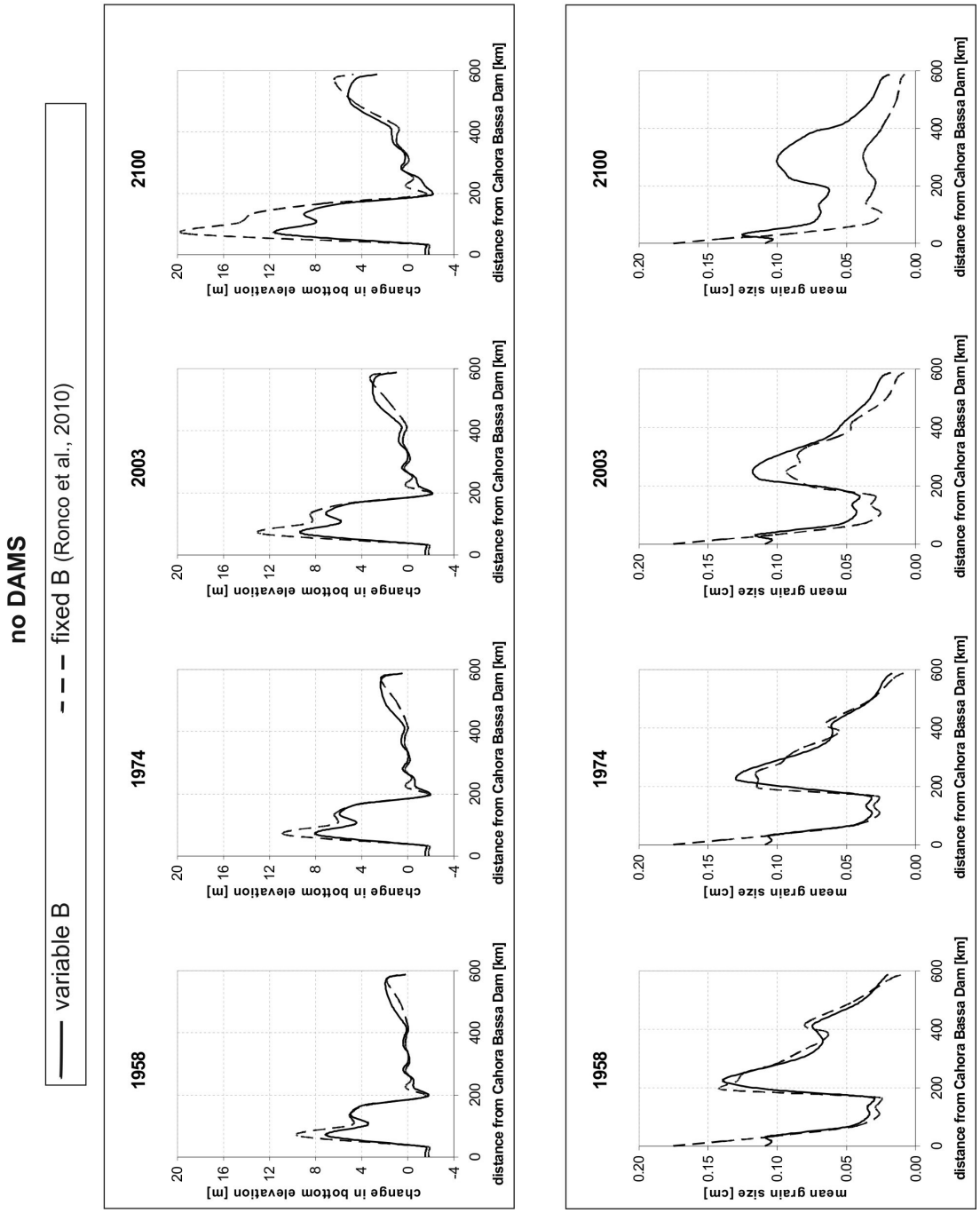


**Figure 5.7:** Comparison between the evolution of the river with fixed river width and with variable river width. Configuration without dams.

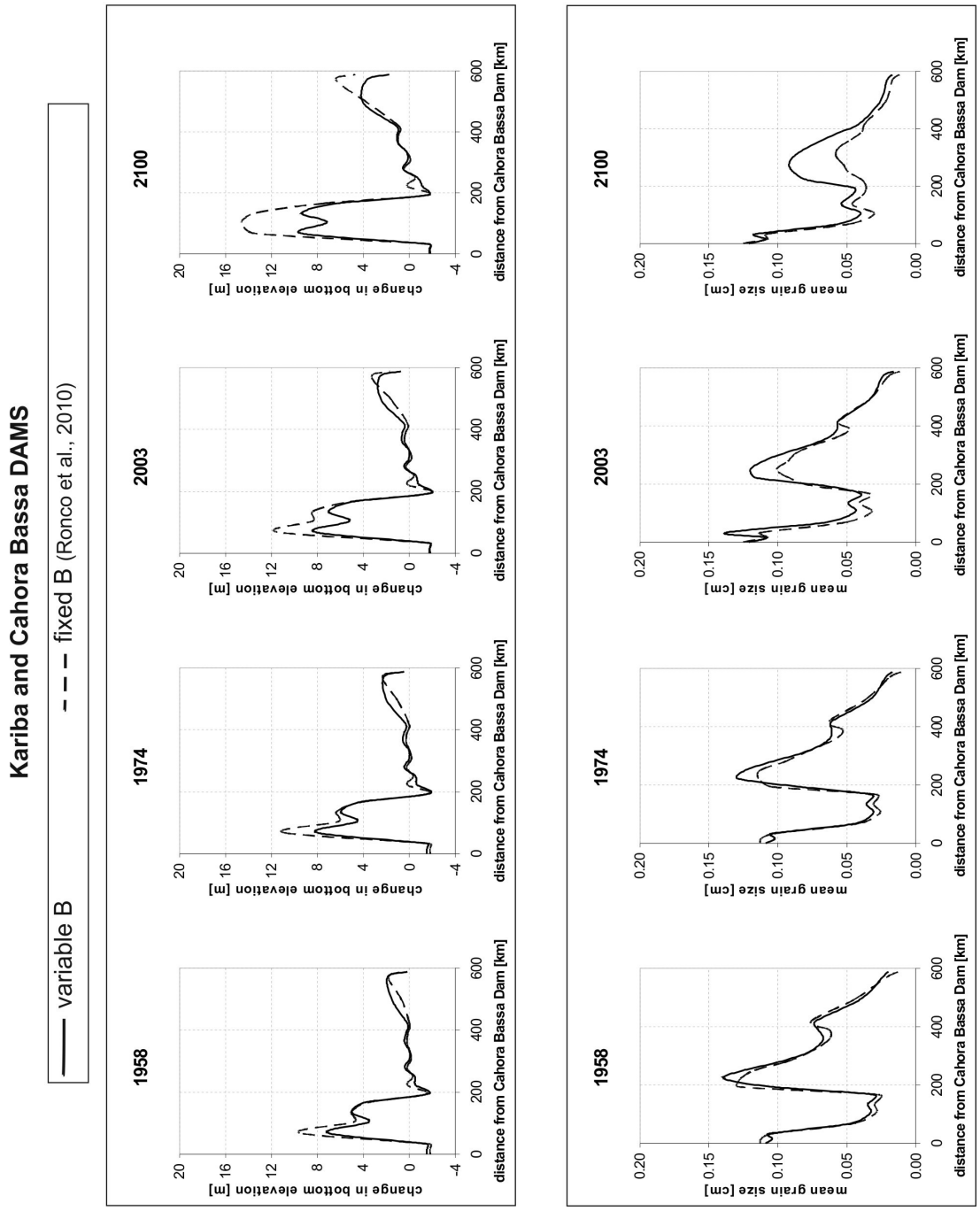


**Figure 5.8:** Comparison between the evolution of the river with fixed river width and with variable river width. Configuration with Kariba Dam and Cahora Bassa Dam.

### 5.4.2 Transversal evolution of the river

The next figures (Figure 5.9, Figure 5.10 and Figure 5.11) report the evolution of three significant river cross-sections in presence of the dams. In other words, we will analyze the evolution of the river due to a reduction of the water flow.

It is possible to observe the typical evolution of a braided river (Figure D.1): when the discharge decreases, the river tends to become a meandering river, with wide floodplains, a lower value of $\beta$, a smaller water depth and a deepening of the main channel. This behaviour is evident along the entire course of the river. We have compared the results of the model with some Literature data (Davies et al., 2000), and we observe a quite good agreement (Figure 5.13).

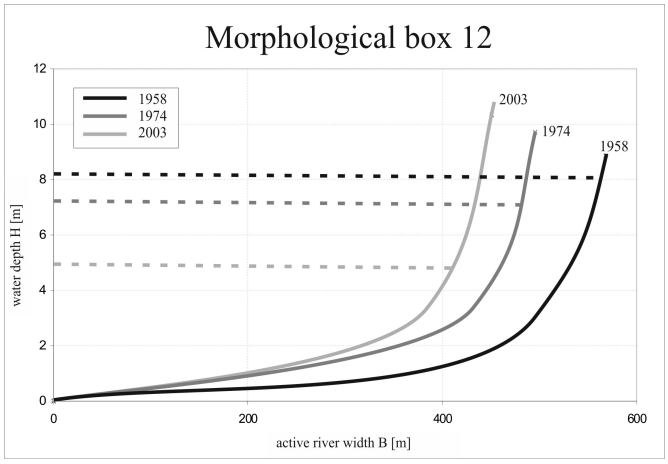


**Figure 5.9:** Simulation of the evolution of the M.B. 12, starting from the 1907 configuration.

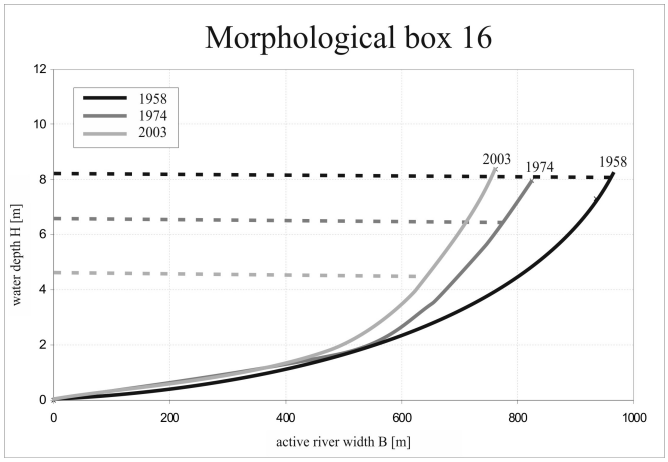


**Figure 5.10:** Simulation of the evolution of the M.B. 16, starting from the 1907 configuration.

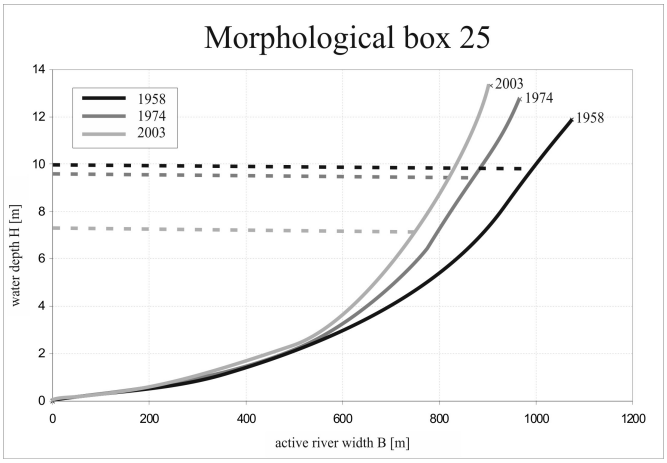


**Figure 5.11:** Simulation of the evolution of the M.B. 25, starting from the 1907 configuration.

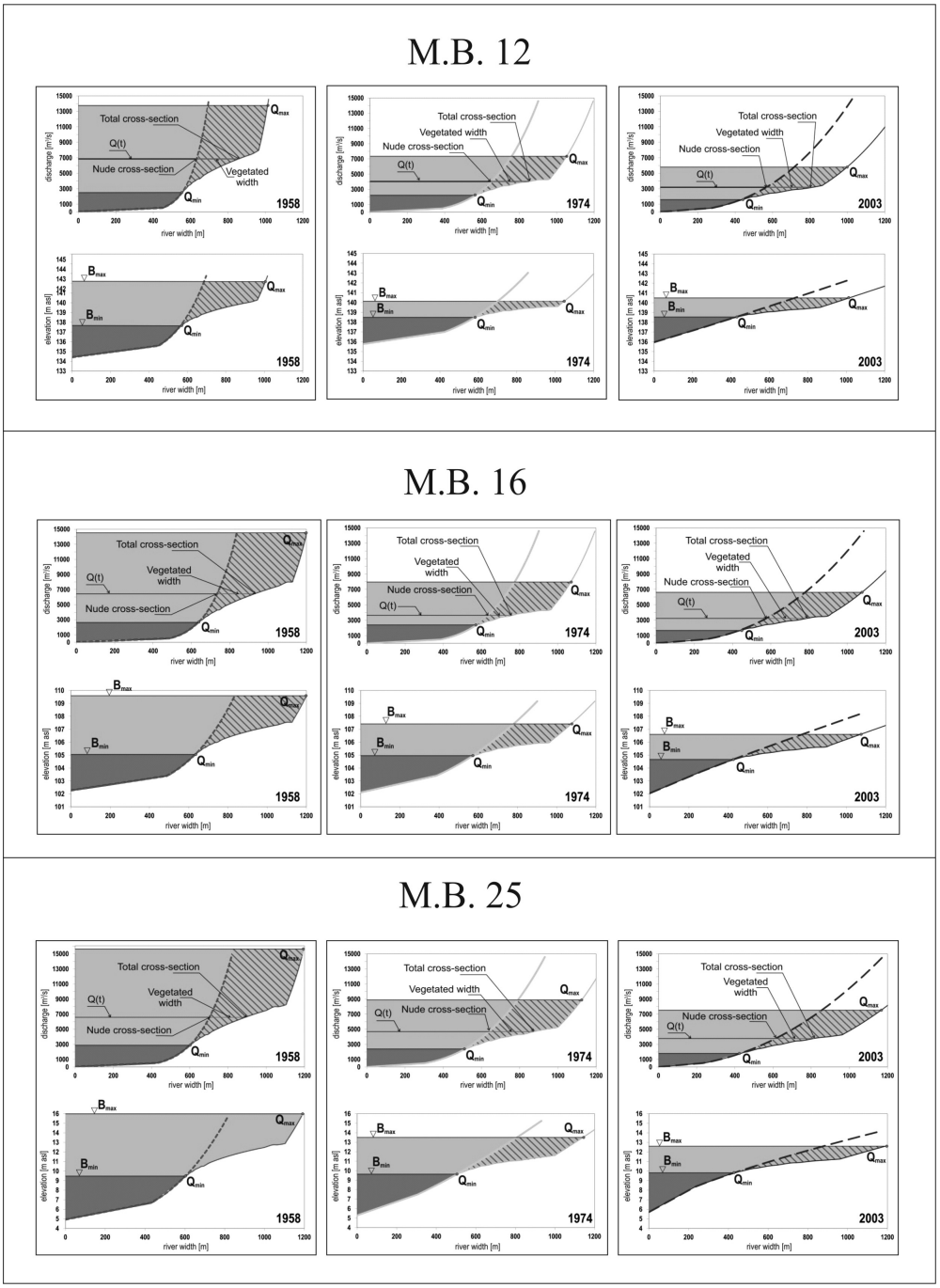


**Figure 5.12:** Simulation of the evolution of the morphological boxes 12, 16 and 25, starting from the 1907 configuration.

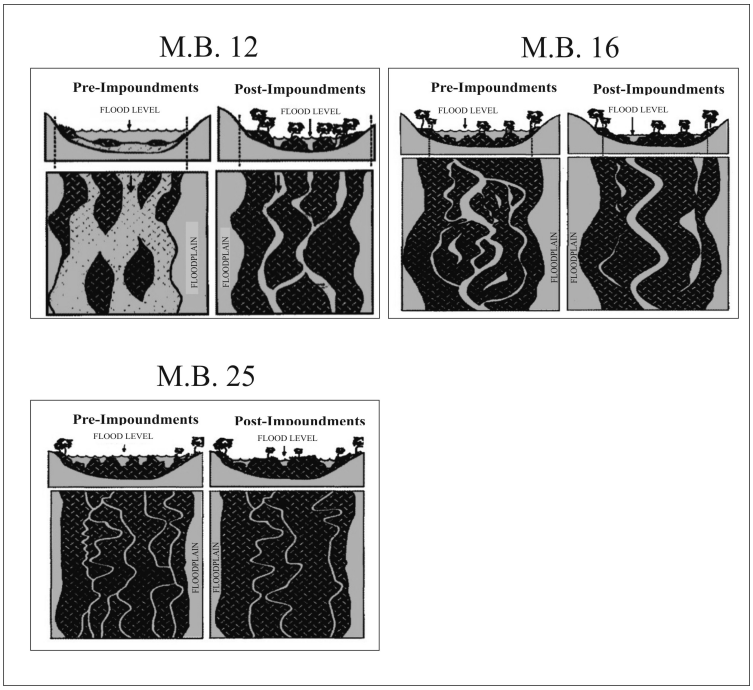


**Figure 5.13:** Evolution of the river patterns; adapted from Davies et al., 2000.

### 5.4.3 Evolution of the river delta

The evolution of the delta coastline has been recognized as an important indicator of the magnitude of the sediment yield in various rivers of the world (Walling, 2008). Besides sediment yield, other complex physical mechanisms are involved in the evolution of the delta morphology and extension, such as sea level fluctuations, subsidence, human intervention, and, above all, sediment redistribution made by the sea. Different methods have been developed to quantify the delta evolution: aerial photo, radar images, satellite images, ground penetrating radar, sonar bathymetry, sediment sampling, grain size distribution analysis and mathematical models able to simulate sediment transport by waves and currents (Liu et al., 2000; Sun et al., 2002; Pelpola et al., 2004; Trebossen et al., 2005).

Some Authors (Walling, 1984; Walford et al., 2005) evaluated the Zambezi delta evolution and the river sediment load history of the last 120 Ma ($120 \cdot 10^6$ y) using a seismic reflection profile system, making some assumptions on the compaction history in order to construct various isochore maps of solid sediment load and yield as a function of the geological time. In their works these Authors analyze three different periods of elevated sediment flux: the first one in Late Cretaceous times (9065 Ma), the second during the Oligocene times (3424 Ma) and the last one during the Late Miocene times (10 Ma), which can be attributed to the doubling of the Zambezi catchment area from the capture of the upper part of the river

(Nugent, 1990).

In this last geological period (last 5 Ma), they estimated the annul sediment yield within the range of 6-13·$10^6$ $m^3$/y, quite larger than our estimate in the present conditions (Figure 5.14). At historical time-scale, the effects on the Zambezi delta from both hydrological and sedimentological natural changes (caused by the presence of the impoundments) have been highlighted by recent studies on the Marromeu wetland system (Anderson et al., 1990; Beilfuss et al., 1996).

By comparison of field ecological survey analysis and aerial satellite images (from 1960 up to 2000), it was observed that the delta of the river is much drier at the end of the dry season than it was in natural (pre-impoundments) conditions, together with a reduction of wetlands and open water areas, infestation of stagnant waterways with exotic vegetation, intrusion of saltwater and decrease of grazing, fisheries and flood recession agriculture. Further, it was observed that the water level in the delta was lower the former bankfull conditions during the flood season (Ronco et al., 2010).

It is unquestionable that frequency, timing, magnitude, duration and sediment load of the Zambezi River floods now differ greatly from historic flooding conditions (Bolton, 1983; Suschka et al., 1986); in fact, up to now, no quantitative and systematic evaluation of the effects of these phenomena on the delta coastline evolution has been carried on.

Therefore, we have made a preliminary evaluation of the delta shoreline evolution, estimating the variation of the delta area of an arbitrary reference surface, calculated from various Landsat images available for the last 40 years. This analysis is performed in the same way as the analysis reported in a recent paper (Ronco et al., 2010).

In particular, we analyzed six different satellite images of the delta taken from the USGS database (USGS, 2011).

- Landsat MSS, 1972/09/24
- Landsat MSS, 1979/08/28
- Landsat TM, 1991/06/14
- Landsat ETM+, 2000/07/16
- Landsat ETM+, 2004/11/08
- Landsat TM, 2010/11/09

In the next table we have summarized the measured area of the Zambezi Delta for each satellite images and reported a preliminary analysis of the temporal evolution of this area during the analyzed period.

| year | Area of the delta [$km^2$] | Loss/increase of area [$km^2$] | Annual rate [$km^2/y$] | Cumulative from 1972 [$km^2$] |
|---|---|---|---|---|
| 1972 | 13920 | - | - | - |
| 1979 | 13903 | -17.25 | -2.46 | -17.25 |
| 1991 | 13881 | -21.80 | -1.82 | -39.05 |
| 2000 | 13905 | 23.66 | 2.63 | -15.39 |
| 2004 | 13894 | -10.92 | -2.73 | -26.31 |
| 2010 | 13882 | -11.59 | -1.93 | -37.90 |

**Table 5.2:** Area of the Zambezi delta and pattern of variations over the considered period of time (1972-2010).

In the following figure we have represented the evolution of the delta area and the trend of the computed change of sediment supply. In this graph the solid line represents the simulation made with the quasi 2-D sub-model, while the dashed line indicates the simulation made by the pure 1-D hydro-morphodynamic model with fixed river width.

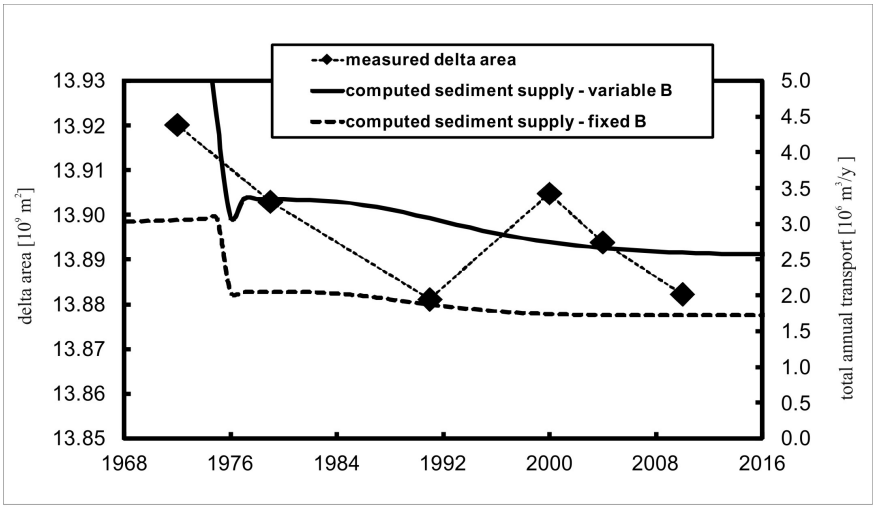


**Figure 5.14:** Measured change of the delta area extension (1972-2010) and computed change of sediment supply with fixed and variable active river width.

These preliminary measurements confirm the general negative trend of the delta area extension, with a loss of about 2.5 $km^2/y$ for the period 1972-1979, a less marked loss in the period 1979-1991 (-1.8 $km^2/y$), an overturning of the erosion/deposition phenomena with an important increase of the extension of the river delta during the period 1991-2000 (around 2.6 $km^2/y$), a decrease of the delta area in the period 2000-2004 (-2.7 $km^2/y$) and a final decrease of the extension of the delta area during the period 2004-2010

(about -1.9 $km^2$/y).

The delta shoreline evolution apparently display a negative trend over the years: from the 1972 measurements the erosion process seems to prevail against the depositional process, with a total loss of area of about 38 $km^2$.

Even if these variations do not exclusively depend on the sediment yield of the Zambezi River, we may compare the delta area evolution to the total sediment supply of the delta computed by the two models in the last section of the river, by assuming the present hydrological conditions (Figure 5.14). While the immediate influence of the Kariba Dam in term of water flow reduction apparently is not so strong (no considerable difference before and after the year 1958), the model predicts a slowly decrease of sediment load for the period 1964-1972, just before the construction of the Cahora Bassa Dam. The sediment discharge strongly decreases after the construction of the Cahora Bassa Dam, and then decreases again to an almost stationary rate for both the two model results.

The time-history of the sediment transport computed in the last section of the delta confirms how the natural trend of aggradation of the delta has been perturbed in a complex way (immediate effect of water flow reduction and delayed effect of sediment interception) by the two impoundments. The computed changes of the sediment supply are congruent with the measured variations of the delta area, when one considers that the surface area has been measured instantaneously and that the morphodynamics of the delta also depends on the conditions of the Indian Ocean.

### 5.4.4 Sensitivity analysis

In this study we can see that the input data required by the numerical model are quite limited. The numerical parameters of the equations expressing the physical processes can be obtained by Literature or by a site-specific calibration against experimental informations.

If we study the growth of the riparian vegetation, there are a lot of parameters which varies with the species of the vegetation (namely the marginal damages). In this work we use a simple description of the vegetational patterns (Timberlake, 2000), and so we assume only one parameter for each morphological box: the maximum aggregate carrying capacity $K_0(x)$, related to the median discharge.

For a complete sensitivity analysis, the variation of the maximum carrying capacity is repeated with the same conditions (dam configuration) for the three morphological boxes that we have considered, characterized by different morphology and riparian vegetation (M.B. 12, M.B. 16 and M.B. 25).

The variation of the carrying capacity affects the vegetated width: when the carrying capacity increases, the vegetated river width increases and the active river width decreases.

By the application of the transport formula (eq. B.3), it is possible to compute the total sediment

transport and notice that, when the active river width decreases, the sediment transport increases. This variation reflects differently along the river: in the morphological boxes 12 and 16 the bottom elevation decreases when the carrying capacity increase, while in the morphological box 25 the bottom elevation vary proportionaly with the variation of the biological term.

In terms of mean grain size, the variation of the carrying capacity is important only in the anabranching zone (namely in the M.B. 16); in the other two boxes, the variation of the carrying capacity has a negligible influence on the mean grain size. If we observe the Figure 5.16, we can note that the variation on the mean diameter is not only local, but it influences a long river reach, both upstream and downstream the morphological box 16.

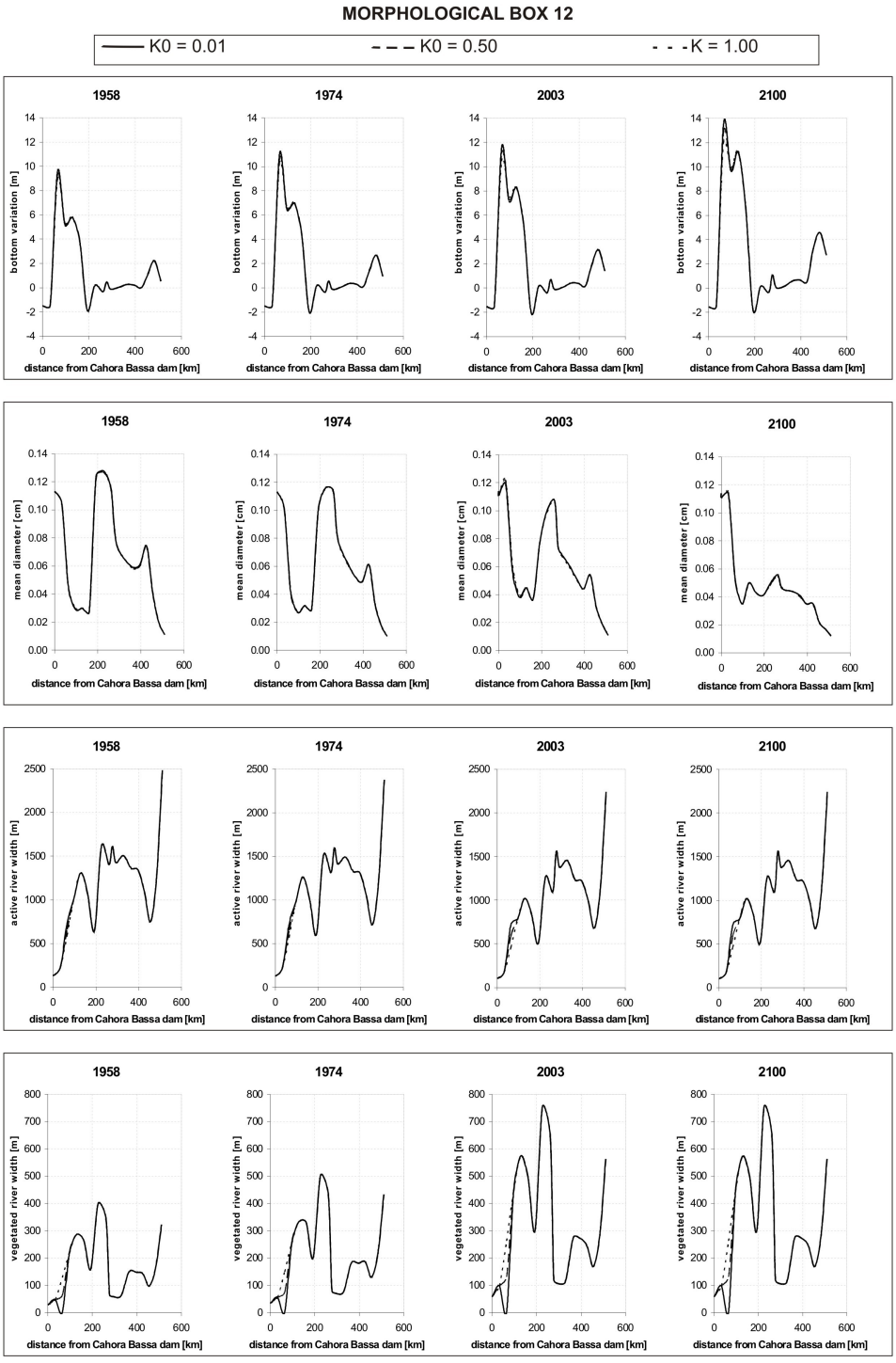


**Figure 5.15:** Simulation of the river evolution starting from the 1907 configuration. Sensitivity analysis by varying the carrying capacity of the M.B. 12.

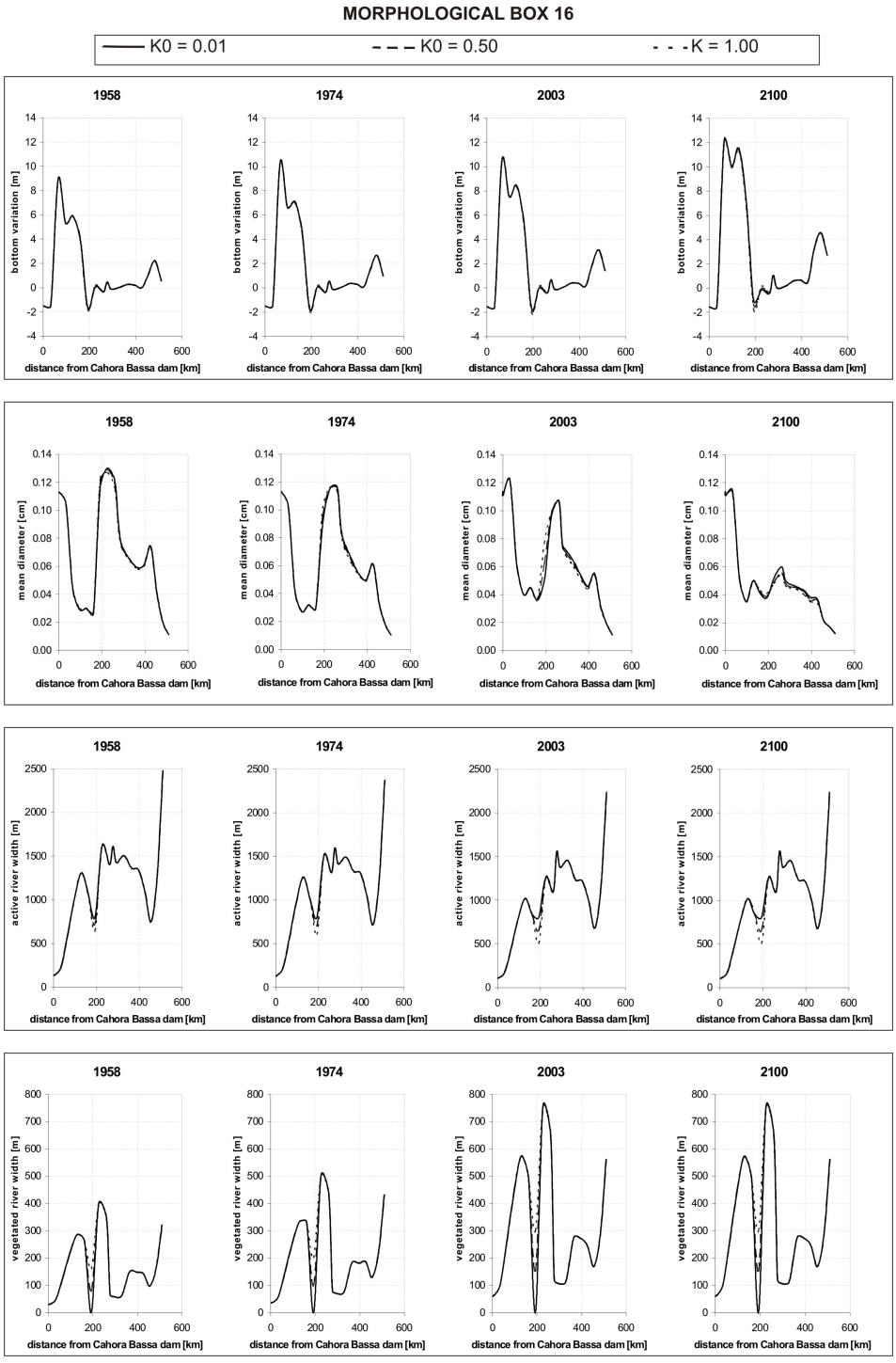


**Figure 5.16:** Simulation of the river evolution starting from the 1907 configuration. Sensitivity analysis by varying the carrying capacity of the M.B. 16.

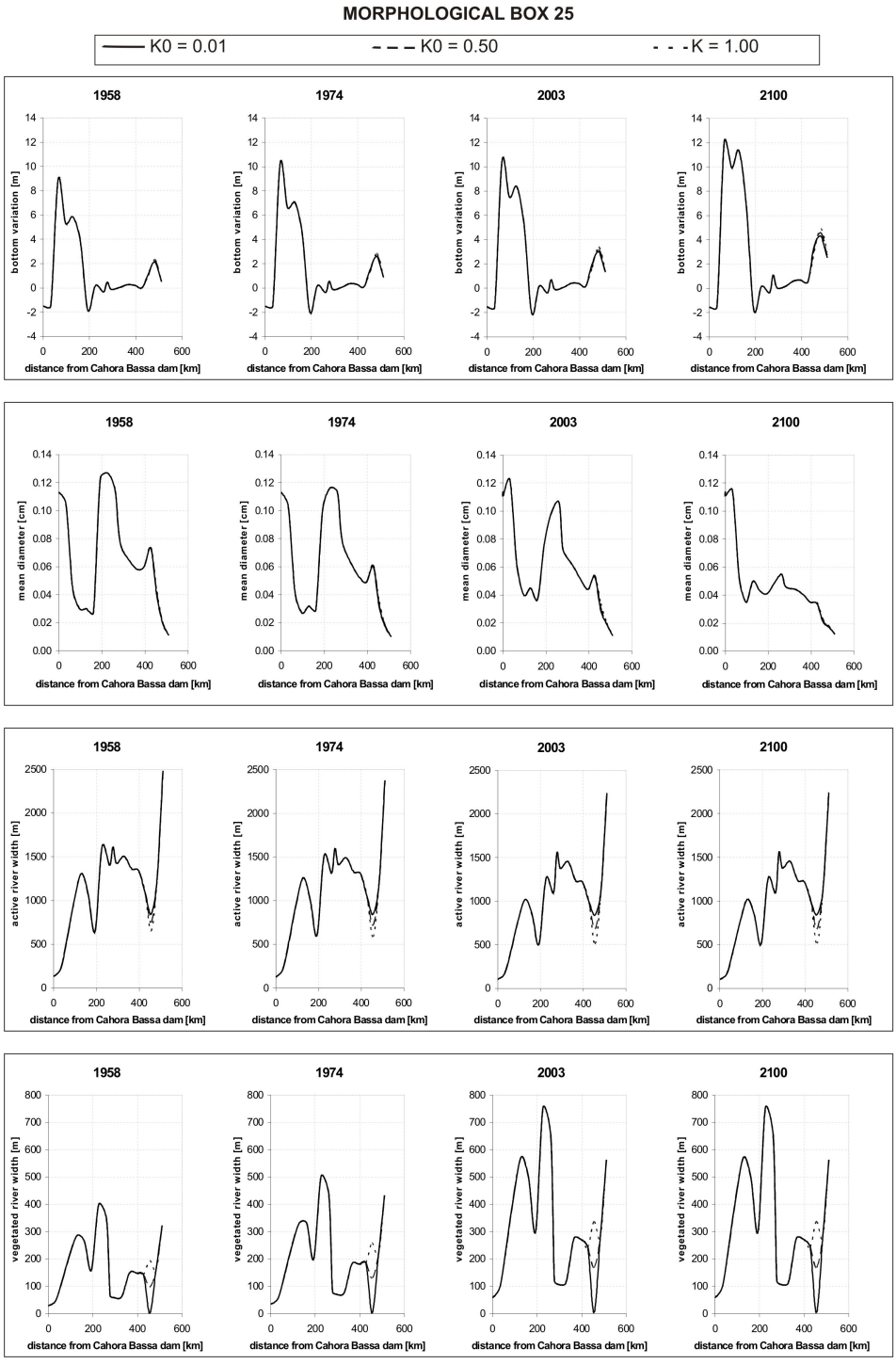


**Figure 5.17:** Simulation of the river evolution starting from the 1907 configuration. Sensitivity analysis by varying the carrying capacity of the M.B. 25.

### 5.4.5 Comparison between measurements and model results

The computational results of the pure hydro-morphodynamic 1-D model with fixed river width have been already compared with the (scarce) field data in another paper (Ronco et al., 2010).
In particular, the turbidity measurements performed in 1973-1974 have been utilized for the calibration of the transport formula. This data are reported in Hall et al., 1977.
As far as the longitudinal morphological evolution is concerned, the only available information is represented by the relatively recent evolution of the river delta between 1972 and 2010. As reported in a previous study (Ronco et al., 2010), the variations of the delta surface are fairly well related to the variation of the total annual transport through the river mouth computed by the model.
As mentioned in the Section 5.4.1, the introduction in the hydro-morphodynamic 1-D model of the quasi 2-D component reproducing the river cross-section, does not change significantly the longitudinal evolution of the river. Consequently, we can conclude that this coupled model reproduces quite good the trend of the annual sediment input to the delta (Section 5.4.3).
Unfortunately, no quantitative data are available regarding the transversal evolution of the river. However, the qualitative informations reported in Figure 5.13, together with the sensitivity analysis performed in Section 5.4.4, indicates a reasonably good predictive capacity of the present coupled model.

## 5.5 Computation of the shape factor

For making a preliminary analysis of the river cross-section profile, we use an iterative method (Appendix C.7) for the computation of the shape factor $\beta$ (eq. 3.3).
In the analysis we use the marginal damages as reported in the Section 3.5, assuming an important contribution due to anoxia and wilting ($\delta_A = \delta_W$=0.90), but a smaller damage related to extirpation and bank erosion ($\delta_E = \delta_B$=0.10), because we assume that the river flows very slow.
For this study, we divide the Zambezi River into three different zones, related to the two dams: one reach upstream the Kariba Dam, one between the Kariba Dam and the Cahora Bassa Dam, and another one downstream the Cahora Bassa Dam.
In the following figures we have reported the trend of the exponent $\beta$ for each iteration. The morphological boxes are numbered from upstream to downstream of each river reach. Analyzing the various morphological boxes, it is possible to notice that the iterative processes is quite quick.

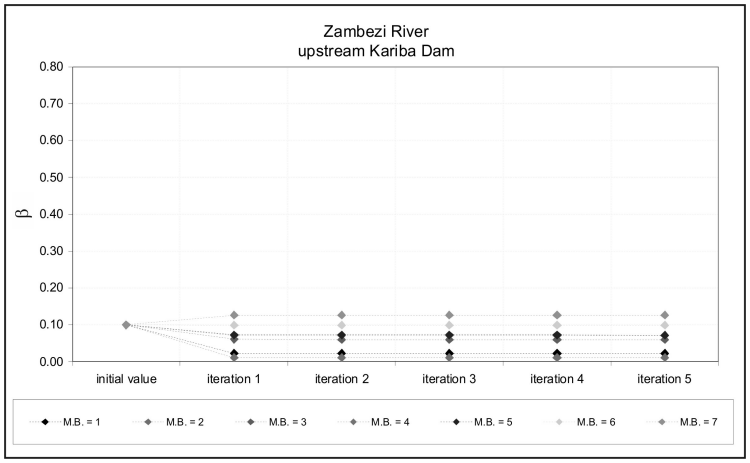


**Figure 5.18:** Variation of the exponent $\beta$ of the river cross-section of the Middle Zambezi River upstream the Kariba Dam.

Upstream the Kariba Dam there are various gorges, and so the river is more straight and can not be wandering. For this reason the shape of the transversal river cross-sections are quite rectangular, with low values of the exponent $\beta$.

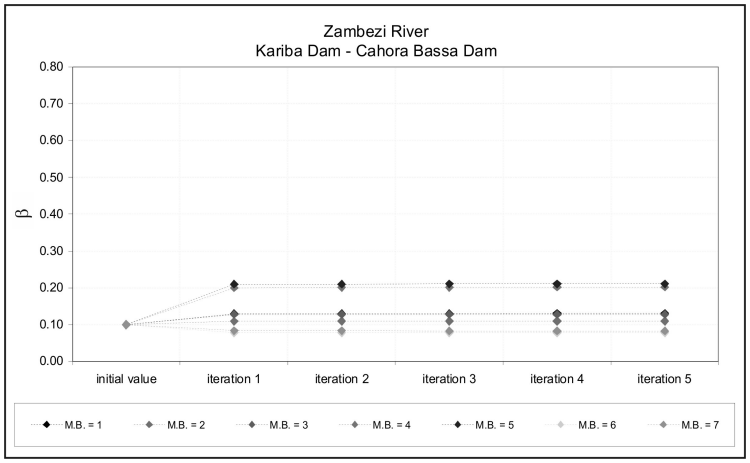


**Figure 5.19:** Variation of the exponent $\beta$ of the river cross-section of the Middle Zambezi River between the Kariba Dam and the Cahora Bassa Dam.

From the Kariba Dam to the Cahora Bassa Dam the river flows between narrow levees, and so the exponents $\beta$ remain quite low, closer to 0.10-0.20.

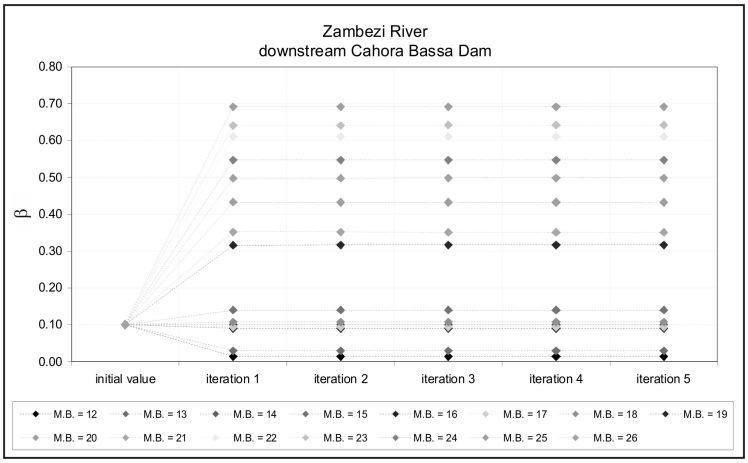


**Figure 5.20:** Variation of the exponent $\beta$ of the cross-section of the Lower Zambezi River downstream the Cahora Bassa Dam.

As we can see in the Figure 5.2, downstream the Cahora Bassa Dam there are two zones of gorges, and so the value of the exponent $\beta$ remains low, similar to the case of the Middle Zambezi. Also in the mobile sand zone the value of $\beta$ is low, closer to 0.10, while in the distributary zone the values of the exponents become higher. In the last part, near to the delta, the river has a quite triangular shape, with high values of the exponent $\beta$.

## 5.6 Conclusions

A combination of a simplified 1-D hydro-morphodynamic model, based on the Local Uniform Flow hypothesis, and a quasi 2-D sub-model, able to describe the evolution of the transversal cross-sections, has been applied to the Lower Zambezi River, from the Cahora Bassa Dam to the Indian Ocean. The coupled model described here is an attempt to simulate the interaction between hydrology, morphology and riparian vegetation on unsurveyed rivers by resorting to satellite informations.

The transversal profile sub-model indicates that the conventional bathymetric survey may be conveniently substituted by periodic satellite images, reproducing different inundated areas due to different water flow, also for unsurveyed rivers. By applying opportune procedures, in facts, these images provide both a synthetic description of the river cross-section profile and a description of the density and the growing of the riparian vegetation.

The main results are the following: i) during the last and the next centuries the largest part of Lower Zambezi in undisturbed conditions shows a continuous and almost constant bottom aggradation and sediment fining; ii) this “natural” trend is affected by the construction of the Kariba Dam (1959) and

the Cahora Bassa Dam (1975), but only in a relatively minor way; iii) the perturbations created by these impoundments, respectively in terms of water flow and sediment interception, appear to propagate along the river with different celerities and with different consequences on the bottom profile and grain size composition; iv) the construction of the two dams has produced an erosion of the delta area, which seems however somehow recovering.

The simulation results are obviously influenced by the scarce and uncertain information utilized for input data and the model calibration. The prediction, however, seems to be quite robust, at least in qualitative terms, as shown by the sensitivity analysis carried on in a precedent study (Ronco et al., 2010).

The model proves to be extremely flexible, inasmuch it can make use of a variety of data differently distributed in space and time. Consequently, its prediction capacity will certain improve as the available data will increase in quantity and quality. The description of the river cross-section appears quite realistic, but a more detailed analysis of the the riparian vegetation can be useful for a better description of the biological parameters.

Finally, the model flexibility permits us to apply this methodology for studying morphodynamic processes at much longer time-scale. In this case the portion of the river to be reproduced must be correspondingly larger up to the entire Zambezi watershed.

# Chapter 6

# Discussion and future developments

The knowledge of sediment budget at watershed scale and extended over long period of time (namely at historical or geological scale) appears to be more and more important for predicting and possibly mitigating the anthropogenic impact of large hydraulics works (dams, sediment mining, etc.) on fluvial and coastal system.

Indeed, due to the gradually slow response of the fluvial systems to perturbations (Fasolato et al., 2011), the effects of engineering interventions require long period of time to propagate along the river network from the upper part to the delta. Therefore, in principle, long simulations should correspondingly be carried on over the entire watershed.

Simulations at watershed scale can provide some informations about the evolution of the river and the variation of the sediment transport all over the basin, often necessary before taking decisions regarding the river basin management. Moreover, these informations may be used for prescribing boundary conditions for 2-D or 3-D models of limited part of the river network, necessary for studies about the detailed morphological evolution of a single river reach.

The main difficulties for implementing the conventional, complete models at watershed scale are the scarce quality and the quantity of the available data (geometrical, topographical, hydrological and sedimentological) distributed over the entire basin, especially in the case of large unsurveyed rivers. It has been therefore necessary to develop a series of less demanding models, useful for these circumstances.

In this thesis we have developed a combination between a 1-D hydro-morphodynamic model and a quasi 2-D cross-section sub-model, which requires extremely simple and aggregated topographic data (easily available from remote sensing analysis), quite coarse hydrological informations (to be obtainded from simple hydrological models) and non-detailed sedimentological informations.

The model is quite accurate in reproducing the space-and time-variations of the geometry and the grain size composition, in spite of its simplified description of the liquid and the solid phase.

Part of the dissertation is devoted to establish the validity and the limits of the simplified models, especially regarding the quasi 2-D sub-model. The Local Uniform Flow hypothesis is valid for large rivers, where the flood waves are much longer than the river reach and the dimension of the morphological boxes is adequate to describe the evolution of these rivers. The description of the evolution of the river cross-section profile is useful for describing the interaction between hydrology, morphology and growth of the riparian vegetation along the river, in order to better understanding the evolution of the entire river network.

The simplified structure of the model is useful for studying the evolution of a river at long-time scale, and for studying the interactions between the river and various forcing terms (construction of dams, sediment mining, climatic change, etc.). The model can substitute, in an adequate manner, other 1-D morphodynamic models, which necessitate to detailed data, for describing the evolution of a river with limited computational effort.

The model is applied to the Middle and Lower Paraná River, for describing the evolution of this water course during the last century and for making a comparison between this model and an other morphodynamic model. The results of the two models are quite similar, and are plausible respect to the few information about the evolution of the river. For a more reliable verification of the 1-D simplifyed model, some other data would be necessary, especially for better calibrating the annual duration curve of the river width and the behaviour of the main channel of the river. The extension of the model to the entire watershed of the Paraná River and to long-term simulations would very likely improve the model performances. Detailed data about the riparian vegetation present along the banks of the Paraná River are necessary for a better evaluation of the morphology of the river cross-section due to the growth of the vegetation.

The 1-D hydro-morphodynamic model is also applied to the case of the Zambezi River, for studing the longitudinal and the transversal evolution of this water course due to the construction of two hydropower reservoirs. In this case it is possible to observe a general similarity between the results of the model and the scarce data available in Literature, also regarding the vegetational patterns. Other data about the growth of the riparian vegetation along the Lower Zambezi River is necessary for better describing the interactions between hydrology, morphology and vegetation. More data about the entire water course permit the extension of the model to the entire watershed of the Zambezi River.

# Bibliography


Abad J.D., Buscaglia G.C., Garcia M.H. (2007). 2D stream hydrodynamic, sediment transport and bed morphology model for engineering applications. Hydrological Processes.

Adam J.A. (2003) Mathematics in Nature. Princeton University Press, pp. 360.

Alarcón J.J., Szupiany R., Montagnini M.D., Gaudin H., Prendes H.H., Amsler M.L. (2003) Evaluación del transporte de sedimentos en el tramo medio del Río Paraná. only in Spanish.

Albertson J.D., Kiely G. (2001). On the structure of soil moisture time series in the context of Land Surface Models. J. Hydrol.

Allen P.A., Densmore A.L. (2000). Sediment flux from an uplifting fault block. Basin Res., vol. 12, pp. 367 380.

Amsler M.L., Ramonell C.G., Toniolo H.A. (2005). Morphologic changes in the Paraná River channel (Argentina) in the light of the climate variability during the 20th century. Geomorphology, vol. 70, pp. 257-278.

Amsler M.L., Drago E.C., Paira A.R. (2007). Fluvial Sediments: Main Channel and Floodplain Interrelationship. M.H. Iriondo, J.C. Paggi, and M.J. Parma (Eds.) The Middle Paraná River: Limnology of a Subtropical Wetland, Springer-Verlag Berlin Heidelberg, Germany.

Amsler M.L., Drago E.C. (2009). A review of the suspended sediment budget at the confluence of the Paraná and Paraguay Rivers. Hydrological Processes 23, pp. 3230-3235.

Anderson J., Dutton P., Goodman P., Souto B., (1990). Evaluation of the Wildlife Resource in the Marromeu Complex with recommendations for its Further Use. LOMACO, Maputo, Mozambique.

Armanini A., Di Silvio G. (1988). A one-dimensional model for the transport of a sediment mixture in non equilibrium flow conditions. Journal of Hydraulics Research, vol. 26, no. 3.

Attwell R.I.G. (1970). Some effects of Lake Kariba on the ecology of a floodplain of the mid-Zambezi valley of Rhodesia. Biological Conservation, vol. 2, no. 3, pp. 189-196.

Auble G.T., Friedman J.M., Scott M.L. (1994). Relating riparian vegetation to oresent and future streamflows. Ecological Applications, vol. 4, no. 3, pp. 544-554.

Baxter R.M. (1977). Environmental effects of dams and impoundments. Annual Review of Ecology and Systematics 8, pp. 255-283.

Barsoum N. (2002). Relative contributions of sexual and asexual regeneration strategies in Populus nigra and Salix alba during the first years of establishment on a braided gravel bed river. Evolutionary Ecology 15, pp. 255-279.

Basile P., Peviani M.A. (1996). Morphodynamic mathematical model for non-uniform grainsize sediment s: an application to the exceptional flood event of 1987 in the Mallero river (Italy). Internal report of FRIMAR Project.

Basile P.A., Riccardi G.A., Zimmermann E.D., Stenta H.R. (2010). Simulation of erosion-deposition processes at basin scale by a physically-based mathematical model. International Journal of Sediment Research 25, pp. 91-99.

Basson G. (2004). Proposed Zambezi River Case Study for ISI: Africa. Confidential technical report IHP-UNESCO ISI Steering Committee, Paris, France.

Bates P.D., Anderson M.G., Baird L., Walling D.E., Simm D. (1992). Modelling floodplain flow with a two dimensional finite element scheme. Earth Surface Processes and Landform 17, pp. 575-588.

Bates P.D., Anderson M.G., Hervouet J.M. (1995). An initial comparison of 2-dimensional finite element codes for river flood simulation. Proc. Inst. Civ. Engrs. Water: Maritime and Energy 112, pp. 238-248.

Baum R.L., Savage W.Z., Godt J.W. (2002). TRGRS - A Fortran program for transient rainfall infiltration and Gps-based regional slope stability analysis. U.S. Geological Survey, Open-File Report 02-424.

Beilfuss R.D., Allan D.G. (1996). Wattled Crane and Wetland Surveys in the Great Zambezi Delta, Mozambique. Proceedings of African Crane and Wetland training workshop, pp. 345-354.

Beilfuss R.D., Davies B.R. (1999). Prescribed flooding and wetlands rehabilitation in the Zambezi Delta, Mozambique. An Int. Perspective on Wetland Rehabilitation, pp. 143-158.

Beilfuss R., Dos Santos D. (2001). Patterns of Hydrological Change in the Zambezi Delta, Mozambique. Program for the Sustainable Management of Cahora Bassa Dam and the Lower Zambezi Valley. Working Paper no. 2. Direco Nacional das Aguas, Maputo, Mozambique.

Beilfuss R., Moore D., Bento C., Dutton P. (2001). Patterns of Hydrological Change in the Zambezi Delta, Mozambique. Program for the Sustainable Management of Cahora Bassa Dam and the Lower Zambezi Valley. Working Paper no. 3. Direco Nacional das Aguas, Maputo, Mozambique.

Bendix J., Hupp C.R. (2000). Hydrological and geomorphological impacts on riparian plant communities. Hydrological Processes 14, pp. 2977-2990.

Bertoldi W., Gurnell A.M., Surian N., Tockner K., Zanoni L., Ziliani L., Zolezzi G. (2009). Understanding reference processes: linkages between river flows, sediment dynamics and vegetated landforms along the Tagliamento river, Italy. River Research and Applications, no. 25, pp. 501-516.

Bertoldi W., Zanoni L., Tubino M. (2010). Assessment of morphological changes induced by flow and flood pulses in a gravel bed braided river: The Tagliamento River (Italy). Geomorphology, vol. 114, pp. 348-360.

Beven K. (1989). Changing ideas in hydrology - The case of physically based model. Journal of Hydrology, vol. 105, pp. 157-172.

Biedenharn D.S., Copeland R.R., Thorne C.R., Soar P.J., Hey R.D., Watson C.C. (2000). Effective Discharge Calculation: A Practical Guide. Coastal and Hydraulics Laboratory, US Army Corps of Engineers.

Bhowmik N.G., Stall J.B. (1979). Hydraulic Geometry and Carrying Capacity of Floodplains. University of Illinois, UILU-WRC-79-0145, Research Report 145.

Bolla Pittaluga M., Seminara G. (2003). Depth integrated modelling of suspended sediment transport. Water Resources Research 39(5), 1137.

Bolton P. (1983). The regulation of the Zambezi in Mozambique: a study of the origins and impact of the Cabora Bassa project. Ph.D. Thesis, University of Edinburgh, England.

Bombino G., Gurnell A.M., Tamburino V., Zema D.A., Zimbone S.M. (2008). Sediment size variation in torrents with chech dams: Effects on riparian vegetation. Ecological Engineering 32, pp. 166-177.

Bonaldo D. (2008). Implicazione idrauliche, morfometriche e vegetazionali delle variazioni di larghezza dei corsi d'acqua. Tesi di Laurea Magistrale, Universitá degli Studi di Padova, Italy. only in Italian

Bonetto A.A., Wais J.R., Castello H.P. (1989). The increasing damming of the Paraná basin and its effects on the lower reaches. Regualted Rivers: Research and Management, vol. 4, pp. 333-346.

Boulanger J.P., Leloup J., Penalba O., Rusticucci M., Lafon F., Vargas W. (2005). Observed precipitation in the Paraná-Plata hydrological basin: long-term trens, extreme conditions and ENSO teleconnections. Climate Dynamics 24, pp. 393-413.

Bowmaker A.P. (1960). A Report on the Kariba Lake Area and Zambezi River Prior to Inundation, and the Initial Effects of Inundation with Particular Reference to the Fisheries. Training Centre on Fishery Survey for the Countries of African Region (Report), FAO Library Fiche AN: 59986. Rome, Italy.

Bradley C., Smith D.G. (1984). Meandering Channel Response to Altered Flow Regime: Milk River, Alberta and Montana. Water Resources Research, vol. 20, no. 12, pp. 1913-1920.

Brandt S.A. (2000). Classification of geomorphological effects downstream of dams. Catena 40, pp. 375-401.

Bristow C.S., Best J.L. (1993). Braided rivers: perspective and problems. Braided Rivers, Geological Society, Special Publication no. 75, pp. 1-11.

Brookes C.J., Hooke M.J., Mant J. (2000). Modelling vegetation interactions with channel flow in river valleys of the Mediterranean region. Catena, vol. 40, pp. 93-118.

Bruk S. (2003). Sediment research and social response: Regional Accents and the International Sediment Initiative of IHP. Proceedings of the ICCORES-UNESCO Workshop: From watershed slope to coastal areas: sedimentation processes at different scales. Venice, Italy.

Brown A.G., Harper D., Peterken G.F. (1997). European floodplain forests: structure, functioning and management. Global Ecology and Biogeography Letters, no. 6, pp. 169-178.

Camilloni I.A., Barros V.R. (2002). Extreme Discharge Events in the Paraná River and their Climate Forcing. Journal of Hydrology 278, pp. 94-106.

Camporeale C., Ridolfi L. (2006). Riparian vegetation distribution induced by river flow variability: A stochastic approach. Water Resources Research, vol. 42.

Camporeale C., Ridolfi L. (2010). Interplay among river meandering, discharge stochasticity and riparian vegetation. Journal of Hydrology 382, pp. 138-144.

Cao Z., Rodney D., Shinji E. (2002). Coupled and decoupled numerical modeling of flow and morphological evolution in alluvial rivers. Journal of Hydraulic Engineering, vol. 128, no. 3.

Carton W. (1986). Carrying capacity and the limits to freedom. Social Ecology Session, vol. 1.

Castro S.L., Cafaro E.D., Gallego M.G., Ravelli A.M., Alarcón J.J., Ramonell C.G., Amsler M.L. (2007). Evolución morfológica histórica del cauce del Río Paraná en torno a Rosario (km 456-406). only in Spanish.

Catuneanu O., Wopfner H., Eriksson P.G., Cairnecross B., Rubidge B.S., Smith R.M.H., Hancox P.J. (2005). The Karoo basins of south central Africa. Journal of African Earth Sciences 43, pp. 211-253.

Cea L., Puertas J., Vázquez-Cendón M.-E. (2007). Depth Averaged Modelling of Turbulent Shallow Water Flow with Wet-Dry Fronts. Archives of Computational Methods in Engineering 14, pp. 303-341.

Chenje M. (2000). State of the Environment Zambezi Basin. SADC/IUCN/ZRA/SARDC, Maseru/Lusaka/Harare.

Chitale S.V. (1970). River channel patterns. Journal of the Hydraulics Division, vol. 96, no. 1, pp. 201-221.

Church M. (1995). Geomorphic response to river flow regulation: case studies and time-scales. Regulated Rivers: Research & Management, vol. 11, pp. 3-22.

Church M. (2002). Geomorphic thresholds in riverine landscapes. Freshwater Biology, vol. 47, pp. 541557.

Claris LPB (2011). Report D9.13: Model of the geomorphology and sediments in the Lower Paraná River. Claris LPB. http://www.claris-eu.org/.

Cooper D.J., Merritt D.M., Andersen D.C., Chimner R.A. (1999). Factors controlling the establishment of Fremont cottonwood seedlings on the upper Green River, USA. Regulated Rivers: Research and Management, vol. 15, no. 5, pp. 419-440.

Cotton J.A., Wharton G., Bass J.A.B., Heppell C.M., Wotton R.S. (2006). The effects of seasonal changes to in-stream vegetation cover on patterns of flow and accumulation of sediment. Geomorphology, vol. 77, pp. 320-334.

Coulthard T.J., Hicks D.M., Van De Wiel M.J. (2007). Cellular modelling of river catchments and reaches: Advantages, limitations and prospects. Geomorphology, vol. 90, pp. 192-207.

Cugier P., Le Hir P. (2002). Development of a 3D Hydrodynamic Model for Coastal Ecosystem Modelling. Application to the Plume of the Seine River (France). Estuarine, Coastal and Shelf Science, vol. 55, pp. 673-695.

Cui Y., Parker G., Paola C. (1996). Numerical simulation of aggradation and downstream fining. Journal of Hydraulic Research, vol. 34(2). pp. 195-204.

Cui Y., Parker G. (2005). Numerical model of sediment pulses and sedimentsupply disturbances in mountain rivers. Journal of Hydraulic Engineering, vol. 131, no. 8, pp. 646-656.

Curran J., Wilcock P.R. (2005). Effect of sand supply on transport rates in a gravel-bed channel. Journal of Hydraulic Engineering, vol. 131, no. 11.

Dal Monte L., Di Silvio G. (2004). Sediment concentration in tidal lagoons. A contribution to long-term morphological modelling. Journal of Marine Systems, vol. 51, no. 1-4, pp. 243-255.

Dade W.B., Friend P.F. (1998). Grain-Size, Sediment-Transport Regime, and Channel Slope in Alluvial Rivers. Journal of Geology, vol. 106, pp. 661-675.

Davies R.D., Hall A., Jackson P.B.N. (1975). Some ecological aspects of the Cabora Bassa Dam. Biol. Conserv. 8, pp. 189-201.

Davies R.D. (1986). The Zambezi River system. The Ecology of River Systems, vol. 60, pp. 225-267.

Davies R.D., Beilfuss R.D., Thomas M.C. (2000). Cahora Bassa Retrospective, 1974-1997: effects of flow regulation on the Lower Zambezi River. Limnology in the developing world 27, pp. 1-9.

De Vriend H.J., Capobianco M., Chesher T., De Swart H.E., Latteux B., Stive M.J.F. (1993). Approaches to long-term modelling of coastal morphology: a review. Coastal Engineering, vol. 21, n 1-3, pp. 225-269.

De Vriend H. J. (1996). Mathematical modelling of meso-tidal barrier island coasts. Part I: Empirical and semi-empirical models. Advances in coastal and ocean engineering, pp. 21152149.

Defina A. (2000). Two-dimensional shallow flow equations for partially dry areas. Water Resources Research, vol. 36, no. 11, pp. 3251-3264.

Defina A. (2003). Numerical experiments on bar growth. Water Resources Research, vol. 39, no. 4.

Denconsult (1998). Sector Studies under ZACPLAN. Zambezi River system action plan.

Depetris P.J., Probst J.-L., Pasquini A.I., Gaiero D.M. (2003). The geochemical characteristics of the Paraná River suspended sediment load: an initial assessment. Hydrological Processes 17, pp. 1267-1277.

De Rosa P. (2008). Un approccio modellistico per il fenomeno delle occlusioni d'alveo per frane: una modifica al modello CAESAR. Giornale di Geologia Applicata, vol. 8, no. 2, pp. 277-284. only in Italian

Di Silvio G. (1983) Modelli matematici per lo studio di variazioni morfologiche dei corsi d'acqua a lunga e breve scala temporale. Studi e Ricerche, no. 356, Istituto di Idraulica, Universitá degli Studi di Padova, Italy. only in Italian

Di Silvio G. (1986). Validity and limitations of different Transport Models with particular reference to sediment transport. Agricultural Nonpoint Source Pollution: Model Selection and Application. Developments in Environmental Modeling 10, Elsevier, New York. 1986. pp. 191-212.

Di Silvio G., Peviani M. (1989). Modelling Short- and Long-Term evolution of mountain rivers: an application to the torrent Mallero (Italy). Int. Workshop on Fluvial Hydraulics of Mountain Regions, Trento (Italy). Also in: Lecture Notes in Earth Sciences no. 37, Fluvial Hydraulics of Mountain Regions, A. Armanini and G. Di Silvio, eds. Springer-Verlag, 1991, pp. 293-315.

Di Silvio G. (1991). Sediment exchage between stream and bottom: a four layer model. Proceedings of a Seminar on Grain Sorting, Ascona, Svizzera.

Di Silvio G., Marin A. (1996a). Analysis and evalutation of various simplifying hypothesis in morphological one-dimensional models, Commission of the European Communities, Directorate General XII for Science, Research and Development, Research and Technical Developmnet Programme in the Field of Environment. FRIMAR Project, Techinal Report no. 1.

Di Silvio G., Marin A. (1996b). Analytical approach to river morphodynamics: effects of space-and time-irregularities and grain-size non-uniformity. Commission of the European Communities, Directorate General XII for Science, Research and Development, Research and Technical Development Program in the Field of Environment, FRIMAR Project, Technical Report no. 2, pp. 48.

Di Silvio G. (2004). Review of state-of-the-art research on erosion and sediment dynamics from catchment to coast (a Northern perspective. Meeting of the Task Force Group of ISI (International Sediment Initiative) of UNESCO-IHP (technical report), Paris, France.

Di Silvio G. (2006). Sediment sources and causes: Approaches to sediment yield evaluation. Proceedings of the International Sediment Initiative Conference (ISIC), Khartoum, Sudan.

Di Silvio G. (2007). Simulating long-term river morphodynamics at watershed scale. Invited Speech, Symposium to honour Professor Selim Yalin, Winnipeg, Maritoba, Canada.

Di Silvio G., Nones M., Guarino L. (2009a). Bilancio di sedimenti a scala di bacino: un modello per il fiume Adige. Rivista ufficiale Autoritá di Bacino del fiume Adige: Adige-Etsch, no. 1/2. only in Italian

Di Silvio G., Bonaldo D., Nones M. (2009b). Morphological and vegetational response to hydrological changes in rivers. Proceedings of the $33^{rd}$ IAHR Congress, Vancouver, British Columbia, Canada.

Di Silvio G., Nones M., Bonaldo D. (2010a). A synthetic river cross-section for one-dimensional models, Proceedings of the $11^{th}$ International Symposium on River Sedimentation (ISRS), Stellenbosch, South Africa.

Di Silvio G., Dall'Angelo C., Bonaldo D., Fasolato G. (2010b). Long-term of planimetric and bathymetric evolution of a tidal lagoon. Continental Shelf, vol. 30, pp. 894-903.

Di Silvio G., Nones M. (2011a). What strategic response to long-term morphological changes of large rivers?. Proceeding of the International Conference on the Status and Future of the World's Large Rivers. Vienna, Austria.

Di Silvio G., Franzoia M., Nones M., Bonaldo D., Zaggia L., Lorenzetti G., Dall'Angelo C. (2011b). Evaluating sediment input of rivers flowing in the Lagoon of Venice. Scientific Research and Safeguarding of Venice, Corila. Volume VII, 2007-2010 results.

Diaz A.F., Studzinski C.D., Mechoso C.R. (1998). Relationships between Precipitation Anomalies in Uruguay and Southern Brazil and Sea Surface Temperature in the Pacific and Atlantic Oceans. Journal of Climate, vol. 11, pp. 251-271.

Dollar E.S.J. (1998). Palaeofluvial geomorphology in southern Africa: a review. Progress in Physical Geography 22 (3), pp. 325-349.

Douglas D.A. (1995). Seed germination, seedling demography, and growth of Salix Setchelliana on glacial river gravel bars in Alaska. Canadian Journal of Botany, vol. 73, no. 4, pp. 1182-1187.

Drago E.C., Amsler M.L. (1988). Suspended sediment at a cross section of the Middle Paraná River: concentration, granulometry and influence of the main tributaries. Proceedings of the Porto Alegre Symposium, IAHS Publ. no. 174.

Du Toit R.F. (1984). Some environmental aspects of proposed hydro-electric schemes on the Zambezi river, Zimbabwe. Biological Conservation 28, pp. 73-87.

Duarte P., Meneses R., Hawkins A.J.S., Zhu M., Fang J., Grant J. (2003). Mathematical modelling to assess the carrying capacity for multi-species culture within coastal waters. Ecological Modelling 168, pp. 109-143.

Dunham K.M. (1989). Vegetation-environment relations of a Middle Zambezi floodplain. Vegetatio 82, pp. 13-24.

Egiazaroff I.V. (1965). Calculation of non-uniform sediment concentration. Journal of Hydraulic Div. 91, pp. 225-248.

Edwards P.J., Kollmann J., Gurnell A.M., Petts G.E., Tockner K., Ward J.V. (1999). A conceptual model of vegetation dynamics on gravel bars of a large Alpine river. Wetlands Ecology and Management 7, pp. 141-153.

Engelund F., Hansen E. (1967). A monograph on sediment transport in alluvial streams. Teknisk Forlag, Copenhagen, Denmark.

Earth Resources Observation & Science (EROS) (2000). HYDRO1K Africa Documentation. Elevation Derivative Database. U.S. Geological Survey, Sioux Falls. U.S.A. http://eros.usgs.gov/#/Find_Data/Products_and_Data_Available/gtopo30/hydro.

FAO (2001). Dams, fish and fisheries: Opportunities, challenges and conflict resolution. FAO Fisheries Technical Paper. eds Marmulla G., pp. 166.

Fasolato G., Ronco P., Tregnaghi M. (2006). Morphodynamics of mountains rivers following repeated sediment release from reservoirs. Proceedings of the International Conference on Fluvial Hydraulics, Riverflow 2006. Lisbon.

Fasolato G. (2008). Simplified Models for Morphological Evolution of River and Lagoon System. PhD Thesis, Universitá degli Studi di Padova, Italy.

Fasolato G., Ronco P., Di Silvio G. (2009). How fast and how far do variable boundary conditions affect river morphodynamics?. Journal of Hydraulic Research, vol. 47, no. 3, pp. 329-339.

Fasolato G., Ronco P., Langendoen E.J., Di Silvio G. (2011). Validity of Uniform Flow Hypothesis in One-Dimensional Morphodynamic Models. Journal of Hydraulic Engineering, ASCE, vol. 37, no. 2, pp. 183-195.

Francis R.A., Gurnell A.M., Petts G.E., Edward P.J. (2005). Survival and growth responses of Populus nigra, Salix elaeagnos and Alnus incana cutting to varying levels of hydric stress. Forest Ecology and Management, no. 210, pp. 291-301.

Franz E.H., Bazzaz F.A. (1977). Simulation of vegetation response to modified hydrological regimes: A probabilistic model based on niche differentiation in a floodplain forest. Ecology, vol. 58, pp. 176-183.

Friedman J.M., Auble G.T. (1999). Mortality of riparian box elder from sediment mobilization and extended inundation. Regulated Rivers: Research & Management, vol. 15, no. 5, pp. 463-476.

Friend P.F., Sinha R. (1993). Braiding and meandering parameters. Braided Rirvers, Geological Society, Special Publication no. 75, pp. 105-111.

Gabriel J.-P., Saucy F., Bersier L.-F. (2005). Paradoxes in the logistic equation?. Ecological Modelling 185, pp. 147-151.

Galappatti R. (1983). A depth integrated model for suspended sediment transport. TU Delft, Internal Report 83-7.

Garcia N.O., Vargas W.M. (1996). The spatial variability of runoff and precipitation in the Río de la Plata basin. Hydrological Sciences, vol. 41, no. 3, pp. 279-299.

Garcia N.O., Vargas W.M. (1998). The temporal climatic variability in the "Río del La Plata" basin displayed by the river discharges. Climatic Change 38, pp. 359-379.

Garcia N.O., Vargas W.M., Venecio M. (2002). About of the 1970/71 climatic jump on the Río de la Plata basin. Proceedings of the $16^{th}$ Conference on Hydrology. American Meteorological Society, pp. 138-141.

Garcia N.O., Mechoso C.R. (2005). Variability in the discharge of South American rivers and in climate. Hydrological Sciences - Journal des Sciences Hydrologiques, vol. 50, no. 3, pp. 459-478.

Garde R.J. (2006). River morphology. eds. New Age International. pp. 479.

Gavrilovic Z. (1988). The Use of an Empirical Method (Erosion Potential Method) for Calculating Sediment Production and Transportation in Unstudied or Torrential Streams. Proceedings of the International Conference on River Regime, Wallingford, England.

Gavrilovic Z., Stefanovic M., Milojevic M, Bacevac J. (2004). The Erosion potential Method and Remote Sensing. Proceedings of the MECEO Conference 2004.

Gee D.M., Anderson M.G., Baird L. (1990). Large floodplain modelling. Earth Surface Processes and Landform 15, pp. 513-523.

Germanoski D., Ritter D.F. (1988). Tributary response to local base level lowering below a dam. Regulated Rivers: Research Management 2, pp. 11-24.

Gerrits A.M.J. (2005). Hydrological modelling of the Zambezi catchment for gravity measurements. Master Thesis, TU Delft.

Gordon E., Meentemeyern R.K. (2006). Effects of dam operation and land use on stream channel morphology and riparian vegetation. Geomorphology, vol. 82, pp. 412-429.

Graf W.L. (2006). Downstream hydrologic and geomorphic effects of large dams on American river. Geomorphology, vol. 79, pp. 336-360.

Gran K., Paola C. (2001). Riparian vegetation controls on braided stream dynamics. Water Resources Research, vol. 37, no. 12, pp. 3275-3283.

Griffiths G.A. (1989). Conversion of braided gravel-bed rivers to single-thread channels of equivalent transport capcacity. Journal of Hydrology, vol. 28, no. 1, pp. 63-75.

Grimm A.M., Barros V.R., Doyle M.E. (2000). Climate Variability in Southern South America Associated with El Ninõ and La Ninã Events. Journal of Climate, vol. 13, pp. 35-58.

Grimm A.M. (2011). Interannual climate variability in South America: impacts on seasonal precipitation, extreme events, and possible effects of climate change. Stochastic Environmental Research and Risk Assessment, vol. 25, pp. 537-554.

Gupta A. (1988). Ecology and Development in the Third World. eds. Routledge, pp. 117.

Gupta A. (2007). Large Rivers: Geomorphology and Management. eds. J. Wiley & Sons, pp. 712.

Gurnell A.M. (1997). The Hydrological and Geomorphological Significance of Forested Floodplains. Global Ecology and Biogeography Letters 3/4 (6), pp. 219-229.

Gurnell A.M., Petts E., Hannah d.M., Smith B.P.G., Edwards P.J., Kollmann J., Ward J.V., Tockner K. (2001). Riparian vegetation and island formation along the gravel-bed fiume Tagliamento, Italy. Earth Surface Processes and Landforms 26, pp. 3162.

Guerrero M., Szupiany R.N., Amsler M. (2011). Comparison of acoustic backscattering techniques for suspended sediments investigations. Flow Measurements and Instrumentation 22, pp. 392-401.

Guy P.R. (1980). River bank erosion in the mid-Zambezi valley, downstream of Lake Kariba. Biological Conservation 19, pp. 199-212.

Hall A., Valente I., Davies B.R. (1977). The Zambezi River in Mozambique: the physicochemical status of the Middle and Lower Zambezi prior to the closure of the Cabora Bassa Dam. Freshwater Biology 7, pp. 187-206.

Hancock G.S., Anderson R.S. (2002). Numerical modeling of fluvial strath-terrace formation in response to oscillating climate. Geological Society of America Bulletin, vol. 114, pp. 1131-1142.

Hardy R.J., Bates P.D., Anderson M.G. (1999). The importance of spatial resolution in hydraulic models for floodpalin environments. Journal of Hydrology, vol. 216, pp. 124-136.

Hartmann S. (2004). Sediment management of alpine reservoirs considering ecological and economical aspects. Proceedings of the $9^{th}$ International Symposium on River Sedimentation (ISRS), Yichang, China.

Helmiö T. (2002). Unsteady 1D flow model of compound channel with vegetated floodplains. Journal of Hydrology. no. 269, pp. 89-99.

Hidroeléctrica de Cahora Bassa (HCB) (2004). Technical Reports on Cahora Bassa Project. Songo, Mozambique.

Hirano M. (1971). River bed degradation with armouring. Trans. of JSCE.

Horvath T.G. (2004). Retention of particulate matter by macrophytes in a first-order stream. Acquatic Botany, 78, pp. 27-36.

Howard A.D. (1996). Modelling Channel Evolution and Floodplains Morphology. eds. J. Wiley & Sons, London.

Hu D., Saito Y., Kempe S. (2001). Sediment and nutrient transport to the coastal zone. In: Galloway, J.N., Melillo, J.M. (Eds.), Asian Change in the Context of Global Climate Change: Impact of Natural and Anthropogenic Changes in Asia on Global Biogeochemical Cycles. IGBP Publication Series, vol. 3. Cambridge Univ. Press, Cambridge, pp. 245-270.

Hu W., Wang G., Deng W., Li S. (2008). The influence of dams on ecohydrological conditions in the Huaihe River basin, China. Ecological Engineering 33, pp. 233-241.

Huang H.Q., Nanson G.C., Fagan S.D. (2002). Hydraulic geometry of straight alluvial channels and the principle of least action. Journal of Hydraulic Research 40(2), pp. 153-160.

Hughes R.H., Hughes J.S. (1992). A Directory of African Wetlands. IUUCN/UNEP/WCMC, Gland, Switzerland. pp. 820.

Hughes F.M.R. (1997). Floodplain biogeomorphology. Progress in Physical Geography, vol. 21, pp. 501-529.

Hui C. (2006). Carrying capacity, population equilibrium, and environment's maximal load. Ecological Modelling 192, pp. 317-320.

Hupp C.R., Osterkamp W.R. 1985. Bottomland vegetation distribution along Passage Creek, Virginia, in relation to fluvial landforms. Ecology, vol. 66, no. 3, pp. 670-681.

Hupp C.R. (1988). Plant ecological aspects of flood geomorphology and paleoflood history. in Flood Geomorphology, eds. J. Wiley & Sons, New York.

Hupp C.R., Simon A. (1991). Bank accretion and the development of vegetated depositional surface along modified alluvial channels. Geomorphology, vol. 4, pp. 111-124.

Hupp C.R., Osterkamp W.R. 1996. Riparian vegetation and fluvial geomorphic processes. Geomorphology, vol. 14, pp. 277-295.

Istituto Nacional de Geologia (ING) (1987). Carta Geologica, escala 1:1,000,000. Ministerio dos Recursos Minerais. Mozambique.

Ikeda S., Izumi N. (1990). Width and Depth of Self-Formed Straight Gravel Rivers With Bank Vegetation. Water Resources Research 26 (10), pp. 2353-2364.

Iriondo M. (2004). The littoral complex at the Paraná mouth. Quaternary International 144, pp. 143-154.

Iriondo M.H., Paggi J.C., Parma M.J. (2007). The Middle Paraná River: Limnology of a Subtropical Wetland. eds. Springer-Verlag Berlin Heidelberg, Germany.

Järvela J. (2005). Effect of submerged flexible vegetation on flow structure and resistance. Journal of Hydrology 307, pp. 233-241.

Jia Y., Wang S.S.Y. (1996). A modeling approach to predict local scour around spur dike-like structures. Procedings of the $6^{th}$ FISC, Subcommittee on Sedimentation Interagency Advisory Committee on Water Data, Las Vegas, Nev., vol. 1, pp. 90-97.

Jia Y., Wang, S.S.Y. (1999). Numerical model for channel flow and morphological change studies. Journal of Hydraulic Engineering, ASCE, vol. 125, no. 9, pp. 924-929.

Jia Y., Scott S., Xu Y., Huang S., Wang S.S.Y. (2005). Three-Dimensional Numerical Simulation and Analysis of Flows around a Submerged Weir in a Channel Bendway. Jornal of Hydraulic Engineering, ASCE, vol. 131, pp. 682-694.

Johnson W.C. (2000). Tree recruitment and survival in rivers: influence of hydrological processes. Hydrological Processes 14, pp. 3051-3074.

Jubb R.A. (1967). Freshwater Fishes of Southern Africa. eds. A.A. Balkema, Cape Town, pp. 248.

Kalesnik F., Aceñolaza P. (2008). Regional distribution of native and exotic species in levees of the lower delta of the Paraná river. Acta Sci. Biol. Sci., vol. 30, no. 4, pp. 391-402.

Kalesnik F., Aceñolaza P., Hurtado M., Martínez J. (2011). Relationship between vegetation of the levee neo-ecosystems and environmental heterogeneity in the Lower Delta of the Paraná River, Argentina. Water and Environment Journal 25, pp. 88-98.

Kandus P., Malvárex A.I. (2004). Vegetation patterns and change analysis in the lower delta islands of the Paraná River (Argentina). Wetlands, vol. 24, no. 3, pp. 620-632.

Karrenberg S., Edwards P.J., Kollmann J. (2002). The life history of Salicaceae living in the active zone of floodplains. Freshwater Biology 47, pp. 733-748.

Kassem A.A., Chaudhry M.H. (2002). Numerical evolution of bed evolution in channel bends. Journal of Hydraulic Engineering, ASCE, vol. 128, no. 5, pp. 507-552.

Kassem a.A., Imran J., Khan J.A. (2003). Three-Dimensional Modeling of Negatively Buoyant Flow in Diverging Channels. Journal of Hydraulic Engineering, ASCE, vol. 129.

Kemp J.L., Harper D.M., Crosa G.A. (2000). The habitat-scale ecohydraulics of rivers. Ecological Engineering 16, pp. 17-29.

Knighton D. (1998). Fluvial forms and processes: a new perspective. eds. J. Wiley & Sons, London.

Kondolf G.M. (1997). Hungry water: effects of dams and gravel mining on river channels. Environmental Management 21 (4), pp. 533-551.

Kozlowski T.T. (1984). Responses of woody plants to flooding. Tree Physiology Monograph no. 1, eds. Heron Publishing, Victoria, Canada.

Kramer K., Vreugdenhil S.J., van der Werf D.C. (2008). Effects of flooding on the recruitment, damage and mortality of riparian tree species: a field and simulation study on the Rhine floodplain. Forest Ecology and Management, vol. 255, pp. 3893-3903.

Krepper C.M., Garcia N.O. (2004). Spatial and temporal structures of trends and interannual variability of precipitation over the La Plata Basin. Quaternary International 114, pp. 11-21.

Laflen J.M., Lane L.J., Foster G.R. (1991). WEPP: A new generation of erosion prediction technology. Journal of Soil and Water Conservation 46, pp. 34-38.

Lago M.E., Miralles-Wilhelm F., Mahmoudi M., Engel V. (2010). Numerical modeling of the effects of water flow, sediment transport and vegetation growth on the spatiotemporal patterning of the ridge and slough landscape of the Everglades wetland. Advances in Water Resources, vol. 33, no. 10, pp. 1268-1278.

Lane E.W. (1955). The importance of fluvial morphology in hydraulic engineering. Proceedings of the American Society of Civil Engineers 81, pp. 1-17.

Lane S.N., Richards K.S. (1997). Linking river channel form and processes: time, space and causality revisited. Earth Surface Processes and Landforms, vol. 22, pp. 249-260.

Langbein W.B., Leopold L.B. (1964). Quasi-equilibrium states in channel morphology. American Journal of Science, vol. 262, pp. 782-794.

Langbein W.B., Leopold L.B. (1966). River Meanders - Theory of Minimum Variance. Geological Survey Paper 422-H.

Lanzoni S., Seminara G. (2006). On the nature of meander instability. Journal of Geophysical Research, vol. 111, pp. 14.

Leopold L.B., Maddock T.Jr. (1953). The Hydraulic Geometry of Stream Channels and Some Physiographic Implications. Geolocigal Survey Paper 252.

Leopold L.B., Wolman M.G. (1957). River Channel Patterns: Braided, Meandering and Straight. U.S. Geological Survey Professional Paper, 282-B.

Leopold L.B., Wolman M.G., Miller J.P. (1964). Fluvial processes in geomorphology. Freeman, San Francisco, USA.

Leslie P.H. (1957). An Analysis of the Data for Some Experiments Carried out by Gause with Populations of the Protozoa, Paramecium Aurelia and Paramecium Caudatum. Biometrika, vol. 44, no. 3/4, pp. 314-327.

Li C.W., Zeng C. (2009). 3D Numerical modelling of flow divisions at open channel junctions with or without vegetation. Advances in Water Resources, vol. 32, pp. 49-60.

Ligon F.K., Dietrich W.E., Trush W.J. (1995). Downstream Ecological Effects of Dams. BioScience, vol. 45, no. 3, pp. 183-192.

Lisi F, Villi V. (2001). Chaotic forecasting of discharge time series: a case study. Journal of the American Water Resources Association, vol. 31, no. 2, pp. 271-279.

Lite S.J., Bagstad K.J., Stromberg J.C. (2005). Riparian plant species richness along lateral and longitudinal gradients of water stress and flood disturbance, San Pedro River, Arizona, USA. Journal of Arid Environments 63, pp. 785-813.

Liu J.T., Huang J.S., Hsu R.T., Chyan J.M. (2000). The coastal depositional system of a small mountainous river: a perspective from grain-size distribution. Marine Geology 165, pp. 63-86.

Luchi R., Hooke J.M, Zolezzi G., Bertoldi W. (2010). Width variations and mid-channel bar inception in meanders: River Bollin (UK). Geomorphology, vol. 119, pp. 1-8.

Lytle D.A., Merritt D.M. (2004). Hydrologic regimes and riparian forests: a structured population model for cottonwood. Ecology 85 (9), pp. 2493-2503.

Maciel F., Díaz A., Terra R. (2010). Variabilidad multi-anual de caudales en ríos de La Cuenca del Plata. Proceedings of the XXIV Congreso Latino Americano de hidráulica, Punta del Este, Uruguay. only in Spanish.

Magilligan F.J., Nislow K.H. (2005). Changes in hydrologic regime by dams. Geomorphology, vol. 71, pp. 61-78.

Maheu C., Cazenave A. (2003). Water level fluctuations in the Plata Basin (South America) from Topex/Poseidon Satellite Altimetry. Geophysical Research Letters, vol. 30, no. 0, XXXX, doi:10.1029/2002GL016033.

Mahoney J.M., Rood S.B. (1998). Streamflow requirements for cottonwood seedling recruitment: An integrative model. Wetlands, vol. 18, no. 4, pp. 634-645.

Main M. (1992). Zambezi: Journey of a River. Southern Book Publishers, Halfway House, South Africa. ISBN 1-86812-257-3. 313 pp.

Makaske B. (2001). Anastomosing rivers: a review of their classification, origin and sedimentary products. Earth-Science Reviews 53, pp. 149-196.

Malvárez A.I. (1999). El Delta del Río Paraná como mosaico de humedales. only in Spanish

Marchetti M. (2002). Environmental changes in the central Po Plain (northern Italy) due to fluvial modifications and anthropogenic activities. Geomorphology, vol. 44, pp. 361-373.

Martín-Vide J.P., Ferrer-Boix C., Ollero A. (2010). Incision due to gravel mining: Modeling a case study from the Gállego River, Spain. Geomorphology, vol. 117 (3-4), pp. 261-271.

Matos J.P., Cohen T., Boillat J.L., Schleiss A.J., Portela MM. (2010). Analysis of flow regime changes due to operation of large reservoirs on the Zambezi River. Environmental Hydraulics, pp. 337-342.

McBride J.R., Strahan J. (1984). Establishment and survival of woody riparian species on gravel bars of an intermitten stream. American Midland Naturalist, vol. 122, no. 2, pp. 235-245.

McCartney M. (2009). Living with dams: managing the environmental impacts. Water Policy 11, Supplement 1, pp. 121-139.

McKenney R., Jacobson R.B., Wertheimer R.C. (1995). Woody vegetation and channel morphogenesis in low-gradient, gravel-bed streams in the Ozrak Plateaus, Missouri and Arkansas. Geomorphology, vol. 13, pp. 175-198.

Menéndez A.N., Sarubbi A. (2007). A Model to Predict the Paraná Delta Front Advancement. Santa Fe, Argentina.

Merritt W.S., Letcher R.A., Jakeman A.J. (2003). A review of erosion and sediment transport models. Environmental Modelling & Software 18, pp. 761-799.

Meyer P.S., Ausubel J.H. (1999). Carrying Capacity: A Model with Logistically Varying Limits. Technological Forecasting and Social Change 61, no. 3, pp. 209-214.

Micheli E.R., Kirchner J.W. (2002). Effects of wet meadow riparian vegetation on streambank erosion. 1. Remote sensing measurements of streambank migration and erodibility. Earth Surface Processes and Landforms, vol. 27, pp. 627-639.

Micheli E.R., Kirchner J.W. (2002). Effects of wet meadow riparian vegetation on streambank erosion. 2. Measurements of vegetated bank strength and consequences for failure mechanics. Earth Surface Processes and Landforms, vol. 27, pp. 687-697.

Millar R.G. (2000) Influence of bank vegetation on alluvial channel patterns. Water Resources Research, 37 (4), pp. 1109-1118.

Minetti J.L., Vargas W.M., Poblete A.G., de la Zerda L.R., Acuña L.R. (2010). Regional droughts in southern South America. Theor. Appl. Climatol., vol. 102, pp. 403-415.

MItsch W.J., Gosselink J. (2007). Wetlands. eds. John Wiley & Sons, New York, pp. 582.

Molles Jr.M.C. (2008). Ecology: concepts and applications. eds. McGraw Hill.

Montgomery D.R., Dietrich W.E. (1994). A physically based model for the topographic control on shallow landsliding. Water Resoures Research 30, pp. 1153-1171.

Montgomery D.R., Buffington J.M. (1998). Channel Processes, Classification, and Response. River Ecology and Mangement. eds. Springer-Verlag, pp. 13-42.

Moore R.J. (1984). A Dynamic Model of Basin Sediment Yield. Water Resources Research, vol. 20, no. 1, pp. 89-103.

Mosley M.P. (1982). Analysis of the Effect of Changing Discharge on Channel Morphology and Instream Uses in a Braided River, Ohau River, New Zealand. Water Resources Research, vol. 18, no. 4, pp. 800-812.

Mount N.J., Louis J., Teeuw R.M., Zukowskyj P.M., Stott T. (2003). Estimation of error in bankfull width comparisons from temporally sequenced raw and corrected aerial photographs. Geomorphology, vol. 56, pp. 65-77.

Muleta M.K., Nicklow J.W. (2005). Sensitivity and uncertainty analysis coupled with automatic calibration for a distributed watershed model. Journal of Hydrology, vol. 306, pp. 127-145.

Muneepeerakul R., Rinaldo A., Rodriguez-Iturbe I. (2007). Effects of river flow scaling properties on riparian width and vegetation biomass. Water Resources Research, vol. 43.

Murray J.D. (2002). Mathematical Biology: I. An Introduction. Third Edition. Eds. Springer.

Nagata N., Hosoda T., Nakato T., Muramoto Y. (2005). Three-Dimensional Numerical Model for Flow and Bed Deformation around River Hydraulic Structures. Journal of Hydraulic Engineering, ASCE, vol. 131, pp. 1074-1088.

Naiman R.J., Décamps H. (1997). The ecology of interfaces: Riparian zones. Annual Review of Ecology and Systematics, vol. 28, pp. 621-658.

Naiman R.J., Décamps H., McClain M.E. (2005). Riparia: Ecology, Conservation, and Management of Streamside Communities. eds. Elsevier Academic Press, New York, pp. 430.

Nakamura F., Yajima T., Kikuchi S. (1997). Structure and composition of riparian forests with special reference to geomorphic site conditions along the Tokachi River, northern Japan. Plant Ecology 133, pp. 209-219.

Nanson G.C., Knighton A.D. (1996). Anabranching rivers: their cause, character and classification. Earth Surface Processes and Landforms, vol. 21, pp. 217-239.

National Academy Press (2002). Riparian Areas: Function and Strategies for management. eds. National Academy Press, pp. 444.

Naumburg E., Mata-Gonzales R., Hunter R.G., McLendon T, Martin D.W. (2005). Phreatophytic vegetation and groundwater fluctuations: A review of current research and application of ecosystem response modeling with an emphasis on great basin vegetation. Environmental Management, vol. 35, no. 6, pp. 726-740.

Nepf H.M. (1999). Drag, turbulence, and diffusion in flow through emergent vegetation. Water Resources Research, 35 (2), pp. 479-489.

Nicholas A.P., Walling D.E. (1998). Numerical modelling of floodplain hydraulics and suspended sediment transport and deposition. Hydrological Processes 12, pp. 1339-1355.

Nilsson C., Berggren K. (2000). Alteration of Riparian Ecosystem Caused by River Regulation. BioScience 783, vol. 50, no. 9, pp. 783-792.

Nones M., Di Silvio G., Guarino L. (2007). Fiume Adige: bilancio di sedimenti a scala di bacino. Tesi di Laurea Magistrale, Universitá degli Studi di Padova, Italy. only in Italian

Nones M., Di Silvio G., Guarino L. (2008). Fiume Adige: modello per l'analisi del bilancio di sedimenti a scala di bacino. Proceedings of the XXXI Convegno di Idraulica e Costruzioni Idrauliche - IDRA 2008, Perugia, Italy. only in Italian

Nones M., Bonaldo D., Di Silvio G., Guarino L. (2009). Sediment budget of rivers at watershed scale: the case of Adige River. Proceedings of the European Geosciences Union, General Assembly 2009 (EGU09), Vienna, Austria.

Nones M., Bonaldo D., Di Silvio G. (2010). Water and sediment management at basin scale: the role of riparian vegetation. Proceedings of the $1^{st}$ IAHR Europe Congress, Edinburgh, Scotland.

Nones M., Di Silvio G. (2011a). Synthetic representation of a river cross-section based on hydrological, morphological and vegetational dynamics. Submitted to Geomorphology.

Nones M., Ronco P., Di Silvio G. (2011b). Modelling the morphological impact of large impoundment on the Lower Zambezi River. Submitted to Journal of River Basing Management

Nones M., Guerrero M., Gaeta M.G., Di Silvio G. (2011c). Analysis of the morphological 1-D evolution of the Paraná River. Submitted to International Journal of Sediment Research.

Nugent C. (1990). The Zambezi River: tectonism, climatic change and drainage evolution. Palaeogeography, Palaeoclimatology, Palaeoecology 78, pp. 55-69.

Olsen N.R.B. (2003). Three dimensional CFD modeling of selfforming meandering channel. Journal of Hydraulic Engineering, ASCE, vol. 129, no. 10, pp. 366-372.

Orfeo O., Stevaux J. (2002). Hydraulic and morphological characteristic of middle and upper reaches of the Paraná River (Argentina and Brazil). Geomorphology, vol. 44, pp. 309-322.

Orpen J.L., Swain C.J., Nugent C., Zhou P.P. (1989). Wrench-fault ant half-graben tectonics in the development of the Palaeozoic Zambezi Karoo basin in Zimbabwe - the "lower Zambezi" and "mid-Zambezi" basins respectively - and regional implications. Journal of African Earth Sciences 8 (2/3/4), pp. 215-229.

Osterkamp W.R., Huopp C.R. (1984). Geomorphic and vegetative characteristics along three northern Virginia streams. Geol. Soc. Am. Bull., vol. 95, pp. 1093-1101.

Osterkamp W.R., Costa J.E. (1987). Change accompanying an extraordinary flood on sandbed stream. in Catastrophic Flooding, eds. Allen and Unwin, St. Leonards, Australia.

Ouillon S., Dartus D. (1997). Three-dimensional computation of flow around groyne. Journal of Hydralic Engineering, ASCE, vol. 123, no. 11, pp. 962-970.

Papanicolau A.N., Bdour A., Wicklein E. (2004). One-dimensional hydrodynamic/sediment transport model applicable to steep mountain streams. Journal of Hydraulic Research, vol. 42, no. 4, pp. 357-375.

Parker G.P., Klingeman P.C. (1982). On why gravel bed streams are paved. Water Resources Research, vol. 18, no. 5, pp. 1409-1423.

Parker G., Wilcock P.R., Paola C., Dietrich W.E., Pitlick J. (2007). Physical basis for quasi-universal relations describing bankfull hydraulic geometry of single-thread gravel bed rivers. Journal of Geophysical Research, 112.

Pearlstine L., McKellar H., Kitchens W. (1985). Modelling the impacts of a river diversion on bottomland forest communities in the Santee River Floodplain, South Carolina. Ecological Modelling, vol. 29, no. 1/4, pp. 283-302.

Pelpola C.P., Hickin E.J. (2004). Long-term bed load transport rate based on aerial-photo and ground penetrating radar surveys of fan-delta growth, Coast Mountains, British Columbia. Geomorphology, vol. 57, pp. 169-181.

Penalba O.C., Robledo F.A. (2010). Spatial and temporal variability of the frequency of extreme daily rainfall regime in the La Plata Basin during the 20th century. Climatic Change 98, pp. 531-550.

Perucca E., Camporeale C., Ridolfi L. (2006). Influence of river meandering dynamics on riparian vegetation pattern formation. Journal of Geophysical Research, vol. 111.

Petts G.E., Gurnell A.M. (2005). Dams and geomorphology: research progress and future directions. Geomorphology, vol. 71, pp. 27-47.

Peviani M., Alteraci J., Danelli A. (2006). Morimor-Gis, modello numerico idraulico-morfologico per la simulazione del trasporto di sedimento multigranulare nei corsi fluviali a forte pendenza. Proceedings of the XXX Convegno di Idraulica e Costruzioni Idrauliche - IDRA 2006, Roma, Italy. only in Italian

Picouet C., Hingray B., Olivry J.C. (2001). Empirical and conceptual modelling of the suspended sediment dynamics in a large tropical African river: the Upper Niger river basin. Journal of Hydrology 250, pp. 19-39.

Poff N.L., Olden J.D., Merritt D.M., Pepin D.M. (2007). Homogenization of regional river dynamics by dams and global biodiversity implications. PNAS, vol. 104, no. 14, pp. 5732-5737.

Pollock M.M., Naiman R.J, Hanley T.A. (1998). Plant species richness in riparian wetlands: A test of biodiversity theory. Ecology, vol. 79, no. 1, pp. 94-105.

Power M.E., Parker G., Dietrich W.E., Sun A. (1995). How does floodplain width affect floodplain river ecology? A preliminary exploration using simulations. Geomorphology, vol. 13, pp. 301-317.

Pryce R.S., Ashmore P.E. (2003). The relation between particle path length distributions and channel morphology in gravel-bed streams: a synthesis. Geomorphology, vol. 56, pp. 167-187.

Quiros R. (1990). The Paraná River basin development and the changes in the lower basin fisheries. Intercercia, vol. 15, no. 6, pp. 442-451.

Randhir T.O., Hawes A.G. (2009). Watershed land use and acquatic ecosystem response: Ecohydrologic approach to conservation policy. Journal of Hydrology 364, pp. 182-199.

Re M., Menéndez A.N., Amsler M.L. (2009). Metodologa para la Generacon de Series Temporales de Descarga Sólida de los Ríos Paraná de las palmas y Paraná Guazú. Proceedings of the Cuarto Simposio Regional sobre Hidráulica de Ríos (RIOS09). Salta, Argentina. only in Spanish.

Reeve W.H. (1960). Progress and Geographical Significance of the Kariba Dam. The Geographical Journal, vol. 126, no. 2, pp. 140-146.

Renard K.G., Foster G.A., Weesies D.A., McCool D.K., Yoder D.C. (1997). Predicting Soil Erosion by Water: A Guide to Conservation Planning with the Revised Universal Soil Equation (RUSLE). Agriculture Handbook no. 703, USDA, Washington DC.

Ribberink J.S., van der Sande J.T.M. (1985). Aggradation in rivers due to overloading-analytical approaches. Journal of Hydraulic Research, vol. 23, no. 3, pp. 273-283.

Richter B.D., Richter H.E. (2000). Prescribing flood regimes to sustain riparian ecosystem along meandering rivers. Conservation Biology, vol. 14, no. 5, pp. 1467-1478.

Ridolfi L., D'Odorico P., Porporato A., Rodriguez-Iturbe I. (2000). Duration and frequency of water stress in vegetation: An analytical model. Water Resources Research, vol. 36, no. 8, pp. 2297-2307.

Ridolfi L., D'Odorico P., Laio F. (2006). Effect of vegetation-water table feedbacks on the stability and resilince of plant ecosystems. Water Resources Research, vol. 42.

Ridolfi L., D'Odorico P., Laio F. (2007). Vegetation dynamics induced by phreatophyte-acquifer interactions. Journal of Theoretical Biology, vol. 248, pp. 301-310.

Robertson A.W., Mechoso C.R. (1998). Interannual and Decadal Cycles in River Flows of Southeastern South America. Journal of Climate, vol. 11, pp. 2570-2581.

Ronco P., Fasolato G., Di Silvio G. (2006). The case of the Zambezi River in Mozambique: Some investigations on solid transport phenomena downstream Cahora Bassa Dam. Proceedings of the International Conference on Fluvial Hydraulics, Riverflow 2006. Lisbon.

Ronco P., Fasolato G., Di Silvio G. (2007). Simulating the profile evolution of large unsurveyed rivers: the case of Zambezi (Austral Africa). Proceedings of the $32^{nd}$ Congress IAHR, Venice, Italy.

Ronco P. (2008). Sediment Budget of Unsurveyed Rivers at Watershed Scale: the Case of Lower Zambezi. PhD Thesis, Universitá degli Studi di Padova, Italy.

Ronco P., Fasolato G., Di Silvio G. (2009). Modelling evolution of bottom profile and grainsize distribution in unsurveyed rivers. International Journal of Sediment Research, vol. 24, no. 2, pp. 127-144.

Ronco P., Fasolato G., Nones M., Di Silvio G. (2010). Morphological effects of damming on lower Zambezi River. Geomorphology, vol. 115, pp. 43-55.

Rood S.B., Kalischuk A.R., Mahoney J.M. (1998). Initial cottonwood seedling recruitment following the flood of the century of the Oldam River, Alberta, Canada. Wetlands, vol. 18, no. 4, pp. 557-570.

Rosatti G., Armanini A. (2008). Un modello matematico bidimensionale per lo studio dell'evoluzione morfologica di corsi d'acqua a carattere fluviale. Proceedings of the XXXI Convegno Nazionale di Idraulica e Costruzioni Idrauliche. Perugia, Italy. only in Italian

Rosgen D.L. (1994). A classification of natural rivers. Catena, vol. 22, pp.169-199.

Roughgarden J. (1974). Population Dynamics in a Spatially Varying Environment: How population Size "Tracks" Spatial Variation in Carrying Capacity. The American Naturalist, vol. 108, no. 963, pp. 649-664.

Rulli M.C., Rosso R. (2007). Hydrologic response of upland catchments to wildfires. Advances in Water Research 30(10), pp. 2072-2086.

Sacchi C.F., Price P.W. (1992). The relative roles of abiotic and biotic factors in seedling demography of arroyo salix (Salix lasiolepis: Salicaceae). American Journal of Botany, vol. 79, no. 4, pp. 395-405.

Salman G, Abdula I. (1995). Development of the Mozambique and Ruvuma sedimentary basins, offshore Mozambique. Sedimentary Geology 96, pp. 7-41.

SCC Brokonsult (Scandiaconsult) (2001). Final Report. Three Crossing Schemes. Consulting Services for Zambezi River Crossing at Caia in Mozambique. Ministerio das Obras Publica e Habitaao, Republica de Mozambique. Maputo.

Shafroth P.B., Stromberg J.C., Patten D.T. (2002). Riparian vegetation response to altered disturbance and stress regime. Ecological Applications, vol. 123, no. 1, pp. 107-123.

Schnitzler A. (1997). River dynamics as a forest process: interactions between fluvial systems and alluvial forests in large European river plains. Botanical Review, no. 63, pp. 40-64.

Schumm S.A. (1969). River metamorphosis. Proceedings of the American Society of Civil Engineers, Journal of the Hydraulics Division HY1, pp. 255-273.

Schumm S.A. (1973). Geomorphic thresholds and complex response of drainage system. In: Fluvial Geomorphology, Proceedings of the $4^{th}$ Annual Geomorphology.

Scodanibbio L., Manez G. (2005). The World Commission on Dams: a fundamental step towards integrated water resources management and poverty reduction? A pilot case in the Lower Zambezi, Mozambique. Physics and Chemistry of the Earth 30, pp. 976-983.

Scott M.L., Shafrot M.B., Auble G.T. (1999). Responses of Riparian Cottonwoods to Alluvial Water Table Declines. Environmental Management, vol., 23, no. 3, pp. 347-358.

Shela O.N. (2000). Management of shared river basins: the case of the Zambezi River. Water Policy 2, pp. 65-81.

Shoko D.S.M., Gwavava O. (1999). Is magmatic underplating the cause of post-rift uplift and erosion within the Cahora Bassa basin, Zambezi rift, Zimbabwe?. Journal of African Earth Sciences 28 (2), pp. 465-485.

Sieben J. (1997). Modeling of hydraulics and morphology in mountain rivers. PhD thesis, also Communications on hydraulic and geotechnical engineering. Report no. 97-3, University of Technology, Delft, The Netherlands.

Simon A. (1989). A model of channel response in disturbed alluvial channel. Earth Surface Processes and Landforms, vol. 14, pp. 11-26.

Singer M.B. (2007). The influence of major dams on hydrology through the drainage network of the Sacramento River basin, California. River Research and Application 23, pp. 55-72.

Singh V.P. (2003). On the theories of hydraulic geometry. International Journal of Sediment Research, vol. 18, no. 3, pp. 196-218.

Sivakumar B., Jayawardena A.W., Fernando T.M.K.G. (2002). River flow forecasting: use of phase-space reconstruction and artificial neural networks approach. Journal of Hydrology, vol. 265, pp. 225-245.

SMEC (2004). Final Report - Zambezi River Basin Mozambique Flood Risk Analysis Project. Maputo. 2.

Smulders M.J.M., Cottrell J.E., Lefevre F., van der Schoot J., Arens P., Vosman B., Tabbener H.E., Grassi, F., Fossati T., Castiglione S., Krystufek V., Fluch S., Burg K., Vornam B., Pohl A., Gebhardt K., Alba N., Agúndez D., Maestro C., Notivol E., Volosyanchuk R., Pospskova M., Bordács S., Bovenschen J., van Dam B.C., Koelewijn H.P., Halfmaerten, D., Ivens B., van Slycken J., Vanden Broeck A., Storme V., Boerjan W. (2008). Structure of the genetic diversity in black poplar (Populus Nigra L.) populations across European river systems: Consequences for conservation and restoration. Forest Ecology and Management 255, pp. 1388-1399.

Stanley E.H, Doyle M.W. (2003). Trading off: the ecological effects of dam removal. Front Ecol Environ, vol. 1, no. 1, pp.15-22.

Stefanovic M., Gavrilovic Z. (2003). Identification of the Erosion Areas Based on "EPM". Natural and socio-economic effects of erosion control in mountainous regions. Belgrade. pp. 257.

Stefanovic M., Gavrilovic Z., Milojevic M. (2004). "Erosion Potential Method" and Erosion risk zoning in mountainous regions. Proceedings of the Interpraevent 2004.

Steiger J., Tabacchi E., Dufour S., Corenblit D., Peiry J.L. (2005). Hydrogeomorphic processes affecting riparian habitat within alluvial channel-floodplain river system: A review for the temperate zone. River Research and Applications, vol. 21, pp. 719-737.

Stevaux J.C., Martins D.P., Meurer M. (2009). Changes in a large regulated tropical river: The Paraná River downstream from the Porto Primavera Dam, Brazil. Geomorphology, vol. 113, pp. 230-238.

Stockstill R.L., Berger R.C., Ronald E.N. (1997). Two-dimensional flow model for trapezoidal high velocity channels. Journal of Hydraulic Engineering, ASCE, vol. 123, no. 10, pp. 844-852.

Strom K., Papanicolaou A.N., Evangelopoulos N., Odeh M. (2004). Microforms in Gravel Bed Rivers: Formation, Disintegration, and Effects on Bedload Transport. Journal of Hydraulic Engineering, vol. 130, pp. 554-568.

Strom K., Papanicolaou A.N., Constantinescu G. (2007). Flow Heterogeneity over 3D Cluster Microform: Laboratory and Numerical Investigation. Journal of Hydraulic Engineering, vol. 133, pp. 273-286.

Stromberg J.C., Patten D.T. (1991). Instream flow requirements for cottonwoods at Bishop Creek, Inyo County, California. Rivers, vol. 2, pp. 1-11.

Stromberg J.C. (2001). Restoration of riparian vegetation in the south-western United States: Importance of flow regimes and fluvial dynamism. Journal of Arid Environments, vol. 49, pp. 17-34.

Sun T., Paola C., Parker G., Meakin P. (2002). Fluvial fan delta: linking channel processes with large-scale morphodynamics. Water Resources Research, vol. 38, no. 8.

Suschka J., Napica P. (1986). Ten years after the conclusion of Cabora Bassa Dam. The impacts of large water projects on the environment. Proceedings of an international symposium. UNEP/UNESCO, Paris, France.

Surian N., Rinaldi M. (2003). Morphological response to river engineering and management in alluvial channels in Italy. Geomorphology, vol. 50, pp. 307-326.

Taylor D.R., Aarssen L.W., Loehle C. (1990). On the relationship between r/K selection and environmental carrying capacity: a new habitat template for plant life history strategies. Oikos, vol. 58, pp. 239-250

Taylor J.P., Wester D.B., Smith L.M. (1999). Soil disturbance, flood management, and riparian woody plant establishment in the Rio Grande floodpalin. Wetlands, vol. 19, no. 2, pp. 372-382.

Taylor M., Ravilious C., Green E.P. (2003). Mangroves of East Africa. UNEP World Conservation Monitoring Centre.

Tealdi S., Camporeale C., Ridolfi L. (2011). Modeling the impact of river damming on riparian vegetation. Journal of Hydrology 396, pp. 302-312.

Tewari S., Kulhavý J., Rock B.N., Hadaš P. (2003). Remote monitoring of forest response to changed soil moisture regime due to river regulation. Journal of forest science, vol. 49, no. 9, pp. 429-438.

Thomas D.S.G., Shaw P.A. (1992). The Zambezi River: tectonism, climatic change and drainage evolution - is there really evidence for a catastrophic flood? A discussion. Palaeogeography, Palaeoclimatology, Palaeoecology 91, pp. 175-182.

Thorne C.R., Hey R.D., Newson M. D. (1997). Applied fluvial geomorphology for river engineering and management. eds. Wiley. Chichester, England.

Thorne C.R. (2002). Geomorphic analysis of large alluvial rivers. Geomorphology, vol. 44, pp. 203-219.

Timberlake J. (1998). Biodiversity of the Zambezi basin wetlands : review and preliminary assessment of available information. Final Report IUCN, Harare, Zimbabwe.

Timberlake J. (2000). Biodiversity of the Zambezi basin. Occasional Publications in Biodiversity, no. 9.

Tockner K., Malard F, Ward J.V. (2000). An extension of the flood pulse concept. Hydrological processes, vol. 14, pp. 2861-2883.

Toner M., Keddt P. (1997). River hydrology and riparian wetlands: a predictive model for ecological assembly. Ecological Applications, vol. 7, no. 1, pp. 236-246.

Trebossen H., Deffontaines B., Classeau N., Kouame J., Rudant J.P. (2005). Monitoring coastal evolution and associated littoral hazards of French Guiana shoreline evolution with radar images. Geoscience 337, pp. 1140-1153.

Tsujimoto T. (1999). Fluvial processes in streams with vegetation. Journal of Hydraulic Research, vol. 37, no. 6, pp. 789-803.

Twidale C.R. (2004). River patterns and their meaning. Earth-Science Reviews 67, pp. 159-218.

Tyagi J.V., Mishra S.K., Singh R., Singh V.P. (2008). SCS-CN based time-distributed sediment yield model. Journal of Hydrology 352(3-4), pp. 388-403.

Udden J.A. (1914). Mechanical composition of clastic sediments. Bull. Geol. Soc. Am.

US Department of the Interior Bureau of Reclamation (2006). Erosion and Sedimentation Manual. US Department of the Interior Bureau of Reclamation, Technical Service Center, Sedimentation and River Hydraulics Group, Denver, Colorado.

USGS Database (2011). Earth Resources Observation and Science (EROS) Center. USGS Global Visualization Viewer, Landsat Archive. U.S. Geological Survey, Sioux Falls. U.S.A. http://glovis.usgs.gov/.

Valiani A., Caleffi V. (2009). Analytical findings for power law cross-sections: Uniform flow depth. Advances in Water Resources 32, pp. 1404-1412.

Vanden Broeck A. (2003). EUFORGEN Technical Guidelines for genetic conservation and use for European black poplar (Populus nigra). International Plant Genetic Resources Institute, Rome, Italy.

Vandermeer J.H. (1969). The Competitive Structure of communities: An Experimental Approach with Protozoa. Ecology, vol. 50, no. 3, pp. 362-371.

Verhaar P.M., Biron P.M., Ferguson R.I., Hoey T.B. (2008). A modified morphodynamic model for investigating the response of rivers to short-term climate change. Geomorphology, vol. 101, pp. 674-682.

Vianello A., D'Agostino V. (2007). Bankfull width and morphological units in an alpine stream of the dolomites (Northern Italy). Geomorphology, vol. 83, pp. 266-281.

Vreugdenhil C.B, (1994). Numerical methods for shallow-water flow. Water Science and Technology Library, vol. 13. eds. Kluwer Academic Publishers, The Netherlands.

Walford H.L., White N.J., Sydow J.C. (2005). Solid sediment load history of the Zambezi Delta. Earth and Planetary Science Letters 238, pp. 49-63.

Walling D.E. (1984). The sediment yields of African rivers. Challenges in African Hydrology and Water Resources, Proceedings of the Harare Symposium. IAHS Publ. 144, pp. 265-283.

Walling D.E., Fang D. (2003). Recent trends in the suspended sediment loads of the world's rivers. Global and Planetary Change 39, pp. 111-126.

Walling D.E. (2008). The changing sediment loads of the world's rivers. Annals of Warsaw, University of Life Science - SGGW, Land Reclamation 39.

Wang Z.-Y., Wu B., Wang G. (2007). Fluvial processes and morphological response in the Yellow and Weihe Rivers to closure and operation of Sanmenxia Dam. Geomorphology, vol. 91 (1-2), 65-79.

Ward J.V., Tockner K., Arscott D.B., Claret C. (2002). Riverine landscape diversity. Freshwater Biology 47, pp. 517-539.

Wentworth C.K. (1922). A scale of grade and class terms for clastic sediments. Journal of Geology V.

Whipple K.X., Tucker G.E. (1999). Dynamics of the stream-power river incision model: Implications for height limits of mountain ranges, landscape response timescales, and research needs. Journal of Geophysical Research, vol. 104, no. B8, pp. 17661-17674.

Wilkerson G.W., Parker G. (2010). Physical Basis for Quasi-Universal Relations Describing Bankfull Hydraulic Geometry of Sand-Bed Rivers. Journal of Hydraulic Engineering 192.

Williams J.R. (1975). Sediment-yield prediction with Universal Equation using runoff energy factor. Present and Prospective Technology for Predicting Sediment Yields and Sources. ARS-S-40, US Department of Agriculture, Agricultural Research Service, pp. 244-252.

Wilson C.A.M.E., Boxall J.B., Guymer I., Olsen N.R.B. (2003). Validation of a three dimensional numerical code in the simulation of pseudo-natural meandering flows. Journal of Hydraulic Engineering, ASCE, vol. 129, no. 10, pp. 758-768.

Wilson C.A.M.E., Yagci O., Rauch H.-P., Olsen N.R.B. (2006). 3D Numerical modelling of a willow vegetated river/floodplain system. Journal of Hydrology 327, pp. 13-21.

Wischmeier W.H., Smith D.D. (1978). Predicting rainfall erosion losses: A guide to conservation planning U.S.D.A.. Agricultural Handbook no. 537, US Department of Agriculture, Washington, D.C.

Wright S., Parker G. (2005). Modeling downstream fining in sand-bed rivers. Journal of Hydraulic Research, vol. 43, no. 6, pp. 613-631.

Wu W., Wang S., Jia Y. (2000a). Non uniform sediment transport in alluvial rivers. Journal of Hydraulic Research, vol. 38, no. 6, pp. 427-434.

Wu W., Rodi W., Wenka T. (2000b). 3D numerical modeling of flow and sediment transport in open channels. Journal of Hydraulic Engineering, vol. 126, no. 1, pp. 4-15.

Wu W., Vieira D.A, Wang S.S.Y. (2004). One-dimensional numerical model for nonuniform sediment transport under unsteady flows in channel networks. Journal of Hydraulic Engineering, vol. 130, no. 9, pp. 914-923.

Xu J. (1996). Wandering braided river channel pattern developed under quasi-equilibrium: an example from the Hanjiang River, China. Journal of Hydrology, vol. 181, pp. 85-103.

Yalin M.S. (1992). River mechanics. eds. Pergamon Press, Oxford, England.

Yanosky T.M. (1982). Effects of flooding upon woody vegetation along parts of the Potamac River floodplain. US Geol. Surv. Prof. Pap., no. 1206.

Ye J., McCorquodate J.A. (1997). Depth-averaged hydrodynamic model in curvilinear collocated grid. Journal of Hydraulic Engineering, ASCE, vol. 123, no. 5, pp. 380-388.

Yukalov V.I., Yukalova E.P., Sornette D. (2009). Punctuated evolution due to delayed carrying capacity. Physica D 238, pp. 1752-1767.

Zaghloul S.S. (2006). Effects of Aswan High Dam on the Nile river regime at delta barrages area. Proceeding of the International Sediment Initiative Conference (ISIC). CD rom. UNESCO Chair in Water Resources, Khartoum, Sudan.

Zedler E.A., Street R.L. (2006). Sediment Transport over Ripples in Oscillatory Flow. Journal of Hydraulic Engineering, vol. 132, pp. 180-194.

Zhou Y., Lu X., Huang Y., Zhu Y. (2004). Anthropogenic impacts on the sediment flux in the dry-hot valleys of southwest China - an example of the Longchuan River. Journal of Mountain Science, vol. 1, no. 3, pp. 239-249.

# Appendix A

| Symbol | Definition | Units | Symbol | Definition | Units |
|---|---|---|---|---|---|
| $Q$ | water discharge | $m^3/s$ | $K(t/\tau)$ | aggregate carrying capacity | - |
| $H$ | water depth | m | $\Delta(t/\tau)$ | aggregate damage | - |
| $U$ | velocity of the current | m/s | $K_A(t/\tau)$ | carrying capacity due to anoxia | - |
| $i$ | bottom slope | - | $K_W(t/\tau)$ | carrying capacity due to wilting | - |
| $j$ | energy slope | - | $K_E(t/\tau)$ | carrying capacity due to extirpation | - |
| $B$ | active river width | m | $K_B(t/\tau)$ | carrying capacity due to bank erosion | - |
| $B_{tot}$ | total river width | m | $\Delta_A(t/\tau)$ | damage due to anoxia | - |
| $B_f$ | flooded river width | m | $\Delta_W(t/\tau)$ | damage due to wilting | - |
| $B_{sv}$ | submerged, vegetated river width | m | $\Delta_E(t/\tau)$ | damage due to extirpation | - |
| $P_s$ | solid discharge | $m^3/s$ | $\Delta_B(t/\tau)$ | damage due to bank erosion | - |
| $d_{eq}$ | equivalent diameter | m | $V_s$ | annual sediment yield | $m^3/y$ |
| $M$ | coefficient of the transport formula | - | $Q_{max}$ | maximum river discharge | $m^3/s$ |
| $m$ | exponent of the transport formula | - | $Q_{mean}$ | mean river discharge | $m^3/s$ |
| $n$ | exponent of the transport formula | - | $Q_{max}$ | minimum river discharge | $m^3/s$ |
| $p$ | exponent of the transport formula | - | $Q_{eq}$ | equivalent river discharge | $m^3/s$ |
| $q$ | exponent of the transport formula | - | $Q_*$ | bankfull river discharge | $m^3/s$ |
| $\alpha'$ | coefficient of the transport formula | - | $\gamma$ | variability coefficient of the river discharge | - |
| $t/\tau$ | seasonal time | - | $\tau$ | annual time | y |
| $a$ | coefficient of the regime formula | - | $\chi$ | Chézy coefficient | $m^{1/2}/s$ |
| $\alpha$ | coefficient of the cross-section formula | - | $\beta$ | exponent of the cross-section formula | - |
| $\Omega$ | morphological parameter | - | | | |

**Table A.1:** List of notations used in the thesis.

# Appendix B

In this section we have reported the mathematical derivations of some values related to the shape factors of the cross-section profile reported in Chapters 2 and 3.

## B.1 Computation of the equivalent discharge

The sediment transport along a river reach is proportional to the liquid discharge.

$$P_s(t/\tau) = M \cdot Q_w(t/\tau)^m \tag{B.1}$$

where the coefficient $M$ represents the ratio between the two quantities.

$$M = \frac{P_s(t/\tau)}{Q_w(t/\tau)^m} \tag{B.2}$$

The coefficient $M$ is related to some characteristics of the river reach, as expressed by the next equation:

$$P_s(t/\tau) = \alpha' \cdot \frac{Q(t/\tau)^m \cdot j(t/\tau)^n}{B(t/\tau)^p \cdot d(t/\tau)^q} \tag{B.3}$$

We can assume that the morphological quantities included in the parameter $M$ (geometry of the river reach, grain size composition of the bottom) do not substantially change during the studied period.
The duration curve of the water discharge is expressed as:

$$Q(t/\tau) = Q_0(\tau) \cdot e^{-\gamma \cdot \frac{t}{\tau}} + Q_{min}(\tau) \tag{B.4}$$

where $Q_0(\tau)$ is the difference between the maximum discharge $Q_{max}(\tau)$ and the minimum discharge $Q_{min}(\tau)$ and the variability coefficient of the river discharge $\gamma$ is expressed by the eq. (B.5).

$$\gamma(\tau) = \frac{Q_0(\tau)}{Q_{mean}(\tau) - Q_{min}(\tau)} = \frac{Q_{max}(\tau) - Q_{min}(\tau)}{Q_{mean}(\tau) - Q_{min}(\tau)} \tag{B.5}$$

The yearly sediment yield is:

$$V_s(\tau) = \int_\tau P_s(t/\tau) d(t/\tau) \tag{B.6}$$

Under the hypothesis that the variability coefficient of the river discharge $\gamma$ is much greater than one, the annual sediment yield becomes:

$$V_s(\tau) = \int_\tau P_s(t/\tau) d(t/\tau) = \frac{1}{m} \cdot Q_0(\tau)^{m-1} \cdot V + Q_{min}(\tau)^m \tag{B.7}$$

with $V$ total annual runoff.
The mean river discharge $Q_{mean}(\tau)$ is related to the total annual runoff.

The equivalent discharge $Q_{eq}(\tau)$, related only to the hydrological data, is expressed as:

$$Q_{eq}(\tau) = \left[\frac{P(\tau)}{M}\right]^{1/m} = \left\{\frac{Q_0(\tau)^{m-1} - [Q_{mean}(\tau) - Q_{min}(\tau)]}{m} + Q_{min}(\tau)^m\right\}^{1/m} \tag{B.8}$$

The computation of the equivalent discharge related to the hydrology and to the shape factor of the river cross-section needs to the description of the relation between the river width and the river discharge.

$$B = \alpha \cdot Q^\beta \tag{B.9}$$

In the eq. (B.3) we can replace the eq. (B.9), and so we obtain:

$$P_s(t/\tau) = \alpha' \cdot \frac{Q(t/\tau)^m \cdot j(t/\tau)^n}{[\alpha \cdot Q(t/\tau)^\beta]^p \cdot d(t/\tau)^q} \tag{B.10}$$

If we substitute the water discharge expressed by the eq. (B.4) into the eq. (B.10) and eq. (B.7), by assuming that the parameter $\gamma$ is much greater than one, we can obtain the expression of the equivalent

river discharge related to the hydrological and morphological data.

$$Q_{eq}(\tau) = \left[ \frac{Q_0(\tau)^{m\cdot(1-\beta)+\beta-1} \cdot \left(\overline{Q}(\tau) - Q_{min}(\tau)\right)}{m\cdot(1-\beta)+\beta} + Q_{min}(\tau)^{m\cdot(1-\beta)+\beta} \right]^{\frac{1}{m\cdot(1-\beta)+\beta}} \tag{B.11}$$

## B.2 Computation of the water depth

We can adopt the Chézy formulation for computing the water depth:

$$H(t/\tau) = \left[ \frac{Q(t/\tau)}{B\cdot\chi\cdot\sqrt{j}} \right]^{2/3} \tag{B.12}$$

We use the exponential description for the active water width (eq. B.13), with the calibration parameters $\alpha$ and $\beta$.

$$B(t/\tau) = \alpha \cdot Q(t/\tau)^{\beta} \tag{B.13}$$

Under the previous assumptions, we can compute the water depth related to the synthetic description of the river cross-section profile.

$$H(t/\tau) = \left[ \frac{Q(t/\tau)^{1-\beta}}{\alpha\cdot\chi\cdot\sqrt{j}} \right]^{2/3} \tag{B.14}$$

The equivalent water depth, related to the equivalent discharge, is expressed by the equation:

$$H_{eq}(\tau) = \left[ \frac{Q_{eq}(\tau)^{0.50}}{a\cdot\chi\cdot\sqrt{j}} \right]^{2/3} \tag{B.15}$$

## B.3 Computation of the flow velocity

Fot the computation of the velocity of the current, we use the expression of the river width (eq. B.13) and the equation of the water depth (eq. B.14). Combining this two expressions we obtain the expression of the flow velocity:

$$U = \frac{Q(t/\tau)^{\frac{1-\beta}{3}} \cdot \chi^{2/3} \cdot j^{1/3}}{\alpha^{1/3}} \tag{B.16}$$

The equivalent velocity, related to the equivalent discharge, is expressed as:

$$U_{eq} = \frac{Q_{eq}^{1/6} \cdot \chi^{2/3} \cdot j^{1/3}}{a^{1/3}} \tag{B.17}$$

# Appendix C

## C.1 Flow duration curve

For describing the aggregate carrying capacity we assume a three-parameters description of the annual flow duration curve.
The submergence time $t/\tau$ is equal to:

$$\frac{t}{\tau} = 1 - \frac{Q^q - Q^q_{min}}{Q^q_{max} - Q^q_{min}} \tag{C.1}$$

In this manner we express the river discharge as:

$$Q(t/\tau) = \left[\left(1 - \frac{t}{\tau}\right) \cdot (Q_{max}(\tau)^q - Q_{min}(\tau)^q) + Q_{min}(\tau)^q\right]^{\frac{1}{q}} \tag{C.2}$$

We can compute the median discharge, related to the submergence time $t/\tau$=0.50, from the exponential description of the flow duration curve (eq. B.4 and from the three-parameters description, and so we can obtain the expression of the coefficent $q$ (eq. 3.10).

## C.2 Carrying capacity related to the anoxia

For the computation of the carrying capacity due to the anoxia we use the description of the flow duration curve with three parameters, expressed by the coefficient $q$.
The single damage due to the anoxia is expressed as:

$$\Delta_A(t/\tau) = \delta_A \cdot \left(1 - \frac{Q(t/\tau)^q - Q_{min}(\tau)^q}{Q_{max}(\tau)^q - Q_{min}(\tau)^q}\right) \tag{C.3}$$

and the related carrying capacity is:

$$K_A(t/\tau) = 1 - \Delta_A \tag{C.4}$$

The extreme values of the submergence time $t/\tau$ are used for computing the maximum and the minimum values of each carrying capacity. for $t/\tau = 0$, $Q(t/\tau) = Q_{max}(\tau)$ $\Rightarrow$ $\Delta_A = 0$, $K_A = 1$
for $t/\tau = 1$, $Q(t/\tau) = Q_{min}(\tau)$ $\Rightarrow$ $\Delta_A = \delta_A$, $K_A = 1 - \delta_A$

## C.3 Carrying capacity related to the wilting

The damage due to the wilting is proportional to the distance between the free surface and the water table ($H - H_{min}$). Under this consideration, for computing this quantity we use the expression of the water depth, computed with the eq. B.14.

$$\Delta_W(t/\tau) = \delta_W \cdot \frac{Q(t/\tau)^{\frac{2}{3}(1-\beta)} - Q_{min}(\tau)^{\frac{2}{3}(1-\beta)}}{Q_{max}(\tau)^{\frac{2}{3}(1-\beta)} - Q_{min}(\tau)^{\frac{2}{3}(1-\beta)}} \tag{C.5}$$

The related carrying capacity is:

$$K_W(t/\tau) = 1 - \Delta_W \tag{C.6}$$

for $t/\tau = 0$, $Q(t/\tau) = Q_{max}(\tau)$ $\Rightarrow$ $\Delta_W = \delta_W$, $K_W = 1 - \delta_W$
for $t/\tau = 1$, $Q(t/\tau) = Q_{min}(\tau)$ $\Rightarrow$ $\Delta_W = 0$, $K_W = 1$

## C.4 Carrying capacity related to the extirpation

The damage due to the extirpation of the riparian vegetation is proportional to the unit power of the current, related to its velocity (eq. 3.17).

$$\Delta_E(t/\tau) = \delta_E \cdot \frac{Q(t/\tau)^{(1-\beta)} - Q_{min}(\tau)^{(1-\beta)}}{Q_{max}(\tau)^{(1-\beta)} - Q_{min}(\tau)^{(1-\beta)}} \tag{C.7}$$

The relative carrying capacity due to the extirpation is expressed as:

$$K_E(t/\tau) = 1 - \Delta_E \tag{C.8}$$

for $t/\tau = 0$, $Q(t/\tau) = Q_{max}(\tau)$ $\Rightarrow$ $\Delta_E = \delta_E$, $K_W = 1 - \delta_E$

for $t/\tau = 1$, $Q(t/\tau) = Q_{min}(\tau)$ $\Rightarrow$ $\Delta_E = 0$, $K_E = 1$

## C.5 Carrying capacity related to the bank erosion

The damage due to the bank erosion is related both to hydrology and to the shape of the river cross-section. The propensity of the river to braiding is represented by the ratio between the active width $B(t/\tau)$ and the hydraulic depth $H(t/\tau)$, both function of the submergence time $(t/\tau)$.

The ratio between the active channel (eq. B.13) and the water depth (eq. B.14) is computed by the expression:

$$\frac{B(t/\tau)}{H(t/\tau)} = \alpha \cdot \left[\alpha \cdot \chi \cdot \sqrt{j}\right]^{\frac{2}{3}} \cdot [Q(t/\tau)]^{\frac{5\beta-2}{3}} \tag{C.9}$$

Under these assumptions, the single damage to to the bank erosion is:

$$\Delta_B(t/\tau) = \delta_B \cdot \left[\frac{Q(t/\tau)}{Q_{min}(\tau)}\right]^{\frac{5\beta-2}{3}} \tag{C.10}$$

The single carrying capacity due to the lateral bank erosion is computed by the equation:

$$K_B(t/\tau) = 1 - \Delta_B \tag{C.11}$$

for $t/\tau = 0$, $Q(t/\tau) = Q_{max}(\tau)$ $\Rightarrow$ $\Delta_B = \delta_B \cdot \left[\frac{Q_{max}(\tau)}{Q_{min}(\tau)}\right]^{\frac{5\beta-2}{3}}$, $K_B = 1 - \delta_B \cdot \left[\frac{Q_{max}(\tau)}{Q_{min}(\tau)}\right]^{\frac{5\beta-2}{3}}$

for $t/\tau = 1$, $Q(t/\tau) = Q_{min}(\tau)$ $\Rightarrow$ $\Delta_B = \delta_b$, $K_B = 1 - \delta_B$

## C.6 Aggregate carrying capacity

As reported in the Section 3.4, the total carrying capacity is computed by a productory of each single carrying capacity.

In the next graph (Figure C.1) we have reported the trend of the various terms composing the aggregate carrying capacity for a river with regular hydrology, while in the Figure C.2 we represents the aggregate carrying capacity for a river with irregular hydrology. In both cases we assume that the shape factor of the river cross-section remains constant during the simulation.

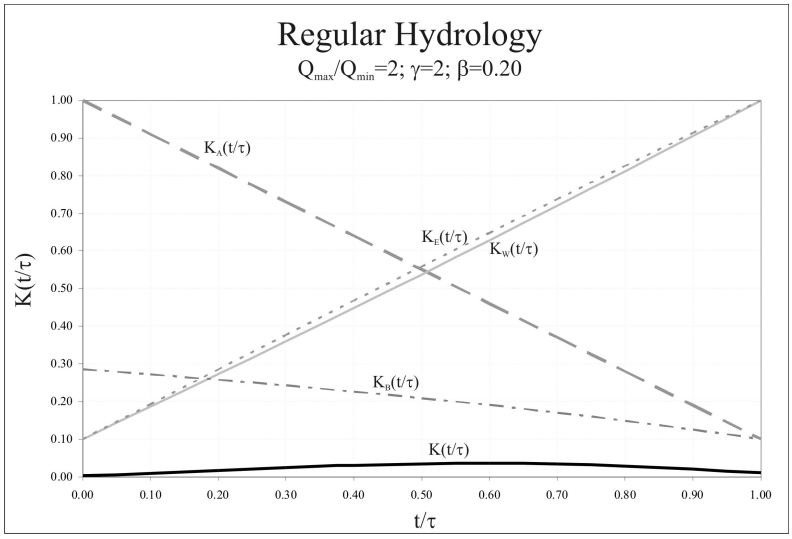


**Figure C.1:** Example of the carrying capcity of a river with regular hydrology.

The aggregate carrying capacity typical of a river with regular hydrology is much low, because the slightly variation of the river discharge does not influence the growth of the riparian vegetation.

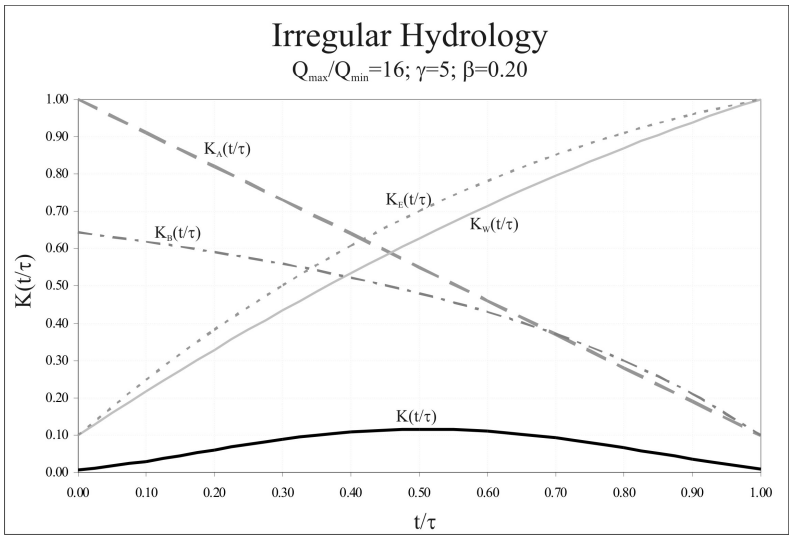


**Figure C.2:** Example of the carrying capcity of a river with irregular hydrology.

A significant variation of the river hydrology creates an important variation of the carrying capacity during the hydrological year, as we can see in the Figure C.2. The most important contribution to the variation of the carrying capacity during the year is due to the lateral bank erosion ($K_B(t/\tau)$), strongly correlated with the hydrological variations (Section C.5).

## C.7 Iterative scheme for the computation of the shape factors

In the next figure we have reported a flow chart of the iterative method used for computing the shape factors $\alpha$ and $\beta$ of the river cross-sections. As mentioned in the previous sections, these parameters are related to the hydrology and the carrying capacity of the riparian submerged vegetation.

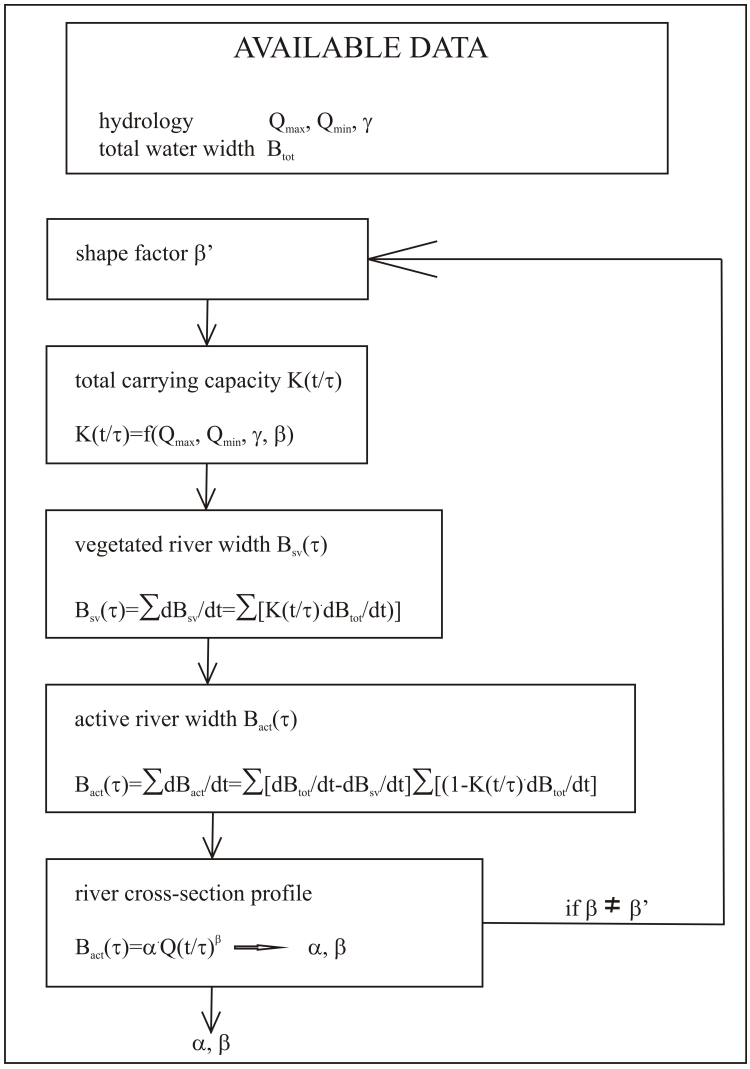


**Figure C.3:** Iterative scheme for the computation of the shape factors of the river cross-sections.

# Appendix D

When no surveys or satellite images are available, there is still the possibility to "create" a synthetic section as a function of some appropriate overall quantity.

The Leopold-Wolman's morphological parameter Ω (Leopold et al., 1953; Leopold et al., 1957; Leopold et al., 1964):

$$\Omega = i \cdot Q_*^{0.44} \tag{D.1}$$

with $i$ average bottom slope and $Q_*$ bankfull discharge, has been recognized as especially significant in this respect (Thorne et al., 1997).

Let us recall, for instance, that when the parameter Ω is smaller than 0.013 a braiding river tends to evolve into a meandering river (Leopold et al., 1957), while when Ω is larger than 0.042 the river tends to be straight and deeply embanked (Figure D.1).

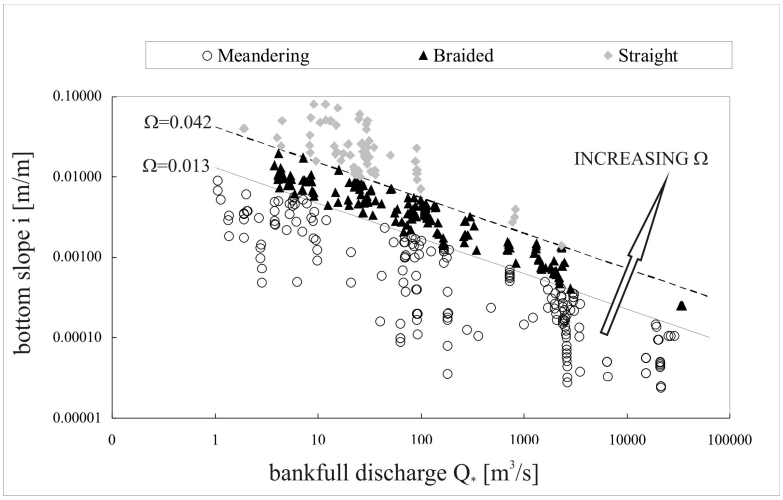


**Figure D.1:** Classification of rivers: bankfull discharge $Q_*$ vs bottom slope $i$ of some river reaches.

Moreover some regime considerations (Yalin, 1992; Knighton, 1998), provide a relationship between the representative river width $B_*(\tau)$ and the bankfull discharge $Q_*(\tau)$:

$$B_*(\tau) = a \cdot Q_*(\tau)^{0.50} \tag{D.2}$$

To define the river cross-section in the expression of $\Omega$ (eq. D.1), however, we use, instead of $Q_*(\tau)$, the equivalent discharge $Q_{eq}(\tau)$ (eq. B.11).

$$B_{eq}(\tau) = a \cdot Q_{eq}(\tau)^{0.50} \tag{D.3}$$

With reference to many measured river cross-sections of different size, both by survey and by satellite images, in temperate and tropical climate, eq. (D.3) appears to be a robust representation of the active equivalent river width, with the coefficient $a$ expressed as:

$$a = 5 \cdot \left(\frac{Bf}{\Omega}\right)^{0.10} \tag{D.4}$$

where $B_f$ is the total distance between the levees or the valley slopes (namely the maximum available river width).

Figure D.2 indicates the relationship between the measured coefficient $a$ and the ratio between the morphological parameter $\Omega$ and the maximum available width $B_f$.

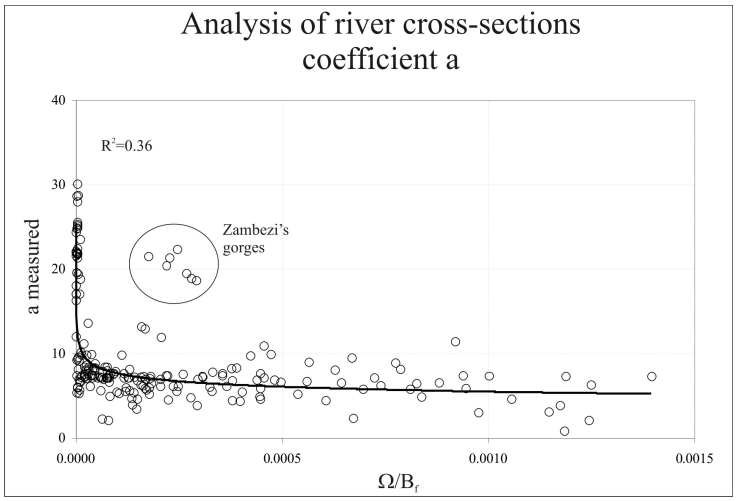


**Figure D.2:** Preliminary prediction of the coefficient $a$ of the river cross-section profile.

By combing eq. (3.3) and eq. (D.3), for $Q(t/\tau) = Q_{eq}(\tau)$ and $B(t/\tau) = B_{eq}(\tau)$, one finds:

$$\alpha = a \cdot Q_{eq}(\tau)^{0.50-\beta} \tag{D.5}$$

namely the coefficient $\alpha$ in eq. (3.3) depends on both the size of the river and on the exponent $\beta$. Combining the eq. (D.5) and the eq. (3.3) it is possible to compute the instantaneous active river width $B(t/\tau)$ as a function of the corresponding instantaneous discharge $Q(t/\tau)$ and of the other quantities.

$$B(t/\tau) = \left[a(\tau) \cdot Q_{eq}(\tau)^{0.50-\beta}\right] \cdot Q(t/\tau)^{\beta} \tag{D.6}$$

These quantities are the equivalent discharge $Q_{eq}(\tau)$ (depending on hydrology), the coefficient $a(\tau)$ (depending on the overall river morphology) and the exponent $\beta$, which can be determined contextually with the carrying capacity (depending on biology) as shown in Section 3.5.